

# Structural and Functional Analogues of the Active Sites of the [Fe]-, [NiFe]-, and [FeFe]-Hydrogenases†

Cédric Tard

Laboratoire d'Electrochimie Moléculaire, Unité Mixte de Recherche Université–CNRS 7591, Université Paris Diderot, 15 rue Jean-Antoine de Baïf, 75013 Paris, France

Christopher J. Pickett\*

Energy Materials Laboratory, School of Chemistry, University of East Anglia, Norwich NR4 7TJ, United Kingdom

Received December 6, 2008

## Contents

1. Introduction	2245
2. [Fe]-Hydrogenase	2246
2.1. Biological Role	2246
2.2. Current Understanding of Structure	2246
2.3. Possible Mode of Action of [Fe]-Hydrogenase	2247
2.4. Synthetic Models	2248
2.4.1. Structure	2248
2.4.2. Function	2249
3. [NiFe]-Hydrogenase	2249
3.1. Structure, Function, and Mechanisms of [NiFe]-Hydrogenases	2249
3.2. Early Chemical Models of the [NiFe]-Hydrogenase Active Site	2250
3.2.1. {Ni-S}-Complexes	2250
3.2.2. {Fe(CO) <sub>x</sub> (CN) <sub>y</sub> }-Complexes	2250
3.3. Structural Models of {NiFe}-Systems	2251
3.3.1. {NiFe}-Complexes	2251
3.3.2. Polymetallic {Ni <sub>x</sub> (μ-S) <sub>z</sub> Fe <sub>y</sub> }-Complexes	2254
3.4. Functionality	2255
4. [FeFe]-Hydrogenase	2256
4.1. Biological Role	2256
4.2. Current Understanding of the Biological Structure	2256
4.2.1. The Catalytic Subunit: The H-Cluster	2256
4.2.2. Nature of the Bridging Dithiolate	2258
4.2.3. Terminal and Bridging CO	2258
4.2.4. The Oxidation State and Spin-Density in the EPR-Active Resting State (H <sub>ox</sub> ) and Its CO-Inhibited Form (H <sub>ox</sub> -CO)	2259
4.2.5. Hydride	2259
4.3. Synthetic Models	2259
4.3.1. Overview	2259
4.3.2. Synthetic Subsite Structures	2260
4.3.3. Protonation and Hydride Binding at Subsite Molecules	2263
4.3.4. Electron Transfer and Electrocatalysis	2264
4.3.5. Photocatalysis of Hydrogen Evolution Using Sacrificial Electron-Donors	2267
5. Concluding Remarks	2268

6. Abbreviations	2269
7. References	2270

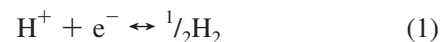
## 1. Introduction

This article sets out to review the chemistry relating to the synthesis of structural and functional analogues of the three classes of hydrogenases. This chemistry has grown explosively over the last 10 or so years since the first X-ray structures of [NiFe]- and [FeFe]-hydrogenase systems were published. There are now some 400 papers covering structural and functional aspects, with the majority of these associated with the di-iron system.

As much emphasized in earlier papers and reviews, there are two principal drivers to research on active site analogues. The first is to provide metric, spectroscopic, and reactivity precedents for the biological systems; the second is the prospect of producing technological materials for a “hydrogen economy” guided by the chemistry of the enzymatic systems.

The literature in this rapidly developing area has been the subject of several major reviews.<sup>1–16</sup> The biological background to the hydrogenases, advances in computational modeling, and fundamental hydrogen chemistry have been most recently covered in the special issue of *Chemical Reviews* entitled “Hydrogen”, of which this contribution forms a companion part.

There is the prospect that hydrogen becomes a major energy vector as the century progresses, by virtue of its clean cold combustion characteristics in fuel cells, a technology which must underpin advances toward a large scale hydrogen economy. Hydrogen can be generated from fossil fuels using well established industrial scale chemistry; while this is clearly not “green”, it can provide the transitional capacity as infrastructure is developed and alternate ways of generating hydrogen using solar, nuclear, hydro, wind, or wave energy come to the fore. Hydrogen fuel or producer cells based on the interconversion of eq 1 will play a major part in such an economy.<sup>17</sup>



However, such interconversion requires an electrocatalyst to proceed in the forward or back direction at diffusion controlled rates without demanding a large driving force—an overpotential—which is greater than  $\pm ca.$  150 mV from the thermodynamic equilibrium potential. The best catalyst is

† This article is part of the Hydrogen special issue.

\* Corresponding author E-mail: c.pickett@uea.ac.uk.



Cédric Tard was born on July 18, 1979, and grew up in Paris. He did his undergraduate studies at Paris-Sud University (Orsay, France). He received his Ph.D. degree at the John Innes Centre (Norwich, U.K.) in 2005 under the guidance of Prof. Chris Pickett. His research involved the synthesis and electrochemical studies of new model complexes related to the [FeFe]-hydrogenase. After two years as a postdoctoral fellow at the Ecole Polytechnique (Palaiseau, France) working with Prof. Jean-Pierre Boilot, he is now an associate scientist at Paris-Diderot University (Paris, France) in the Laboratory of Molecular Electrochemistry led by Profs. Jean-Michel Savéant and Marc Robert. He is currently involved in the mechanistic study of proton-coupled electron transfer in bioinspired organic and organometallic molecules.

platinum or certain of its alloys, and this is utilized, for example, as a nanoparticulate adsorbed onto carbon wool in commercial proton exchange membrane (PEM) fuel cells.<sup>18</sup> The sustainability of platinum in a growing hydrogen economy is very doubtful. Thus, understanding and *expanding* the chemistry of the hydrogenases by the design of artificial enzymes or “convergent” chemical systems which utilize biomechanistic insights provides a Grand Chemical Challenge for the early part of this century.

## 2. [Fe]-Hydrogenase

### 2.1. Biological Role

In some methanogenic archaea, there is a type of hydrogenase, the H<sub>2</sub>-forming methylenetetrahydromethanopterin (Hmd) that does not contain nickel or iron–sulfur clusters and which is induced under nickel limited growth conditions.<sup>19</sup> Hmd, also referred to as iron–sulfur cluster free hydrogenase and abbreviated as [Fe]-hydrogenase, catalyzes the reversible reduction of methenyltetrahydromethanopterin with dihydrogen to methylenetetrahydromethanopterin and a proton (Figure 1).<sup>20,21</sup> The reduction of the methenyl-substrate with H<sub>2</sub> is an intermediary step in the biological conversion of carbon dioxide to methane. The occurrence of this cytoplasmic enzyme is limited to methanogenic archaea also, but it is not universally present in these. This absence in some methanogens is explained by the existence of two other enzymes, a F<sub>420</sub>-reducing [NiFe]-hydrogenase (F<sub>rh</sub>) and a F<sub>420</sub>-dependent methylene-H<sub>4</sub>MPT dehydrogenase (Mtd).

### 2.2. Current Understanding of Structure

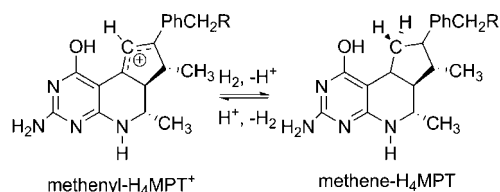
The crystal structure of a native enzyme has not been obtained. However, in elegant work, Shima et al. have described the reconstitution of an [Fe]-hydrogenase apoenzyme from *Methanothermobacter jannaschii* with an iron cofactor from *Methanothermobacter marburgensis* which has allowed the crystallization of an active enzyme and its characterization by X-ray crystallography (1.75 Å resolution,



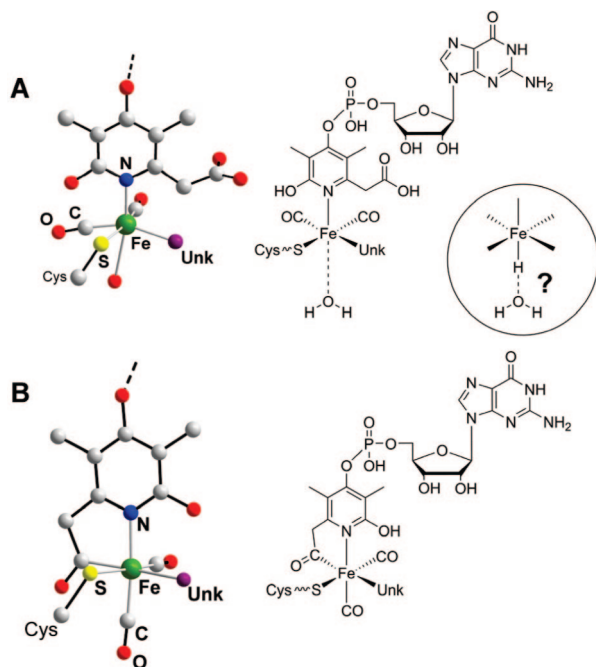
Chris Pickett is Professor of Chemistry at the University of East Anglia, where he is Director of the new Energy Materials Laboratory. He was born on the Isle of Avalon, Somerset, England, in 1950, and educated in Glastonbury, Wells, and Wembley, obtaining a Ph.D. under the guidance of Professor Derek Pletcher at the University of Southampton in 1975. He then joined Professor Chatt's Nitrogen Fixation Laboratory at the University of Sussex and spent the next 30 odd years exploring the chemistry and electrochemistry of molecular nitrogen, discovering along the way new electrochemical transformations of coordinated ligands, including a pathway for electrochemical nitrogen fixation, and a ligand free energy equation. An occasional francophile (when they lose at rugby) and australophile (when they lose the Ashes), Chris has enjoyed many years of great collaborations with Jean Talarmin (Brest), in nitrogen fixation research, and with Stephen Best (Melbourne), in hydrogenase chemistry. Chris is particularly indebted to Dr. Saad Ibrahim for his exceptional research support over the last 15 years and to the many gifted postgraduate and postdoctoral scientists he has and continues to research alongside.

Figure 2A).<sup>22</sup> In this structure, the iron center takes a square pyramidal geometry in which the sp<sup>2</sup>-hybridized N of the pyridinol derivative binds apically to the iron and two *cis*-CO, with a cysteinyl thiolate and an unknown ligand occupying the basal positions. The oxidation state of the iron center remains, however, undefined, but the possibility of an Fe(I) oxidation state can be excluded because this mononuclear center is EPR-silent in the isolated form. Mössbauer experiments are more likely suggesting a low-spin Fe(0) or Fe(II).<sup>23</sup> EXAFS for the isolated cofactor and the enzyme together with X-ray crystallographic data for the latter indicate a distal water molecule “occupying” one coordination site at a distance of 2.7 Å and an additional site which is possibly partially occupied.<sup>22</sup>

The hydroxylate and carboxylate substituents of the pyridinol are not evidently iron ligands; however, the latter is partly disordered, and partial occupancy in this hybrid structure cannot be excluded. Because the planarity of the heterocyclic ring establishes that it is a pyridinol and is not in a pyridone tautomeric form, with the nitrogen atom in a  $\pi$ -accepting sp<sup>2</sup> configuration, it is suggested that the pyridinol group might have ligand back-bonding properties similar to those of cyanide,<sup>24</sup> which acts as an iron ligand in the [NiFe]- and [FeFe]-hydrogenases. Two CO molecules are optimally accommodated between several nonpolar atoms of the polypeptide chain. The CO molecules form an angle of 90°, in agreement with the interpretation of the IR spectrum of the holoenzyme.<sup>25</sup> The other ligand originating from the protein backbone is the thiolate sulfur of Cys176 that points toward the iron. The chemical nature of a “fifth” ligand is unknown, and its electron density cannot definitely be assigned as a monatomic or diatomic ligand, although it is clearly connected with that of the iron and of relatively high occupancy (i.e., corresponds to a completely occupied



**Figure 1.** Reversible reaction catalyzed by the [Fe]-hydrogenase. A hydride is stereospecifically transferred from H<sub>2</sub> to the *pro-R* side of methylenetetrahydromethanopterin.



**Figure 2.** X-ray crystal structures and schematic representations of the active site of the [Fe]-hydrogenase. Unk, unknown ligand; this site appears to bind cyanide. A: Structure from ref 22. B: Structure from ref 31.

water molecule). The “vacant” sixth coordination site of the iron contains a spherical electron density which Shima, Thauer, and co-workers interpret as a monatomic solvent molecule (i.e., a completely occupied water molecule). They note it is, however, at a distance of 2.7 Å, too far away to be considered as a ligand. This site is thought to be the binding position of extrinsic CO, an inhibitor of the [Fe]-hydrogenase.

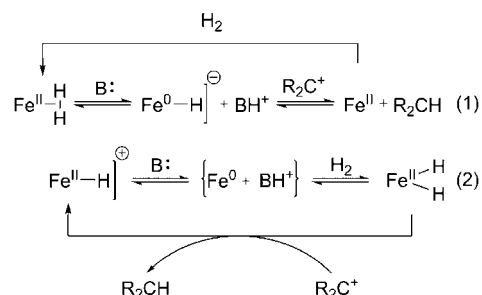
Notably, the water close to the iron interacts with a second water molecule, which in turn is linked to the carbonyl group of the strictly conserved Cys250. Interestingly, the Cys250 → Ala mutant shows reduced enzyme activity.<sup>26</sup> The potential role of hydride–water interaction and hydrogen bonding is developed in the following section.

### 2.3. Possible Mode of Action of [Fe]-Hydrogenase

In the bimetallic hydrogenases, the electrons from the oxidation of dihydrogen flow from the active site through a set of iron–sulfur clusters to an electron acceptor protein partner. In [Fe]-hydrogenase, electrons are not released; rather, the carbocation substrate methenyl-H<sub>4</sub>MPT<sup>+</sup> is thought to directly “accept” hydride from H<sub>2</sub>.

Support for this comes from the X-ray crystal structure of the protein. There is cleft between the peripheral and central units which can accommodate the substrate and allow positioning of the carbocation center close to the iron.

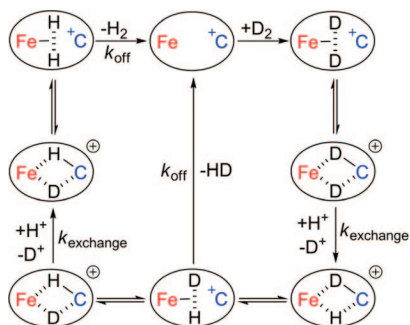
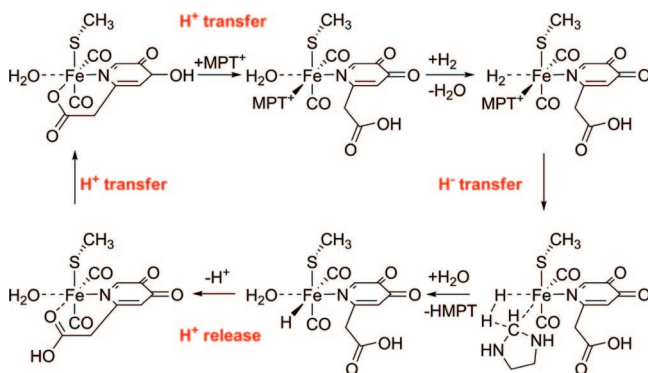
**Scheme 1**



Shima and Thauer suggest that the most attractive hypothesis for the mechanism of H<sub>2</sub> cleavage in [Fe]-hydrogenases is based on a concerted action involving the substrate, the strong hydride acceptor methenyl-H<sub>4</sub>MPT<sup>+</sup>, and the Lewis acid Fe(II) of the active site. The latter is argued to substantially lower the pK<sub>a</sub> value of H<sub>2</sub> when this is bound in a side-on conformation, and this has a well established chemical precedent.<sup>27</sup> The problem with this is that lowering the pK<sub>a</sub> would actually deactivate H<sub>2</sub> with respect to it acting as a hydride source. Perhaps a more reasonable scenario involving an Fe(II) center is that dihydrogen coordinates and then a neighboring base heterolytically splits dihydrogen by removing a proton; this would leave a hydride on the metal center for concerted or sequential transfer to the carbocation substrate, as shown in Scheme 1, mechanism 1. Base cleavage of coordinated dihydrogen leaving a hydride on a metal is well established chemistry.<sup>27</sup> As pointed out by Shima and Thauer, there are bases available close to the active site in the enzyme.<sup>22</sup> While mechanism 1 is viable, there is still the aspect of the apparent low-coordination number of the active site, and we might conjecture that, in the crystal structure of the resting state enzyme, a hydride ligand is crystallographically undetected.

An alternative pathway for dihydrogen activation that might be considered is oxidative addition of dihydrogen to an iron(0) center to give a dihydride followed by abstraction of one hydride by the carbocation substrate (Scheme 1, mechanism 2). The regeneration of the dihydride intermediate could occur by proton removal preceding or concerted with dihydrogen ligation to the monohydride. Again, there are well established precedents for this type of reaction. This requires that the crystallographic form is actually the protonated intermediate (Figure 2A); while this putative hydride has yet to be detected, the possibility is nevertheless attractive, in that the apparent low-coordination number associated with the long distance between a water molecule and the iron site is accommodated by a hydrogen bonded hydride. Chemical precedent for intramolecular hydride ligand hydrogen bonding has been established.<sup>27,28</sup>

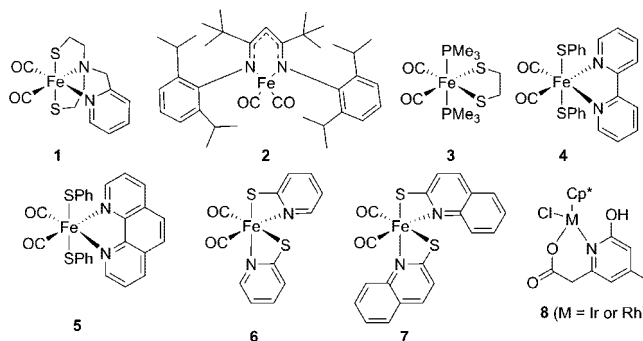
[Fe]-hydrogenase catalyzes an active exchange of H<sub>2</sub> with protons of water; however, this activity is dependent on the presence of the hydride-accepting methenyl-H<sub>4</sub>MPT<sup>+</sup> substrate.<sup>20</sup> In its absence, the exchange activity is not observed. There is a parallel formation of HD and H<sub>2</sub> from D<sub>2</sub> and H<sub>2</sub>O in this exchange catalysis; there is not a lag in the formation of H<sub>2</sub>, as would be observed in a sequential pathway.<sup>29</sup> Thus, HD is not an intermediate on the pathway to D<sub>2</sub>. To explain this mechanism, Shima and Thauer have suggested that the catalytic cycle starts with the formation of an (η<sup>2</sup>-D<sub>2</sub>)Fe complex which is in electronic equilibrium with the cationic (μ-D)<sub>2</sub> complex. This is followed by an exchange of the (μ-D)<sub>2</sub> complex with protons of bulk water

**Scheme 2. Proposed H/D Exchange Mechanism (Adapted from Ref 29)****Scheme 3. Mechanism for H<sub>2</sub> Cleavage Catalyzed by the Model Active Site with MPT<sup>+</sup> (Adapted from Ref 31)**

and either by a rotation of HD in the ( $\eta^2$ -HD)Fe complex followed by a second exchange, or by the dissociation of the complex with the release of HD. The parallel formation of HD and H<sub>2</sub> at equal rates can be explained assuming that  $k_{\text{off}} = k_{\text{exchange}}$  and that all other steps in the catalytic cycle are not rate-limiting. They draw the interesting parallel in the mechanism shown in Scheme 2 that the carbocation behaves as a second metal center.<sup>29</sup> The elegant study by Ogo and co-workers<sup>30</sup> on parallel formation of HD and D<sub>2</sub> by a {RuNi}-system parallels the exchange studies of Vogt et al.<sup>29</sup>

A DFT analysis of the possible mechanism of action of [Fe]-hydrogenase has been undertaken by Hall and Yang.<sup>31</sup> They have chosen to model a structure in which the oxo group on the pyridine has been shifted from the enzymic 2- to the unnatural 3-position because this avoids interactions of the oxygen with S and *cis*-CO (perhaps even N,O chelation?). The calculations successfully model the strict dependence of H<sub>2</sub>/H<sup>+</sup> isotopic exchange on the presence of the substrate. They argue that the ability of the pyridone to change its donor ability provides a trigger mechanism. Its strong donor strength prevents heterolytic H<sub>2</sub> cleavage from occurring and only in the presence of the substrate does the donor strength of the pyridone efficiently assist the transfer of hydride to the substrate (Scheme 3).

Very recent development studies on a mutant protein (Cys176 → Ala) have provided a new interpretation of the structure. A better refinement of the pyridone substituent was achieved;<sup>32</sup> rather than it being a disordered carboxylate, it now looks as if it is a coordinated acyl group. This opens up novel aspects, notably the possibility of CO-insertion into a metal-carbon  $\sigma$ -bond or the reverse deinsertion of CO. In addition to the acyl ligand, the coordination sphere is completed by S- and O-coordination from *exogenous* dithiothreitol (Figure 2B). The two infrared  $\nu(\text{CO})$  frequencies and

**Figure 3. Synthetic models of [Fe]-hydrogenase.**

intensities for this modified protein at 1996 and 1928 cm<sup>-1</sup> are typical for a *cis*-CO arrangement. An acyl band has not been identified, presumably because it is masked by water absorption at frequencies below *ca.* 1700 cm<sup>-1</sup>.

## 2.4. Synthetic Models

### 2.4.1. Structure

Model studies of the [Fe]-hydrogenase system are necessarily at an early stage, as knowledge from EXAFS and crystallographic studies of the enzyme have only recently been published. As with the [FeFe]-hydrogenase system, *vide infra*, there is available some early background chemistry which includes the synthesis of iron centers with *cis*-CO, thiolate, and pyridine ligands, and these are illustrated in Figure 3 and Table 1.

Given that hitherto biologically unknown iron(I) oxidation states are now established to occur in the [FeFe]-hydrogenase (see section 4.2.4), the question has naturally arisen as to whether or not the heterolytic cleavage of H<sub>2</sub> by this [Fe]-hydrogenase enzyme was facilitated by a Lewis superbase in the form of a low oxidation state Fe(0) metal center, in combination with a Lewis superacid, viz. the carbonium ion center of the substrate. In this context, Wang et al. have correlated CO stretching frequencies in their model complex **1**, with that of the cofactor, the enzyme, and some 130 complexes in the literature which possess the {Fe(*cis*-CO)<sub>2</sub>}-motif.<sup>33</sup> From this correlation, it was concluded that the oxidation state of iron in both the isolated cofactor and the enzyme is Fe(II). Furthermore, Mössbauer spectral data for the enzyme and the synthetic model were found to be in good agreement, lending further support to this assignment.

The apparent low coordination number of the enzyme structure, the superbase proposition, and the Fe(II) oxidation state could all be accommodated if one (or two) hydride(s) occupied the so-called low occupancy positions. If a superbase is indeed involved, it would be unlikely that it could be easily isolated in a deprotonated form. It is much more likely to have scavenged a proton to form a hydride. Indeed, the photolability of the cofactor might owe more to H atom or H<sub>2</sub> photolability than to CO loss.<sup>34</sup>

Low-coordinate number dicarbonyl iron species have been synthesized. Thus, Holland and co-workers have isolated and crystallographically characterized a four-coordinated iron dicarbonyl species (**2**) by using an electron rich and sterically constricting bis(imino) ligand.<sup>35</sup> However, this is a paramagnetic Fe(I) species and does not possess a coordinated thiolate.<sup>23,25</sup>

Guo et al. have discussed the nuclear resonance vibrational spectroscopy (NRVS) for [Fe]-hydrogenase and that for a

**Table 1.** {Fe(*cis*-CO)<sub>2</sub>}-Complexes' Infrared Data and Mössbauer Parameters of [Fe]-Hydrogenase Models

complex	$\nu(\text{CO})$ (cm <sup>-1</sup> )	Mössbauer parameters, i.s./q.s. (mm·s <sup>-1</sup> )	ref
[Fe]-hydrogenase (native)	1944, 2011 (pH 8.0)	0.06/0.65	25
[Fe]-hydrogenase (cofactor)	1972, 2031 (pH 9.0)	0.03/0.43	25
[Fe( <i>cis</i> -CO) <sub>2</sub> (NC <sub>5</sub> H <sub>5</sub> )CH <sub>2</sub> N(CH <sub>2</sub> CH <sub>2</sub> SH) <sub>2</sub> ] (1)	1973, 2026 (MeOH)	0.10/0.79	33
[Fe(CO) <sub>2</sub> {2,2,6,6-tetramethyl-3,5-bis-[(2,6-diisopropylphenyl)imino]hept-4-yl}] (2)	1915, 1994 (neat)	nd	35
[Fe( <i>cis</i> -CO) <sub>2</sub> (PMe <sub>3</sub> ) <sub>2</sub> (SCH <sub>2</sub> CH <sub>2</sub> S)] (3)	1939, 1998 (toluene)	nd	36
[Fe( <i>cis</i> -CO) <sub>2</sub> (SPh) <sub>2</sub> (bipy)] (4)	1983, 2029 (MeOH)	nd	37
[Fe( <i>cis</i> -CO) <sub>2</sub> (SPh) <sub>2</sub> (phen)] (5)	1985, 2029 (MeOH)	nd	37
[Fe( <i>cis</i> -CO) <sub>2</sub> (S-C <sub>5</sub> H <sub>4</sub> N) <sub>2</sub> ] (6)	1989, 2044 (THF)	nd	38
[Fe( <i>cis</i> -CO) <sub>2</sub> (S-C <sub>5</sub> H <sub>4</sub> NC <sub>4</sub> H <sub>4</sub> ) <sub>2</sub> ] (7)	1979, 2030 (Nujol)	0.07, 0.51	39

diphosphine dicarbonyl dithiolate Fe(II) model (3).<sup>36</sup> The authors concluded that NRVS results are consistent with previous FTIR and EXAFS studies and disfavor a strictly tetrahedral Fe center but cannot distinguish between a five-coordinate model with a water ligand or a truncated four-coordinate model.<sup>23,25</sup>

#### 2.4.2. Function

A rhodium complex and its iridium analogue which possess the heterocyclic ligand 6-(carboxymethyl)-4-methyl-2-hydroxypyridine have been synthesized by Rauchfuss and co-workers (8).<sup>40</sup> This ligand has a structural relationship to the GP cofactor of the enzyme. Interestingly, the iridium complex is reported to be an excellent catalyst for the dehydrogenation of PhCH(OH)(Me) to acetophenone, and this dehydrogenation chemistry is thought to be promoted by the 2-hydroxy substituent of the pyridine ligand, which may substantially influence the reactivity of an adjacent open coordination site. The authors suggest that the role of the 2-hydroxy group of the pyridol ligand in the enzyme may similarly confer high activity for the hydrogen transfer to the metal.

Relevant functional chemistry of iron or other metal systems capable of catalyzing carbocation reduction by dihydrogen will undoubtedly develop rapidly in the next few years.

### 3. [NiFe]-Hydrogenase

#### 3.1. Structure, Function, and Mechanisms of [NiFe]-Hydrogenases

The structure, function, and mechanistic aspects of [NiFe]-hydrogenases together with advances in computational modeling of this enzyme have recently been reviewed by several groups.<sup>41–44</sup> The generalist interested in obtaining a broad understanding of the [NiFe]-hydrogenase is most likely to be driven to distraction by the plethora of so-called “states” of the enzyme, some of which have real physiological significance and others of which are artifacts of *in vitro* isolation and processing: these states total eleven in all; see Table 2. Their labeling is somewhat of a historic burden, which all but aficionados are likely to find somewhat trying; nevertheless, these and their interconnectivity are necessarily summarized in Scheme 4.<sup>42</sup>

Early infrared spectroscopic studies established that carbon monoxide (CO) and cyanide (CN) ligands were part of the catalytic center,<sup>45</sup> and the first X-ray structure by Volbeda and co-workers revealed that these diatomic groups were coordinated to the iron atom, maintaining its oxidation state at +II in a low-spin (*S* = 0, diamagnetic) system.<sup>46</sup> This

structure was reported for the *Desulfovibrio gigas* enzyme in its inactive form (Ni-A) and was shortly followed by a series of papers in which the structural features of the inactive Ni-A and Ni-B forms were characterized.<sup>47–49</sup> Subsequently, crystallographic studies reported Ni-C, Ni-R, and Ni-CO structures and probed potential proton and gas-channel pathways.<sup>50–53</sup>

Common to all the crystallographically defined states are the following:

- (i) the {Ni( $\mu$ -SCys)<sub>2</sub>Fe}-butterfly arrangement formed by the bridging cysteinyl ligands
- (ii) a distorted square-planar arrangement of the four cysteinyl ligands about the Ni center
- (iii) the {Fe(CO)(CN)<sub>2</sub>}-motif.

The structure of the metal center in the inactive forms of the enzyme as isolated under aerobic conditions, Ni-A and Ni-B, is represented by Figure 4. In Ni-A, the bridging group has been suggested to be a peroxide; in Ni-B, it is thought to be a hydroxide group. Reductive activation removes these bridging groups and produces the active Ni-SI forms. The distance between the two metals ranges from about 2.9 Å for the inactive forms Ni-A and Ni-B to about 2.5 Å for the reduced active form Ni-SI.<sup>47–49</sup>

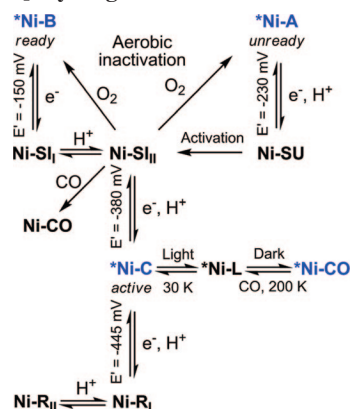
These different redox states of [NiFe]-hydrogenases present a complex scheme with inactive and active forms as well as CO-inhibited states as summarized in Scheme 4. Not all are fully structurally characterized; some are postulated from computational studies combined with spectroscopic and magnetic experiments (Table 2). The nickel atom is the redox active species in the bimetallic center, and it can be probed by its EPR signal when it is oxidized by one electron from its EPR silent Ni(II) state (in Ni-SU, Ni-SI<sub>I</sub>, Ni-SI<sub>II</sub>, Ni-R<sub>I</sub>, Ni-R<sub>II</sub>, Ni-R<sub>III</sub>, Ni-CO) to its Ni(III) state (in Ni-A, Ni-B, Ni-C) or reduced to Ni(I) (in Ni-L). It is argued on the basis of extensive FTIR, EPR, and ENDOR spectroscopy that the iron(II) is not redox active during the catalytic cycle; nevertheless, the presence of CO and CN ligands provides an FTIR probe of the electronic density around the iron atom in the various {NiFe}-states.

The Ni site is believed to be the primary dihydrogen binding site because of its position at the end of the H<sub>2</sub> transfer channel, as well as from CO-inhibition experiments. But some controversy on this point has led some authors to favor the iron(II) as the binding metal for H<sub>2</sub>, based on DFT calculations and the affinity of low spin d<sup>6</sup> metals for dihydrogen.<sup>42,43</sup> From computational studies, a postulated mechanism for dihydrogen oxidation has been proposed by Pardo et al. and is presented in Scheme 5.<sup>54</sup> This mechanism takes the iron center as the binding site for the dihydrogen molecule. For a complete overview of DFT calculations for H<sub>2</sub> activation mechanisms in [NiFe]-hydrogenases, reviews

**Table 2. Vibrational frequencies, *g* values, Ni-Fe distances and standard potentials of the redox states of the [NiFe]-hydrogenases.**

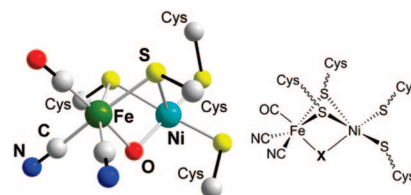
redox state	<i>A. vinosum</i>		<i>D. gigas</i>		<i>D. fructosovorans</i>		<i>D. vulgaris</i>	
	$\nu(\text{CO})$	$\nu(\text{CN})$	$\nu(\text{CO})$	$\nu(\text{CN})$	$\nu(\text{CO})$	$\nu(\text{CN})$	$\nu(\text{CO})$	$\nu(\text{CN})$
<b>FTIR<sup>a</sup> (<math>\text{cm}^{-1}</math>)</b>								
Ni-A	1945	2082, 2093	1947	2083, 2093	1947	2084, 2096	1956	2084, 2094
Ni-B	1943	2079, 2090	1946	2079, 2090	1946	2080, 2091	1955	2081, 2090
Ni-SU	1948	2088, 2100	1950	2089, 2099	1950	2091, 2101	1946	2075, 2086
Ni-SI <sub>I</sub>	1910	2052, 2067	1914	2055, 2069	1913	2054, 2069	1922	2056, 2070
Ni-SI <sub>II</sub>	1931	2073, 2084	1934	2075, 2086	1933	2074, 2087	1943	2075, 2086
Ni-C	1951	2073, 2085	1952	2073, 2086	1951	2074, 2086	1961	2074, 2085
Ni-R <sub>I</sub>	1936	2059, 2072	1940	2060, 2073	1938	2060, 2074	1948	2061, 2074
Ni-R <sub>II</sub>	1921	2048, 2064	1923	2050, 2060	1922	2051, 2067	1933	nd
Ni-R <sub>III</sub>	1913	2043, 2058	nd	nd	nd	nd	nd	nd
Ni-CO	1929, 2060	2069, 2082	1932, 2056	2070, 2083	1931, 2055	2069, 2084	nd	nd
Ni-L	1898	2044, 2060	nd	nd	nd	nd	1911	2048, 2062
<b>EPR<sup>b</sup> (<math>g_x, g_y, g_z</math>)</b>								
Ni-A	2.32, 2.24, 2.01		2.31, 2.23, 2.01		2.31, 2.23, 2.01		2.32, 2.23	
Ni-B	2.33, 2.16, 2.01		2.33, 2.16, 2.01		2.33, 2.16, 2.01		2.33, 2.16	
Ni-C	2.21, 2.15, 2.01		2.19, 2.16, 2.01		2.20, 2.16, 2.01		2.19, 2.15, 2.01	
Ni-CO	2.12, 2.07, 2.02		nd		nd		nd	
Ni-L	2.26, 2.12, 2.05		nd		nd		nd	
<b>Ni-Fe Distance<sup>c</sup> (Å)</b>								
Ni-A	nd		2.90, 2.69		2.92		2.80	
Ni-B	nd		nd		2.74, 2.88		2.69	
Ni-C/Ni-R	nd		nd		nd		2.60	
Ni-CO	nd		nd		nd		2.61	
<b>Standard Potentials<sup>d</sup> (mV, pH 8, 30 °C, V vs NHE)</b>								
Ni-B/Ni-SI <sub>I</sub>	nd		−150		nd		−151	
Ni-A/Ni-SU	nd		−230		nd		−96 (pH 6)	
Ni-SI <sub>II</sub> /Ni-C	nd		−380		nd		−375	
Ni-C/Ni-R <sub>I</sub>	nd		−445		nd		−436	

<sup>a</sup> Data from refs 45 and 58–61. <sup>b</sup> Data from refs 58 and 62–64. <sup>c</sup> Data from refs 46, 47, and 49–52. <sup>d</sup> Data from refs 58 and 61.

**Scheme 4. Different Redox States of the Active Site of Standard [NiFe]-Hydrogenases<sup>a</sup>**

<sup>a</sup> The paramagnetic EPR-active states are marked with an asterisk. Those states structurally characterized by X-ray crystallography are labeled in blue. The formal redox potentials (at pH 8.0), energy barriers, and  $pK_a$  correspond to those measured by FTIR-spectroelectrochemistry of *Desulfovibrio gigas* hydrogenase.<sup>45</sup> Ni-A, Ni-B, Ni-SU, Ni-SI<sub>I</sub>, Ni-SI<sub>II</sub>, Ni-CO, and Ni-R are named in some references as Ni<sub>II</sub>, Ni<sub>I</sub>, Ni<sub>II</sub>-S, Ni<sub>I</sub>-S, Ni<sub>II</sub>-S, Ni-S-CO, and Ni-SR, respectively (adapted from ref 42).

by Siegbahn and co-workers and by Brushi and co-workers provide an excellent insight into this field of bioinorganic chemistry.<sup>43,55</sup> Recently, there was a seminal breakthrough in understanding the role of hydride in the [NiFe]-hydrogenase system, and this was the detection of bridging hydride in the Ni-C state by Lubitz and co-workers using the HYSCORE and ENDOR techniques.<sup>56,57</sup> This work is reviewed in the companion article by Lubitz and co-workers.<sup>41</sup>

**Figure 4.** X-ray structure and schematic representation of the metallo-center of the aerobically isolated, inactive form of the [NiFe]-hydrogenase (X = HOO<sup>−</sup> for Ni-A and HO<sup>−</sup> for Ni-B).

### 3.2. Early Chemical Models of the [NiFe]-Hydrogenase Active Site

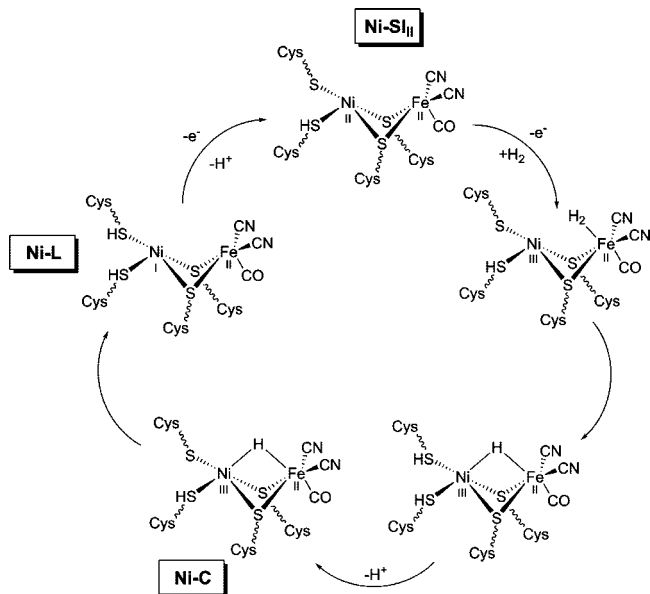
#### 3.2.1. {Ni-S}-Complexes

Prior to X-ray crystallography showing that the active site of the [NiFe]-hydrogenase was comprised of a nickel and an iron connected by bridging thiolates, it was believed that mononuclear nickel provided the catalytic center. Iron was considered as only involved as a constituent of the {Fe<sub>4</sub>S<sub>4</sub>}-clusters' electron-transfer relay. EXAFS studies suggested the environment surrounding the nickel atom was a tetragonal [Ni(SR)<sub>4</sub>]<sup>2−</sup> unit, and this stimulated a renewed interest in nickel thiolate chemistry.<sup>65–73</sup> Reviews by Halcrow and Christou<sup>74</sup> and Bouwman and Reedijk<sup>7</sup> summarize this period of research.

#### 3.2.2. {Fe(CO)<sub>x</sub>(CN)<sub>y</sub>}-Complexes

As discussed above, the {Fe<sup>II</sup>(CO)(CN)<sub>2</sub>}-pyramidal fragment of the active site of the [NiFe]-hydrogenase remains intact throughout the catalytic cycle. The chemistry of mononuclear iron with carbon monoxide and cyanide ligands has been developed by several groups, with Koch and co-workers contributing particularly systematic studies.

**Scheme 5. Proposed Catalytic Cycle for H<sub>2</sub> Oxidation by the Active Site of [NiFe]-Hydrogenase Based of DFT Calculations (Adapted from Ref 54)**



Pertinent to infrared studies of the [NiFe] and [FeFe] and [Fe]-hydrogenases, spectroscopic data for various  $\{\text{Fe}^{\text{II}}, \text{III}(\text{CO})_x(\text{CN})_y\}$  units are gathered in Table 3. Not unexpectedly, oxidation of the metal center from +II (1) to +III (2) gives rise to a shift toward the higher frequencies for both the CO and CN stretching vibrations of about 130 and 25  $\text{cm}^{-1}$  respectively.<sup>75</sup> A similar positive shift is observed when the number of CO ligands is increased around an iron(II) center, compare to, for example, complexes **9**, **11**, **12**, and **13**.<sup>75–79</sup>

Studies to mimic the electronic influence of the Ni-center and its surrounding ligands on the  $\{\text{Fe}(\text{CO})(\text{CN})_2\}$ -unit led Darensbourg and co-workers to develop a set of  $\eta^5$ -cyclopentadienyl (Cp) iron complexes (complexes **17–24**, Figure 5).<sup>80,81</sup> Notably, when the infrared spectrum of complex  $[\text{Fe}(\text{Cp})(\text{CO})(\text{CN})_2]^-$  (**18**) and that of the natural active site of the oxidized form (Ni-A or Ni-B) of [NiFe]-hydrogenase are overlaid, an almost precise match is observed.<sup>58,81</sup> The electronic influence of the Cp unit on the CO and CN ligands was therefore argued to be comparable to that of the S-bridged Ni-center found at the active site. A quasi-reversible one-electron oxidation wave is observed for the Fe(II/III) redox couple of complex **18** at +0.42V vs SCE (+0.66 V vs NHE). This value is substantially positive of the redox couples detected in the natural system (Table 2), consistent with the Fe-center of the enzyme being redox inactive under physiological conditions.

Synthetic studies in which sulfur ligation has been introduced at a  $\{\text{Fe}(\text{CO})_x(\text{CN})_y\}$ -unit have been widely explored, and some typical examples are illustrated in Figure 6.<sup>78–80,82–85</sup> However, none of the *fac*- $\{\text{Fe}(\text{CO})(\text{CN})_2\}$  examples among these (**28**, **30**, **31**, **35**, **36**, **39**) present FTIR data are comparable to that observed in the enzyme. Interestingly, complex **35** prepared by Sellmann and co-workers can be protonated by  $\text{HBF}_4$  at one of the thiolate groups to give complex **36**, which possesses an uncommon coordinated SH group with  $\nu(\text{SH}) = 2383 \text{ cm}^{-1}$ .<sup>82</sup>

### 3.3. Structural Models of {NiFe}-Systems

#### 3.3.1. {NiFe}-Complexes

Although biochemical studies of the NiFe-hydrogenases are at least as extensive if not exceeding those of [FeFe]-hydrogenase, chemical studies of model {NiFe}-systems are dramatically fewer than those of their di-iron counterparts. There are still relatively few examples of structures possessing {NiFe}-motifs with pertinent ligation around the metal atoms. Those so far reported in this admittedly challenging area are given in Table 4. This contrasts with structural models for the active site of the [FeFe]-hydrogenase, which are extensive (and perhaps somewhat over abundant, *vide infra*).

**3.3.1.1.  $\{\text{N}_x\text{Ni}(\mu\text{-S})_y\text{Fe}\}$ -Motifs.** The challenge of assembling compartmentalized Ni and Fe centers in a single molecule was first met by employing N,S ligands around the Ni center which could then allow S bridging to electron-poor Fe centers cationically charged or possessing electron-withdrawing CO groups (Figure 7 and Table 4).

Thus, Darensbourg and co-workers first developed the synthesis of a heterometallic  $[\text{Ni}(\text{bme-daco})\text{Fe}(\text{CO})_4]$  complex (**45**), soon after the publication of the crystal structure of the [NiFe]-hydrogenase enzyme.<sup>86</sup> For the single thiolate bridge between the two metals, the  $\text{Ni}\cdots\text{Fe}$  distance (3.76(1) Å) is rather long compared to the natural system (2.5–2.9 Å), but the presence of carbonyl ligands around the iron(0) was a first step toward structural and electronic model complexes.

The preparation of the dithiolate bridged complex **49** by the group of Pohl led to a complex with a shorter  $\text{Ni}\cdots\text{Fe}$  distance (2.797(1) Å).<sup>87</sup> The synthesis of complex **46** by Schröder and co-workers with a distorted square pyramidal geometry around the nickel and the short  $\text{Ni}\cdots\text{Fe}$  distance (2.539(4) Å) provided a rather good structural model.<sup>88</sup> The bent Ni–Fe  $\sigma$ -bond described by density functional theory investigations explained the diamagnetism of this complex and raised the possibility of a metal–metal bonding interaction during the catalytic cycle of the enzyme. The same group also investigated the use of Schiff-base type ligands to prepare the unusual  $[\text{Ni}(\text{tsalen})\text{Fe}(\text{CO})_3]$  complex **48**.<sup>89</sup> The nickel center is surrounded by imine  $\pi$ -bonds and two bridging thiolates. The relatively short  $\text{Ni}\cdots\text{Fe}$  distance (2.8924(6) Å) may also imply an interaction between the two metals.

Steinfeld et al. have prepared complex **47**, in which both metals are entrapped in an octahedral geometry;<sup>90</sup> again the  $\text{Ni}\cdots\text{Fe}$  distance is too long for metal–metal bonding (3.030(1) Å), but magnetic susceptibility measurements and cyclic voltammetry show clearly a mutual influence.

**3.3.1.2.  $\{\text{P}_2\text{Ni}(\mu\text{-S})_2\text{Fe}\}$ -Motifs.** In parallel to work on N,S binuclear assemblies, structures possessing P,S coordination spheres have been developed (Figure 8, Table 4).

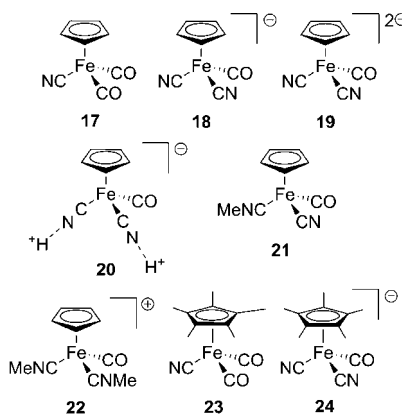
Evans and co-workers developed a strategy to prepare heterometallic complexes **50–54** using bidentate phosphine ligands 1,2-bis(diphenylphosphino)ethane (dppe) and 1,3-bis(diphenylphosphino)propane (dppp) together with tris-(ethylthiolato)amine ligands, **50–54**.<sup>91–95</sup> Except for complex **53**, all the nickel centers are found to be five-coordinate in a square pyramidal pattern with a chlorine atom in the apical site. For complexes **50–52**, the iron atom is octahedrally coordinated, whereas, for the two mononitrosyl complexes **53** and **54**, a trigonal bipyramid environment surrounds the ferric ion. The  $\text{Ni}\cdots\text{Fe}$  distances are longer than 3 Å; thus,

**Table 3.** {Fe(CO)<sub>x</sub>(CN)<sub>y</sub>}-Complexes Infrared Spectroscopic Data in  $\nu(\text{CO})$  and  $\nu(\text{CN})$  Regions

complex	condition	$\nu(\text{CO})$ (cm <sup>-1</sup> )	$\nu(\text{CN})$ (cm <sup>-1</sup> )	ref
[Fe(CO)(CN) <sub>5</sub> ] <sup>3-</sup> ( <b>9</b> )	DMSO	1931	2075	75
[Fe(CO)(CN) <sub>5</sub> ] <sup>2-</sup> ( <b>10</b> )	DMF	2064	2098	75
[Fe( <i>trans</i> -CO) <sub>2</sub> (CN) <sub>4</sub> ] <sup>2-</sup> ( <b>11</b> )	DMSO	1992	2104	77
[Fe( <i>cis</i> -CO) <sub>2</sub> (CN) <sub>4</sub> ] <sup>2-</sup> ( <b>12</b> )	DMF	1967, 2022	2080, 2106	76
[Fe( <i>fac</i> -CO) <sub>3</sub> (CN) <sub>3</sub> ] <sup>-</sup> ( <b>13</b> )	DMF	2062, 2108	2136, 2148	76
[Fe(Br)(CO) <sub>3</sub> (CN) <sub>2</sub> ] <sup>-</sup> ( <b>14</b> )	THF	2035, 2056, 2099	2127, 2139	79
[Fe(Br)(CO) <sub>2</sub> (CN) <sub>3</sub> ] <sup>2-</sup> ( <b>15</b> )	CH <sub>3</sub> CN	1984, 2039	2105, 2115, 2123	78
[Fe(CO) <sub>2</sub> (CN) <sub>3</sub> (MeCN)] <sup>-</sup> ( <b>16</b> )	CH <sub>3</sub> CN	2023, 2068	2118, 2127, 2133	78
[Fe(Cp)(CO) <sub>2</sub> (CN)] ( <b>17</b> )	CH <sub>3</sub> CN	2014, 2059	2121	80
[Fe(Cp)(CO)(CN) <sub>2</sub> ] <sup>-</sup> ( <b>18</b> )	CH <sub>3</sub> CN	1949	2088, 2094	81
[Fe(Cp)(CO)(CN) <sub>2</sub> ] <sup>2-</sup> ( <b>19</b> )	CH <sub>3</sub> CN	1863, 1898	2063, 2071	80
H[Fe(Cp)(CO)(CN) <sub>2</sub> ] ( <b>20</b> )	CH <sub>3</sub> CN	1988	2096, 2107	80
[Fe(Cp)(CO)(CN)(MeNC)] ( <b>21</b> )	CH <sub>3</sub> CN	1988	2195, 2200 <sub>(CNR)</sub>	80
[Fe(Cp)(CO)(MeNC) <sub>2</sub> ] <sup>+</sup> ( <b>22</b> )	CH <sub>3</sub> CN	2021	2211 <sub>(CNR)</sub> , 2231 <sub>(CNR)</sub>	80
[Fe(Cp*)(CO) <sub>2</sub> (CN)] ( <b>23</b> )	CH <sub>3</sub> CN	1983, 2032	2112	80
[Fe(Cp*)(CO)(CN) <sub>2</sub> ] <sup>-</sup> ( <b>24</b> )	CH <sub>3</sub> CN	1924	2079, 2085	80
[Fe(SPh)( <i>trans</i> -CO) <sub>2</sub> (CN) <sub>3</sub> ] <sup>2-</sup> ( <b>25</b> )	CH <sub>3</sub> CN	1973, 2023	2100, 2111, 2118	78
[Fe(S-C <sub>6</sub> H <sub>4</sub> Br)( <i>trans</i> -CO) <sub>2</sub> (CN) <sub>3</sub> ] <sup>2-</sup> ( <b>26</b> )	CH <sub>3</sub> CN	1978, 2028	2101, 2112, 2119	78
[Fe(S,S-CN(Et) <sub>2</sub> )( <i>cis</i> -CO) <sub>2</sub> (CN) <sub>2</sub> ] <sup>-</sup> ( <b>27</b> )	THF	1973, 2027	2112, 2119	79
[Fe(S,S-CN(Et) <sub>2</sub> )(CO)(CN) <sub>2</sub> ] <sup>-</sup> ( <b>28</b> )	THF	1985	2102, 2109	79
[Fe(S,S-COEt)( <i>cis</i> -CO) <sub>2</sub> (CN) <sub>2</sub> ] <sup>-</sup> ( <b>29</b> )	THF	1984, 2038	2112, 2122	79
[Fe(S,S-COEt)(CO)(CN) <sub>2</sub> ] <sup>-</sup> ( <b>30</b> )	THF	1996	2105, 2113	79
[Fe(S <sub>2</sub> C <sub>6</sub> H <sub>4</sub> )(CO)(CN) <sub>2</sub> ] <sup>2-</sup> ( <b>31</b> )	CH <sub>3</sub> CN	1897	2080, 2075	83
[Fe(S,S-CS)( <i>cis</i> -CO) <sub>2</sub> (CN) <sub>2</sub> ] <sup>2-</sup> ( <b>32</b> )	CH <sub>3</sub> CN	1960, 2016	2102, 2111	78
[Fe(S,S-CS)( <i>fac</i> -CO) <sub>3</sub> (CN) <sub>2</sub> ] <sup>-</sup> ( <b>33</b> )	THF	2009, 2033, 2076, 2090	2123	78
[Fe(SPh) <sub>2</sub> ( <i>cis</i> -CO) <sub>2</sub> (CN) <sub>2</sub> ] <sup>2-</sup> ( <b>34</b> )	CH <sub>3</sub> CN	1953, 2007	2075, 2094, 2103	83
[Fe(bmps)(CO)(CN) <sub>2</sub> ] <sup>2-</sup> ( <b>35</b> )	KBr	1924	2074	82
[Fe(bmps-H)(CO)(CN) <sub>2</sub> ] <sup>-</sup> ( <b>36</b> )	KBr	1960	2099	82
[Fe(SETSET)( <i>cis</i> -CO) <sub>2</sub> (CN)] <sup>-</sup> ( <b>37</b> )	THF	1954, 2009	2101	78
[Fe(S,N-C <sub>3</sub> H <sub>4</sub> )( <i>cis</i> -CO) <sub>2</sub> (CN) <sub>2</sub> ] <sup>-</sup> ( <b>38</b> )	THF	1983, 2036	2113, 2124	79
[Fe(S,N-C <sub>3</sub> H <sub>4</sub> )(CO)(CN) <sub>2</sub> ] <sup>-</sup> ( <b>39</b> )	THF	1996	2103, 2111	79
[Fe(S,O-C <sub>3</sub> H <sub>4</sub> N)( <i>cis</i> -CO) <sub>2</sub> (CN) <sub>2</sub> ] <sup>-</sup> ( <b>40</b> )	THF	1982, 2041	2109, 2121	79
[Fe( <i>cis</i> -CO) <sub>2</sub> (CN)(S,NH-C <sub>6</sub> H <sub>4</sub> )] <sup>-</sup> ( <b>41</b> )	CH <sub>3</sub> CN	1933, 1997	2099	84
[Fe(CO)(CN)(S-C <sub>4</sub> H <sub>3</sub> N <sub>2</sub> )] <sup>-</sup> ( <b>42</b> )	CH <sub>3</sub> CN	1945	2090	84
[Fe(tppt)(CN)] <sup>2-</sup> ( <b>43</b> )	DMF	nd	2070	85
[Fe(tppt)(CO)(CN)] <sup>2-</sup> ( <b>44</b> )	DMF	1904	2079	85

there is no significant metal–metal bonding in these complexes. As expected, in complex **53** the single bridging thiolate increases the Ni···Fe distance to 3.596(2) Å.<sup>93</sup> For the  $\mu$ -thiolate derivatives, the distances range from 3.0216(5) for complex **54** to 3.343(3) for complex **50**. All the nickel atoms are in a +II oxidation state, with the oxidation state for the iron centers varying from +II (low-spin) for carbonyl derivatives **50** and **52** to +III (high-spin) for nitrosyl complexes **53** and **54**.<sup>91–94</sup> Although not directly relevant to the hydrogenase, compound **53**, which possesses a methyl ligand on Ni, is of considerable relevance to [NiFe]-carbon monoxide dehydrogenase.<sup>96</sup>

Schröder and co-workers utilized the 1,3-propanedithiolate ligand (pdt)—commonly used for [FeFe]-hydrogenase model systems—to bridge Ni and Fe in a butterfly arrangement.<sup>88</sup>

**Figure 5.** {Fe(Cp)(CO)<sub>x</sub>(CN)<sub>y</sub>}-motifs.

This is less sterically restrictive than the tetradentate NS<sub>3</sub> ligands. Thus, the diamagnetic heteronuclear complexes **55–57** possess a bent metal–metal  $\sigma$ -bond (Ni···Fe = 2.4666(6) and 2.4777(7) Å, respectively), which is more elongated in the Cp complex **55** (2.7795(9) Å). In complex **56**, the nickel center switches from a square-planar Ni(II) geometry in the parent compound [Ni(pdt)(dppe)] to a distorted tetrahedral Ni(I) arrangement on binding to the

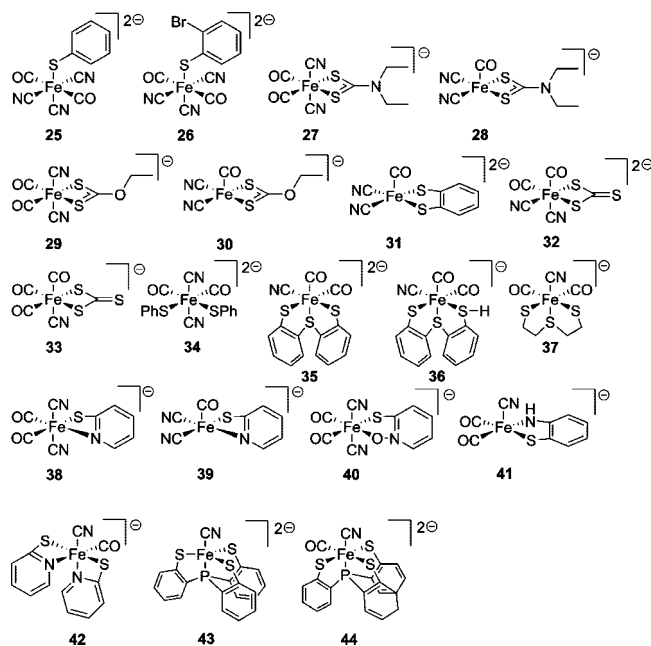
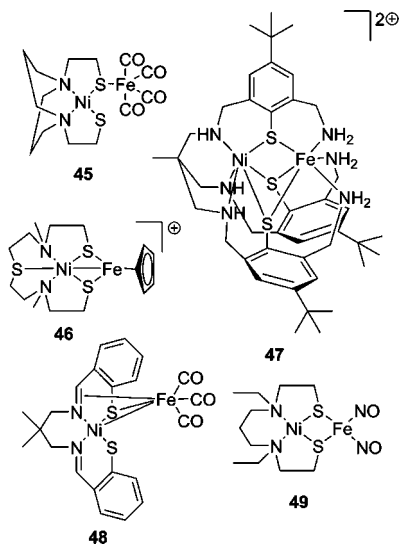
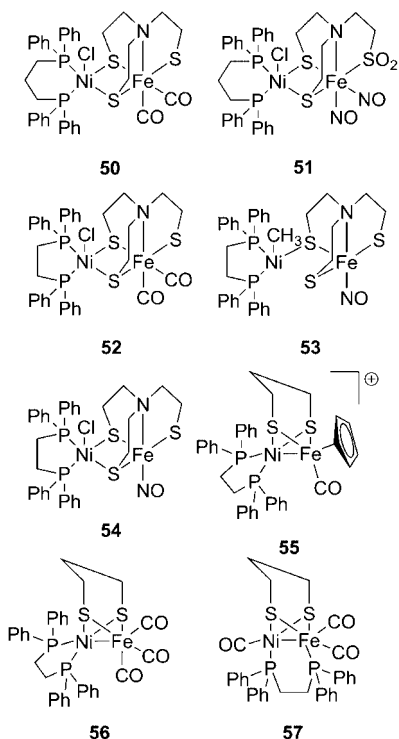
**Figure 6.** {Fe(CO)<sub>x</sub>(CN)<sub>y</sub>(S)<sub>z</sub>}-motifs.

Table 4. Structural and Spectroscopic Parameters for {NiFe}-Complexes.

[NiFe(CO) <sub>4</sub> (CN) <sub>3</sub> ]-complexes	Ni-Fe distance (Å)	$\nu(\text{CO})$ (cm <sup>-1</sup> )	ref
[{ $\mu$ -bis(mercaptoethyl)-1,5-diazacyclooctane}NiFe(CO) <sub>4</sub> ] <b>45</b>	3.76(1)	2030, 1945, 1926, 1907	86
[{ $\mu$ -tris(ethylthiolato)amine]Fe(CO) <sub>2</sub> Ni(Cl)(diphenylphosphino)propane}] <b>50</b>	3.343(3)	2006, 1944	94
[{ $\mu$ -bis(2-mercaptophenyl)sulfido-S,S',S'']Fe(PMe <sub>3</sub> ) <sub>2</sub> (CO)Ni(benzene-1,2-dithiolato)] <b>63</b>	3.323(1)	1948	99
[{ $\mu$ -tris(ethylthiolato)amine]Fe(CO) <sub>2</sub> Ni(Cl)(diphenylphosphino)ethane}] <b>52</b>	3.308(2)	2000, 1944	91, 92
[{ $\mu$ -2-(methylthio)ethanethiolate]Ni( $\mu$ -S'-Bu) <sub>2</sub> Fe(CO) <sub>3</sub> (S'-Bu)] <b>66</b>	3.2877(7)	1959, 2006, 2056	101
[{ $\mu$ -2-( <i>tert</i> -butylthio)benzenethiolate]Ni( $\mu$ -S'-Bu) <sub>2</sub> Fe(CO) <sub>3</sub> (S'-Bu)] <b>68</b>	3.2828(7)	1963, 2006, 2056	101
[{ $\mu$ -2-(methylthio)benzenethiolate]Ni( $\mu$ -S'-Bu) <sub>2</sub> Fe(CO) <sub>3</sub> (S'-Bu)] <b>67</b>	3.2344(7)	1961, 1992, 2002, 2009, 2058	101
[{ $\mu$ -2-(methylthio)phenolate]Ni( $\mu$ -S'-Bu) <sub>2</sub> Fe(CO) <sub>3</sub> (S'-Bu)] <b>69</b>	3.219(2)	1963, 2000, 2011, 2058	101
[{ $\mu$ -2-(methylthio)phenolate](MeOH)Ni( $\mu$ -S'-Bu) <sub>2</sub> Fe(CO) <sub>3</sub> ] <b>71</b>	3.2013(6)	1973, 2004, 2013, 2067	101
[{ $\mu$ -bis(2-mercaptoethyl)-1,2-dimercaptoethane}NiFe(Cp)(CO)] <b>59</b>	3.1727(6)	2038, 1991, 1915	88
[(Br)( $\mu$ -tetramethylthiourea)Ni( $\mu$ -S'-Bu) <sub>3</sub> Fe(CO) <sub>3</sub> ] <b>70</b>	3.1529(7)		
[{Br}(THF)(OAc)Ni( $\mu$ -S'-Bu) <sub>3</sub> Fe(CO) <sub>3</sub> ] <b>72</b>	3.1442(3)	1973, 2006, 2017, 2073	101
[{ $\mu$ -1,3-propanedithiolato]Fe(CO) <sub>2</sub> (CN) <sub>2</sub> Ni(diethyldithiocarbamate)] <b>64</b>	3.1312(4)	1969, 1998, 2008, 2015, 2071	101
[{ $\mu$ -1,3-propanedithiolato]Fe(CO) <sub>2</sub> (CN) <sub>2</sub> Ni(piperidinodithiocarbamate)] <b>65</b>	3.0587(6)	2110 <sub>(CN)</sub> , 2094 <sub>(CN)</sub> , 2044, 2031, 1994	100
[{ $\mu$ -bis(2,2,2-tris(5- <i>tert</i> -butyl-1,2-thio-3-amidomethyl)benzylamidomethyl)ethane}]NiFe] <b>47</b>	3.0364(8)	2110 <sub>(CN)</sub> , 2094 <sub>(CN)</sub> , 2044, 2031, 1996	100
[{ $\mu$ -ethylenebis(thiosalicylideneiminato)]NiFe(CO) <sub>3</sub> ] <b>48</b>	3.030(1)	nd	90
[{ $\mu$ -1,3-propanedithiolato]Fe(Cp)(CO)Ni(diphenylphosphino)ethane}] <b>55</b>	2.8924(6)	2045, 1973	89
[{ $\mu$ -1,3-propanedithiolato]Fe(Cp)(CO)Ni(diphenylphosphino)ethane}] <b>46</b>	2.7795(9)	1944	88
[{ $\mu$ -dimethylbis(2-mercaptoethyl)-bis(aminoethyl)sulfide}NiFe(Cp)] <b>57</b>	2.539(4)	nd	88
[{ $\mu$ -1,3-propanedithiolato]Fe(CO) <sub>2</sub> ( $\mu$ -diphenylphosphino)ethane}Ni(CO)] <b>51</b>	2.4777(7)	2023, 1973, 1920	88
[{ $\mu$ -1,3-propanedithiolato]Fe(CO) <sub>3</sub> Ni(diphenylphosphino)ethane}] <b>56</b>	2.4666(6)	2025, 2006, 1948	88
[{ $\mu$ -bis(4-mercapto-3,3-dimethyl-2-thiabutyl)- <i>o</i> -xylene}NiFe(CO) <sub>4</sub> ] <b>60</b>	nd	2009, 1945, 1860	98
[{ $\mu$ -bis(4-mercapto-3,3-dimethyl-2-thiabutyl)- <i>o</i> -xylene}NiFe <sub>2</sub> (CO) <sub>2</sub> ] <b>62</b>	nd	2048, 2096	98
[{ $\mu$ -tris(ethylthiolato)amine]Fe(CO)Ni(ethanedithiolato)] <b>73</b>	nd	1935	93
[{ $\mu$ -tris(ethylthiolato)amine]Fe(CO)Ni(dithiocarbamate-diisopropylamine)] <b>74</b>	nd	1935	93
{NiFe(NO) <sub>2</sub> }-Complexes			
Ni-Fe distance (Å)			
$\nu(\text{NO})$ (cm <sup>-1</sup> )			
ref			
[{ $\mu$ -tris(ethylthiolato)amine]Fe(NO)Ni(CH <sub>3</sub> )(diphenylphosphino)ethane}] <b>53</b>	3.596(2)	1666	93
[{ $\mu$ -bis((2-mercaptoethyl)amino)ethanesulfonato}Fe(NO) <sub>2</sub> Ni(Cl)(diphenylphosphino)propane)] <b>51</b>	3.372(2)	1733, 1704	95
	3.343(2)		
[{ $\mu$ -tris(ethylthiolato)amine]Fe(NO)Ni(Cl)(diphenylphosphino)ethane}] <b>54</b>	3.0216(5)	1667	92
[{ $\mu$ -bis(2-mercaptoethyl)sulfide}Ni(NO)Fe(NO) <sub>2</sub> ] <b>58</b>	2.8001(6)	1767, 1725	97
[{ $\mu$ -diethyl-3,7-diazanone-1,9-dithiolato}NiFe(NO) <sub>2</sub> ] <b>49</b>	2.797(1)	1663, 1624	87
[{ $\mu$ -bis(4-mercapto-3,3-dimethyl-2-thiabutyl)- <i>o</i> -xylene}NiFe(NO) <sub>2</sub> ] <b>61</b>	nd	1771, 1733	98

Figure 7.  $\{Ni_xNiS_yFe\}$ -motifs.Figure 8.  $\{P_2Ni(\mu-S)_2Fe\}$ -motifs.

$\{Fe(CO)_3\}$ -moiety. Nominally, metal–metal bonding, diamagnetism, and a closed-shell configuration about both metals in these complexes are met by each possessing a Ni(I) center with **55** Fe(III) and **56**, **57** Fe(I). The acute dihedral angle Ni–( $\mu$ -S) $_2$ –Fe found in these three complexes (65.5 to 80.3°) and the short metal–metal bond are comparable with those in the natural enzyme in its reduced active form Ni-SI (88.95° and 2.53 Å).<sup>48</sup>

**3.3.1.3.  $\{S_xNi(\mu-S)_yFe\}$ -Motifs.** Building on earlier work which described NiFe structures with only a partial correspondence of the primary coordination environment of the two metals with the natural system, more recent efforts have focused on meeting the challenge of assembling structures possessing the  $\{S_2Ni(\mu-S)_2Fe\}$ -core. All currently known examples of these are shown in Figure 9, **58–74**, and their key properties are summarized in Table 4.

The neutral complex **58** is severely constrained because the apical thioether in the bis-mercaptoethylenesulfide (bmes) ligand forces distortion around the nickel center toward a tetrahedral geometry.<sup>97</sup> The Ni $\cdots$ Fe distance is relatively short (2.8001(6) Å) but is rather too long for a metal–metal bond. The nitrosyl ligand on the nickel(0) is assigned as NO<sup>+</sup> on the basis of its infrared frequency and the linearity of the nickel–nitrosyl arrangement in the crystal structure.

Zhu et al. developed the synthesis of complex **59**, showing a nickel center in a square-planar geometry linked to a pseudooctahedral  $\{Fe(CO)Cp\}$ -unit by a bridging dithiolate.<sup>88</sup> The Ni $\cdots$ Fe distance is *ca.* 3.16 Å, and there is a relatively small Ni–( $\mu$ -S) $_2$ –Fe dihedral angle, *ca.* 41°. Other related thioether–thiolate complexes have been described by Bouwman and co-workers (**60**, **61**, and **62**).<sup>98</sup>

The first tetrathiolate  $\{NiFe\}$ -assemblies were described by Evans (**73**),<sup>93</sup> Sellmann (**63**), and their respective co-workers.<sup>99</sup> Thus, complex **63** has a planar Ni(II) coordinated by four thiolate groups with both metals in a low-spin configuration and the complex in a diamagnetic EPR silent state. The Ni $\cdots$ Fe distance, 3.323(1) Å, is relatively long compared to that determined in the enzyme states (2.6–2.9 Å, Table 2), whereas the  $\nu(CO)$  frequency at 1948 cm<sup>−1</sup> is in the range of that found in the various (insensitive) enzyme states Ni-A, -B, -C, and -SU, *ca.* 1943–1956 cm<sup>−1</sup>. It is argued that the two trimethylphosphine ligands confer electron density on the Fe similar to that of two cyanide ligands on the CO in the common *fac* arrangement. This suggested parity between PMe<sub>3</sub> and CN<sup>−</sup> comes up again in the discussion of the chemistry of  $[FeFe]$ -hydrogenase model systems.

Importantly, Tatsumi et al. reported the first syntheses of bridging-dithiolate  $\{NiFe\}$ -complexes **64** and **65**, in which the iron is coordinated by *both* carbonyl and cyanide ligands.<sup>100</sup> The two compounds have similar structural features, and metal–metal as well as metal–sulfur distances are comparable to that found in the oxidized forms of  $[NiFe]$ -hydrogenase (*Desulfovibrio gigas* and *Desulfovibrio fructosovorans*).<sup>46,49,63</sup> From <sup>1</sup>H NMR studies, both complexes **64** and **65** are diamagnetic, presumably consisting of low-spin Ni(II) and Fe(II) ions. In both complexes, an “extra” carbonyl ligand is bound to the iron center, whereas spectroscopic and X-ray crystallographic studies of the CO-inhibited form of the enzyme suggest that for the Ni–CO state the “extra” CO is bound to the nickel.<sup>42</sup> Nevertheless, these complexes provide one of the closest models for the active site of the  $[NiFe]$ -hydrogenase.

More recent work from the Tatsumi laboratory has described the preparation of several complexes with  $\mu$ -thiolate ligands that are thermally unstable in solution and have to be synthesized and manipulated at −40 °C.<sup>101</sup> Whereas the iron(II) center is in an octahedral geometry in all cases, the nickel site can adopt geometries ranging from square planar (**66–69**), through distorted square pyramidal (**70**), to octahedral (**71**, **72**). It is proposed that this remarkable flexibility of geometry of the nickel center could be responsible for dihydrogen activation in the natural active site. It will be most interesting to see how and whether these models display functionality with respect to hydrogen uptake/evolution.

### 3.3.2. Polymetallic $\{Ni_x(\mu-S)_zFe_y\}$ -Complexes

There are some 20  $\{Ni_x(\mu-S)_zFe_y\}$ -complexes **75–94** with three or four metal atoms held together, at least in part, by

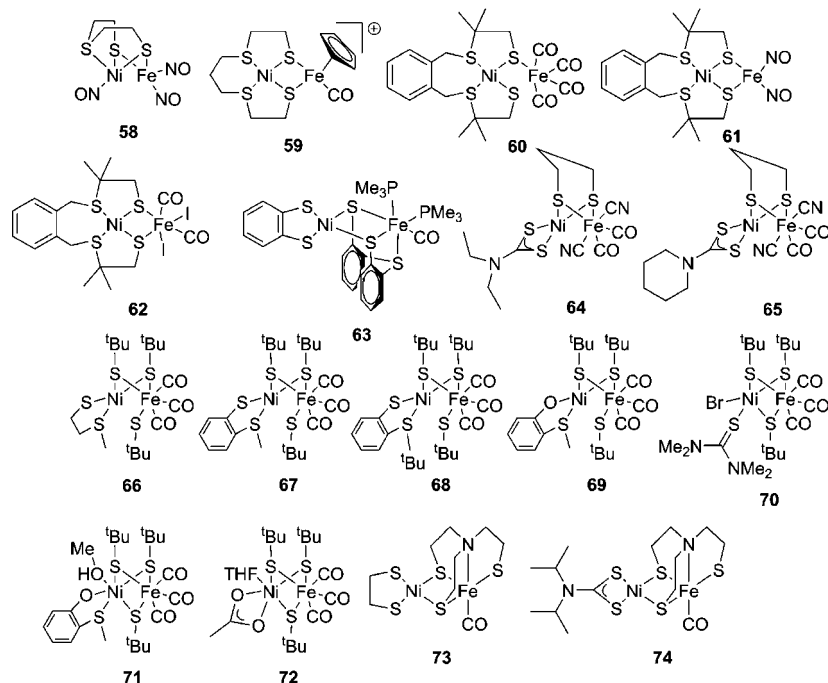


Figure 9.  $\{S_xNi(\mu-S)_yFe\}$ -motifs.

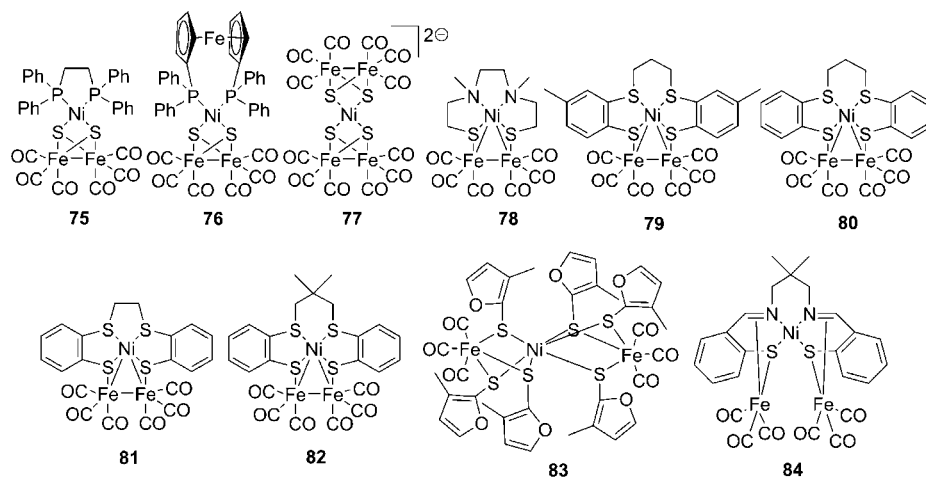


Figure 10.  $\{Ni(\mu-S)_2Fe_2(CO)_6\}$ -complexes.

bridging sulfur ligation. Those incorporating an  $\{Fe_2(CO)_6\}$ -unit are illustrated in Figure 10 (**75**–**84**), and those built from other units are shown in Figure 11 (**85**–**94**). Table 5 summarizes pertinent spectroscopic data. Although all such complexes have been discussed in terms of their relevance to  $\{NiFe\}$ -hydrogenase, there is arguably no outstanding structural chemistry that goes beyond that discussed for the more relevant dinuclear systems.

However, of the  $\{Ni_x(\mu-S)_zFe_y\}$ -systems described herein, there are only two complexes, **79** and **92**, which are reported to show electrocatalytic behavior, and these are *trinuclear* species. Notably, **79** contains an  $\{Fe_2S_2(CO)_6\}$ -motif commonly found in electrocatalytic systems for proton reduction (*vide infra*). The Sellmann system **92** is remarkable in that proton reduction occurs at a relatively positive potential of  $-0.48$  V vs NHE, and it is suggested that this is associated with the ability of the system to protonate on sulfur ligated to Ni, an argument supported by DFT calculations. Notably, the role of protonation at sulfur in a heterolytic cleavage of dihydrogen, albeit at a mononuclear iridium center, has been recently described by Tatsumi and co-workers.<sup>102</sup>

### 3.4. Functionality

As noted above, despite the synthesis of some 50  $\{NiFe\}$ -model systems, only *two* are reported to show electrocatalytic activity, and this for the reduction of protons rather than dihydrogen oxidation. Moreover, hydride chemistry of  $\{NiFe\}$ -systems is as yet unknown. However, here it is worth recalling the very elegant chemistry reported by DuBois and DuBois and co-workers, who have shown that mononuclear nickel diphosphine systems **95** with pendant proximal bases cleave dihydrogen (Scheme 6).<sup>117–125</sup> This work has been reviewed recently<sup>126</sup> and in the earlier companion *Chemical Reviews* article by Gregory Kubas.<sup>27</sup>

Rauchfuss has shown that dinuclear ruthenium thiolate systems form well-defined hydrides and can catalyze proton reduction (see section 4.3.4.1) and has further developed some interesting  $\{NiRu\}$ -systems related to these. The capability of  $\{NiRu\}$ -complexes to electrocatalyze proton reduction has been reported, but whether this is actually Ni-based has not been determined.<sup>12,127,128</sup> In seminal chemistry, Ogo and co-workers have shown that, in aqueous media,

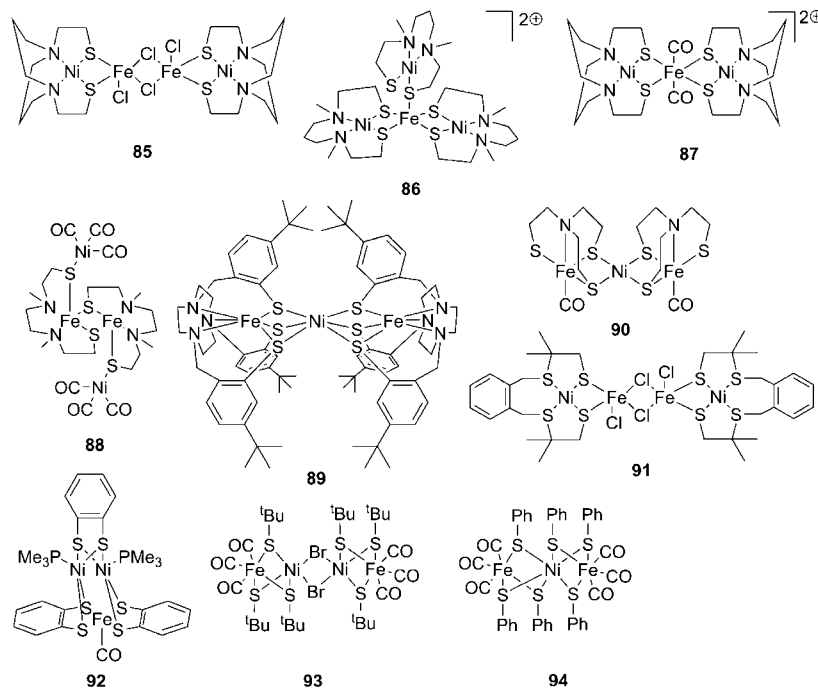
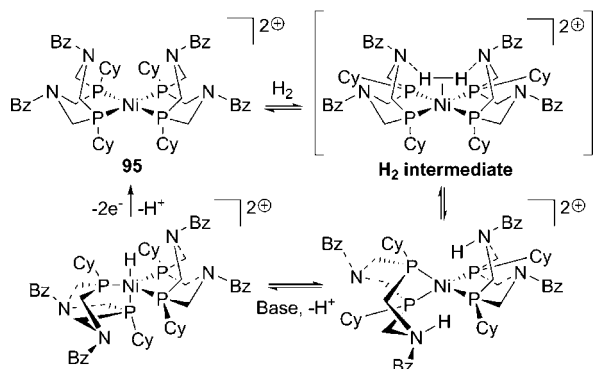


Figure 11. Polymetallic  $\{Ni_x(\mu-S)_2Fe_x\}$ -complexes.

Scheme 6. Proposed Catalytic Cycle for the  $H_2$  Oxidation (Adapted from Ref 119)



dihydrogen can be cleaved at a  $\{NiRu\}$ -unit (**96**) to give a bridging hydride between Ni and Ru (Figure 12),<sup>129</sup> and this has considerable resonance with the spectroscopic work of Lubitz and co-workers (see section 3.1).<sup>57</sup> A recent paper also by the Ogo group concluded that the  $\mu-H$  ligand of complex **96** has both protic character (at pH 4–6) and hydridic character (at pH 7–10) for this water-soluble species and can catalyze the isotope exchange of HD and D<sub>2</sub>.<sup>30</sup>

Finally, we must mention the intriguing chemistry of Tatsumi and co-workers, whom have recently shown that an extraordinary  $\{GeRu\}$ -system (**97**) can support  $\mu-S$ ,  $\mu-O$ ,  $\mu-OH$ , and  $\mu-H$  bridging groups, which are analogous with some enzyme states; moreover, this system supports the reversible interconversion of  $(H_2 + OH^-)/(H^- + H_2O)$  (Scheme 7).<sup>130</sup>

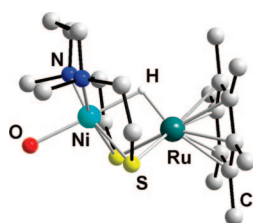


Figure 12. X-ray structure of the  $\{Ni(\mu-H)Ru\}$ -complex **96**.

## 4. [FeFe]-Hydrogenase

### 4.1. Biological Role

[FeFe]-hydrogenases play a central role in microbial energy metabolism, catalyzing the reversible interconversion of protons and electrons into dihydrogen, but are usually committed to catalyze hydrogen evolution.<sup>131,132</sup> The location of hydrogenases in the bacterial cell reflects the enzyme's function.<sup>133</sup> The periplasmic *Desulfovibrio desulfuricans* [FeFe]-hydrogenase (DdH) is involved in dihydrogen uptake. Protons resulting from this dihydrogen oxidation create a gradient across the membrane that is thought to be coupled to ATP synthesis in the cytoplasm. *Clostridium pasteurianum* [FeFe]-hydrogenase I (CpI) is a cytoplasmic enzyme that accepts electrons from ferredoxin and generates dihydrogen with protons as electron acceptors. This reaction permits the regeneration of oxidized ferredoxin. Molecular masses of [FeFe]-hydrogenases can vary from 45 to 130 kDa. Unlike [NiFe]-hydrogenases, [FeFe]-hydrogenases are mainly monomeric (in the cytoplasm), but dimeric, trimeric, and tetrameric enzymes are also known (in the periplasm).<sup>133</sup>

### 4.2. Current Understanding of the Biological Structure

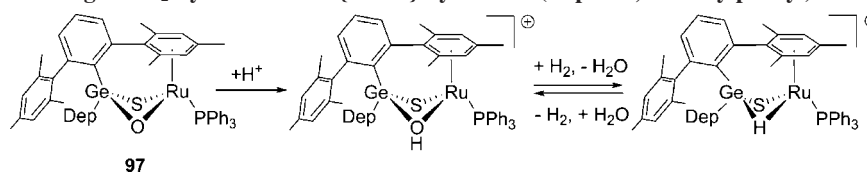
#### 4.2.1. The Catalytic Subunit: The H-Cluster

The H-cluster X-ray crystallographic structure for [FeFe]-hydrogenase has been unraveled conjointly by two independent groups in 1998 from two different organisms (DdH and CpI).<sup>134,135</sup> The active site is buried deeply within the protein. A continuous hydrophobic channel has been observed between the surface and the H-cluster and is conserved in the two [FeFe]-hydrogenases studied. As these enzymes are involved in different reactions ( $H_2$  uptake for DdH and  $H_2$  evolution for CpI), it suggests that the same pathway is used by dihydrogen to migrate to or from the active site.

The H-cluster is composed of an  $\{Fe_4S_4\}$ -cubane core linked by a cysteinyl residue to a  $\{2Fe2S\}$ -subsite (Figure

Table 5. Structural and Spectroscopic Parameters for {Ni( $\mu$ -S) $_2$ Fe $_3$ (CO) $_6$ }- and {Ni $_x$ ( $\mu$ -S) $_z$ Fe $_x$ }-Complexes

	{Ni( $\mu$ -S) $_2$ Fe $_2$ (CO) $_6$ }-Complexes		{Ni $_x$ ( $\mu$ -S) $_z$ Fe $_x$ }-Complexes		$\nu$ (CO) (cm $^{-1}$ )	ref
	Ni-Fe distance (Å)	Fe-Fe distance (Å)	Ni-Fe distance (Å)	Fe-Fe distance (Å)		
[( $\mu$ -diphenylphosphinoethane)NiS $_2$ Fe $_2$ (CO) $_6$ ] <b>75</b>	3.209(5) 3.151(5) 3.121(1)	2.485(6)	2.485(6)	2.485(6)	2061, 2044, 1998	103, 104
[{ $\mu$ -bis(2-methyl-3-furyl)disulfide} $_3$ Fe(CO) $_2$ Ni}] <b>83</b>	2.8928(4)	6.241(1)	6.241(1)	6.241(1)	2076, 2023	105
[{ $\mu$ -ethylenebis(thiosalicylideneiminato)}NiFe $_2$ (CO) $_6$ ] <b>84</b>	2.5130(8)	5.780(4)	5.780(4)	5.780(4)	2050, 2000, 1977	89
[{ $\mu$ -dimethyl-bis(2-sulfanylethyl)ethylenediamine}NiFe $_2$ (CO) $_6$ ] <b>78</b>	2.5061(8) 2.5038(4) 2.4904(8) 2.4789(9) 2.4936(8) 2.4855(6) 2.4859(6) nd	2.6099(5) 2.6435(9)	2.6099(5) 2.6435(9)	2.6099(5) 2.6435(9)	2009, 1956, 1917, 1900, 1885	106
[{ $\mu$ -1,3-bis((2-mercaptophenyl)thio)-2-dimethyl-propane}NiFe $_2$ (CO) $_6$ ] <b>82</b>	2.6279(7)	2.6279(7)	2.6279(7)	2.6279(7)	2033, 1992, 1957	107
[{ $\mu$ -1,3-bis((5-methyl-2-mercaptophenyl)thio)propane}NiFe $_2$ (CO) $_6$ ] <b>79</b>	2.6050(7) 2.509(1)	2.6050(7) 2.509(1)	2.6050(7) 2.509(1)	2.6050(7) 2.509(1)	2035, 1995, 1955	108
[{ $\mu$ -1,3-bis((2-mercaptophenyl)thio)ethane}NiFe $_2$ (CO) $_6$ ] <b>81</b>	2.503(3)	2.503(3)	2.503(3)	2.503(3)	2028, 1993, 1942	107
[{ $\mu$ -diphenylphosphinoferrocene}NiS $_2$ Fe $_2$ (CO) $_6$ ] <b>76</b>	nd	nd	nd	nd	2051, 2008, 1982, 1953, 1935	109
[Ni( $\mu$ -S $_2$ Fe $_2$ (CO) $_6$ ) $_2$ ] <b>77</b>	nd	nd	nd	nd	2018, 1995, 1941	110
Other {Ni $_x$ ( $\mu$ -S) $_z$ Fe $_x$ }-Complexes						
[{ $\mu$ -dimethyl-bis(2-sulfanylethyl)ethylenediamine}Fe $_2$ Ni $_2$ (CO) $_6$ ] <b>88</b>	3.899(1)	3.098(1)	3.098(1)	3.098(1)	2048, 1968, 1949	111
[{ $\mu$ -dimethyl-bis(2-mercaptoethyl)-1,3-propanediamine} $_2$ ( $\mu$ -dimethyl-bis(2-mercaptoethyl)-1,3-propanediamine)Ni $_3$ Fe] <b>86</b>	3.269(4)	nd	nd	nd	nd	112
[{Fe(CO) $_3$ ( $\mu$ -benzenedithiolate) $_3$ Ni $_2$ ] <b>94</b>	3.123(4) 2.976(4) 3.1703(8) 3.1153(7) 3.103 3.088	nd	nd	nd	2025, 2077	101
[{ $\mu$ -bis(mercaptoethyl)-1,5-diazacyclooctane}Ni $_2$ Fe(CO) $_2$ ] <b>87</b>	3.002(1)	nd	nd	nd	2023, 1975	113
[{ $\mu$ -bis(mercaptoethyl)-1,5-diazacyclooctane}NiCl $_2$ Fe] $_2$ <b>85</b>	3.0935(8)	3.725(1)	3.725(1)	3.725(1)	nd	113
[{Fe(CO) $_3$ ( $\mu$ -S-Bu) $_3$ Ni(Br) $_2$ ] <b>93</b>	3.0898(6)	nd	nd	nd	1973, 2000, 2021, 2073	101
[{( $\mu$ -1,4,7-tris(4- <i>tert</i> -butyl-2-mercaptobenzyl)-1,4,7-triazacyclononane)Fe $_2$ Ni][PF $_6$ ] $_x$ <b>89</b>	3.054(1) (x = 2) 3.002(1) (x = 3)	nd	nd	nd	nd	114
[{ $\mu$ -bis(4-mercapto-3,3-dimethyl-2-thiabutyl)- <i>o</i> -xylene}NiCl $_2$ Fe] $_2$ <b>91</b>	3.0403(3)	3.6947(5)	3.6947(5)	3.6947(5)	nd	98
[{( $\mu$ -tris(ethylthiolato)amine)Fe(CO) $_3$ Ni}] <b>90</b>	2.6372(11)	nd	nd	nd	1933	115
[( $\mu$ -1,2-benzenedithiolate) $_3$ Fe(CO)Ni $_2$ (PMe $_3$ ) $_2$ ] <b>92</b>	2.596(1)	nd	nd	nd	1916	116
[( $\mu$ -1,2-benzenedithiolate) $_3$ Fe(CO)Ni $_2$ (PMe $_3$ ) $_2$ ][PF $_6$ ] <b>92</b> $^{+}$	2.582(2)	nd	nd	nd	1976	116

Scheme 7. Heterolytic Cleavage of H<sub>2</sub> by a Dinuclear {GeRu}-System 97 (Dep = 2,6-Diethylphenyl)Table 6. Vibrational Frequencies, *g* Values, and Fe–Fe Distances of the Redox States of the [FeFe]-Hydrogenases

redox state	<i>D. desulfuricans</i> (DdH)		<i>D. vulgaris</i> (CpI)	
	$\nu(\text{CO})$	$\nu(\text{CN})$	$\nu(\text{CO})$	$\nu(\text{CN})$
	<b>FTIR<sup>a</sup> (cm<sup>-1</sup>)</b>			
H <sub>ox</sub> <sup>air</sup>	1848, 1983, 2007	2087, 2106	nd	nd
H <sub>ox</sub>	1802, 1940, 1965	2079, 2093	1802, 1948, 1971	2072, 2086
H <sub>ox</sub> -CO	1810, 1963, 1971, 2016	2088, 2096	1810, 1971, 1974, 2017	2077, 2096
H <sub>red</sub>	1894, 1916, 1965	2040, 2079	nd	nd
	<b>EPR<sup>b</sup> (<i>g</i><sub>x</sub>, <i>g</i><sub>y</sub>, <i>g</i><sub>z</sub>)</b>			
H <sub>ox</sub>	2.10, 2.04, 2.00	2.10, 2.04, 2.00		
H <sub>ox</sub> -CO	2.06, 2.00, 2.00	nd		
	<b>Fe–Fe Distance<sup>c</sup> (Å)</b>			
H <sub>ox</sub> <sup>air</sup>	2.6	2.62		
H <sub>ox</sub> -CO	nd	2.60		

<sup>a</sup> Data from refs 149, 150. <sup>b</sup> Data from refs 149, 151, and 152. <sup>c</sup> Data from refs 134–136.

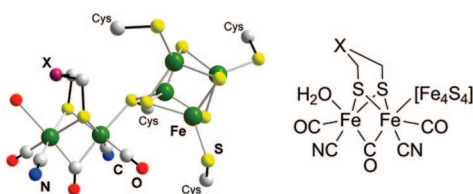
13). The {Fe<sub>4</sub>S<sub>4</sub>}-cluster is anchored to the protein by three cysteines from the backbone of the protein. The binuclear metal center is bridged by a dithiolate ligand with biologically unusual carbonyl and cyanide ligands completing the coordination sphere. Notably, when CO is added to the enzyme at high concentration and under turnover conditions, it results in a complete inhibition (H<sub>ox</sub>-CO state). The structure of CpI showed the terminal binding of CO on the distal iron of the H<sub>ox</sub>-CO form of the [FeFe]-hydrogenase, consistent with the putative role of this site as that at which dihydrogen evolution/uptake occurs.<sup>136</sup>

## 4.2.2. Nature of the Bridging Dithiolate

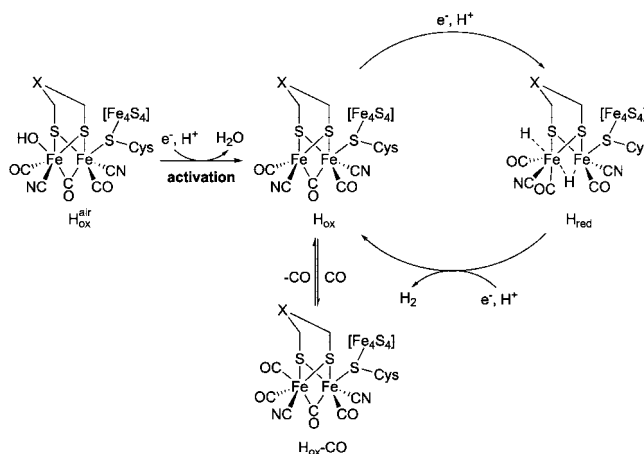
Of major contention related to the structure of the [FeFe]-hydrogenase is the nature of the apical group of the dithiolate ligand, X in Figure 13. Currently, it remains undecided experimentally as to whether X is CH<sub>2</sub>, NH, or O, although high resolution X-ray crystallographic data combined with density functional theory optimizations of the dithiolate ligand embedded in a 3.5–3.9 Å protein environment provided an “unbiased” approach to examining the most likely composition of the ligand.<sup>137</sup> Their study favored X = O. Undoubtedly, further spectroscopic studies including isotopic ENDOR and HYSCORE examinations of the resting H<sub>ox</sub> and CO-inhibited H<sub>ox</sub>-CO paramagnetic states of the enzyme will provide more detailed information in the near future.<sup>41</sup>

## 4.2.3. Terminal and Bridging CO

Spectroelectrochemical studies on the enzyme system and low-temperature FTIR/photolysis studies utilizing enzyme



**Figure 13.** X-ray structure and schematic representation of the active site of the [FeFe]-hydrogenase (X = CH<sub>2</sub>, NH, or O).

Scheme 8. Possible Catalytic Cycle for H<sub>2</sub> Evolution by [FeFe]-Hydrogenases<sup>a</sup>

<sup>a</sup> The postulated proton anchoring sites in H<sub>red</sub> are depicted in red (terminal on the distal iron atom) and in blue (bridging between the two iron atoms). Note, this is a minimal scheme; additional intermediates, for example, protonation at the bridgehead group X, are plausible.

preparations from both DdH and CpI have provided an understanding of the interconversion of bridging and terminal CO states of the enzyme (Table 6).<sup>138–142</sup> These studies have been reviewed comprehensively in the “Hydrogen” issue.<sup>42</sup>

In the H<sub>ox</sub> form of the enzyme, one CO occupies a bridging position. The addition of an electron to give H<sub>red</sub> results in a rearrangement to the all-terminal CO form. In H<sub>red</sub>, the formal oxidation states of the iron atom are Fe(I)–Fe(I), and this is the level at which a proton is thought to interact. The infrared stretching frequencies show a loss of bridging CO observed in H<sub>ox</sub><sup>air</sup> and H<sub>ox</sub>-CO. The increase in the electron density on the Fe(I)–Fe(I) system *vis-à-vis* the Fe(I)–Fe(II) systems is most clearly evident from the lowering of the two cyanide stretching frequencies. Addition of CO inhibits the enzyme generating the H<sub>ox</sub>-CO state, in which the open coordination site at the distal iron atom of H<sub>ox</sub> is occupied by the CO ligand.<sup>136</sup> Scheme 8 summarizes the bridging and terminal CO interconversion observed for the enzyme.

#### 4.2.4. The Oxidation State and Spin-Density in the EPR-Active Resting State ( $H_{ox}$ ) and Its CO-Inhibited Form ( $H_{ox}$ -CO)

In earlier spectroscopic work on the enzyme, it was argued by Nicolet et al. that the cubane cluster components of the H-cluster in the paramagnetic  $H_{ox}$  state, the  $H_{ox}$ -CO state, and the one-electron reduced state were at the  $1+$  level, i.e.  $\{Fe_4S_4\}^{1+}$ .<sup>135</sup> Later studies by Popescu and Munck and reevaluation of Mössbauer, EPR, and ENDOR data have led to the conclusion that in all of these states the cubane center remains at the EPR-silent  $2+$  level, i.e.  $\{Fe_4S_4\}^{2+}$ .<sup>143</sup> These assignments of the cubane oxidation state are now generally accepted.<sup>41</sup>

In the same comprehensive study of the electronic structure of the H-cluster, Popescu and Munck concluded that the subsite was best described as a mixed-valent Fe(II)–Fe(III) combination, although, in light of concurrent chemical studies, they noted that a mixed-valent Fe(II)–Fe(I) arrangement could not be excluded.<sup>143</sup> Cogent arguments by De Lacey et al. based upon isotopic  $^{13}CO$  labeling infrared studies of [FeFe]-hydrogenase from *Desulfovibrio desulfuricans*, together with spectroscopic and spectroelectrochemical studies of model systems (*vide infra*) and detailed DFT calculations by Hall and De Gioia and their co-workers, have led to the generally accepted conclusion that both the  $H_{ox}$  state and its  $H_{ox}$ -CO form were Fe(II)–Fe(I) systems.<sup>43,140,144,145</sup>

Popescu and Munck considered the distribution of spin-density in the paramagnetic  $H_{ox}$  state and the  $H_{ox}$ -CO form of the enzyme.<sup>143</sup> They concluded that in  $H_{ox}$  the unpaired spin-density is localized on one iron site of the subsite. The question arose as to whether this spin-density is on the proximal or distal iron. They note that the  $A$  value associated with the subsite changes from *ca.* 18 MHz on  $H_{ox}$  to 9.5 MHz in  $H_{ox}$ -CO, and they argued that the 50% reduction reflects delocalization of the unpaired spin over both of the two iron sites in  $H_{ox}$ -CO. This being the case, it was further suggested that the spin-density in  $H_{ox}$  is located on the iron atom distal to the cubane because the observed coupling with the cubane is rather weak, being mediated at long distance through the thiolate bridge, the diamagnetic proximal iron site, and the two sulfurs of the dithiolate ligand. The CO binding to the distal iron is argued to induce delocalization, and the attendant transfer of unpaired spins to the proximal iron would increase the exchange interaction between the cubane and the subsite.

The infrared studies on the enzyme and its CO-inhibited form by De Lacey et al., as discussed above, fit well with the unpaired spin-density on the di-iron subsite residing on the distal iron atom and its formal assignment as Fe(I).<sup>140</sup> The frequencies would not sensibly correlate with a distal Fe(III) center, although, in light of the delocalization argument, the binding would be distal at a  $\{FeFe\}^{3+}$  unit.

DFT calculations on the *entire* H-cluster by both the groups of Brunold and De Gioia and their respective collaborators have explored geometric, electronic, and magnetic properties.<sup>146,147</sup> Each of these studies have supported the earlier DFT and spectroscopic interpretation that the unpaired spin-density in the  $H_{ox}$  state is localized on the distal Fe center, whereas it is delocalized over the subsite component in the  $H_{ox}$ -CO form.

Silakov et al. have undertaken a comprehensive Q-band  $^{57}Fe$ -ENDOR and HYSCORE study of the electronic structure of the [FeFe]-hydrogenase from *Desulfovibrio desulfuricans*.<sup>148</sup> In contrast to the conclusions of Munck, they

suggested that for the  $H_{ox}$  state the unpaired spin is distributed almost *equally* over the two iron atoms of the subsite. In the  $H_{ox}$ -CO state, they argue that the unpaired spin is shifted toward the proximal iron. The weak, almost dipolar  $^{57}Fe$  hyperfine coupling attributed to the distal iron supports the view that the spin density is strongly localized on the proximal iron in the  $H_{ox}$ -CO state.

Thus, we were left with a concordant view from FTIR and DFT studies on subsite and H-cluster components, together with magnetic studies, that the di-iron unit is a mixed-valence Fe(I)–Fe(II) assembly. Where we now have disagreement is on whether it is the distal or proximal iron which bears the spin density in the  $H_{ox}$  form.

#### 4.2.5. Hydride

The direct spectroscopic detection of any form of iron-hydride, bridging or terminal, during turnover of [FeFe]-hydrogenase systems remains elusive. Various DFT calculations on subsite and entire H-cluster assemblies have been performed which include discussion of terminal and bridging hydrides.<sup>43,147,153</sup> Chemical precedence for terminal and bridging coordination modes at synthetic di-iron systems is rapidly developing and informing the biochemistry.<sup>16</sup>

### 4.3. Synthetic Models

#### 4.3.1. Overview

The number of di-iron dithiolate and related systems ascribed as models of structural and functional aspects of the active site of the [FeFe]-hydrogenase has grown exponentially since the first structures of the enzyme were reported some 10 years ago. In this overview, we wish to draw out some of the salient features which this chemistry has explored. Scheme 9 summarizes key areas of research on the synthetic systems, which ranges from electrocatalysis and solid state devices, through hydride and mixed-valent systems, to total synthesis of H-cluster structures.

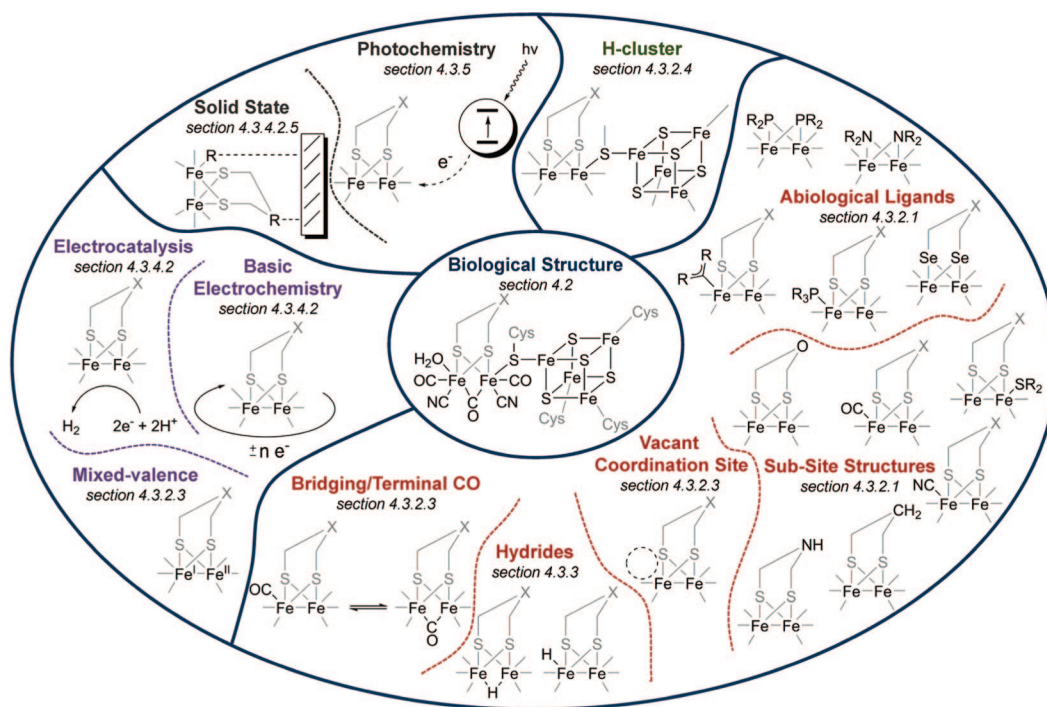
There has been tremendous progress on many fronts summarized in the boxes of Scheme 9. Of major significance have been advances in hydride chemistry of di-iron systems and the synthesis of stable mixed-valent di-iron units, notably by Darensbourg and Rauchfuss and their co-workers.

On the structural side, the cores of the di-iron units rarely match that of the enzyme subsite or H-cluster center. For example, considerable progress has been made in achieving stable mixed-valent sites with bridging CO. However, this chemistry has required much use of abiological phosphine or carbene substituted derivatives. It has been argued that such substitution provides electron density at the iron centers at least partially approaching that of  $CN^-$  ligation; nevertheless, it is perhaps disappointing that new cyanide complexes remain very much under represented.

On the functional side, the following are true:

- (i) Electrocatalysis rarely involves a core which matches that of the enzyme subsite; systems with a dicyanide motif are notably absent.
- (ii) Electrocatalytic systems generally cycle through the Fe(I)–Fe(0) level rather than the natural Fe(II)–Fe(I) level.
- (iii) No electrocatalytic di-iron system has been designed which oxidizes dihydrogen to protons.
- (iv) Electrocatalytic systems operate at potentials considerably negative of that for the reversible  $H^+/H_2$  couple and,

## Scheme 9



where measured, have poor electron transfer kinetics for proton reduction.

#### 4.3.2. Synthetic Subsite Structures

##### 4.3.2.1. The Enzyme Subsite: Di-iron Dithiolate Units.

In 1929, Reihlen et al. described the synthesis of  $[\text{Fe}_2(\text{CO})_6(\mu\text{-SEt})_2]$  (**98**, Figure 14), the X-ray structure of which was reported some 34 years later.<sup>154,155</sup> With the protein crystallographic structures of the  $[\text{FeFe}]$ -hydrogenase available in 1999, the striking resemblance between the subsite of the H-cluster and this type of molecule immediately became evident.<sup>134,135</sup> This chemistry and that developed by Hieber,<sup>156–159</sup> Seyferth,<sup>103,160–184</sup> Poilblanc,<sup>185–193</sup> and others<sup>194–220</sup> set the scene for the synthesis of a range of molecules possessing the  $\{2\text{Fe}_2\text{S}\}$ -core with a distorted tetrahedron butterfly arrangement, as found in the enzyme.

The first advance in the chemistry of these systems in the context of the enzyme was the demonstration in 1999 that two CO ligands of a propane dithiolate hexacarbonyl (**99**) could be replaced by cyanide, to give water-soluble dianions (**100**).<sup>221–223</sup> This was followed by the work of Rauchfuss and co-workers, which showed that the bridgehead  $\text{CH}_2$  group could be formally replaced by NH (**101**),<sup>224</sup> and this

has led to a chemistry which generally parallels that of the propane dithiolate system.<sup>225</sup> Rauchfuss, followed by Song and their respective co-workers, showed that oxygen bridged molecules were also accessible (**102**).<sup>224,226,227</sup> The structural metrics of the  $\text{CH}_2$ , NH, and O hexacarbonyl molecules are closely similar, and perturbations of infrared stretching frequencies are small. The bridging NH (or N-alkyl analogues) molecule can be protonated at the  $\text{sp}^2$  nitrogen atom (**102**, **103**); this modestly perturbs the IR spectrum but induces a considerable change for the redox potential of the system.<sup>224,225,228–244</sup> As discussed above, whether the natural system possesses  $\text{CH}_2$ , NH, or O bridgeheads is unresolved. Recently, syntheses leading to S-bridgehead molecules have also been reported.<sup>245–247</sup>

Following these earlier studies, there has been an immense amount of chemistry developed based on either modification of the bridgehead group or substitution of carbonyl ligands with a biological phosphine,<sup>225,227,237,240,243,248–273</sup> isocyanide,<sup>274–278</sup> N-heterocyclic carbene,<sup>279–288</sup> or nitrosyl ligands.<sup>267</sup> In addition, thiolsates have been replaced by selenide,<sup>110,242,289–292</sup> phosphide,<sup>293–295</sup> amide,<sup>296</sup> and peptide groups.<sup>297,298</sup> The number of modifications of the  $\{\text{Fe}_2\text{S}_2\}$ -core in the last 10 years has been staggering, encompassing more than 200 papers.

The thrust of this chemistry has in part been to confer additional functionality on the systems—for example, for attachment of photoactive groups—or to provide methods for anchoring subsites to electrode surfaces, polymers, or electropolymers (*vide infra*).

Another aspect of the approach is that it has provided materials with modified redox and electrocatalytic properties. However, of major importance is that it has enabled the synthesis both of stable, mixed-valent  $\text{Fe(I)}\text{--Fe(II)}$  systems and of structurally and spectroscopically characterizable hydride intermediates, which have not so far been accessible by studies of the dicyanide systems. This chemistry is discussed in more detail below.

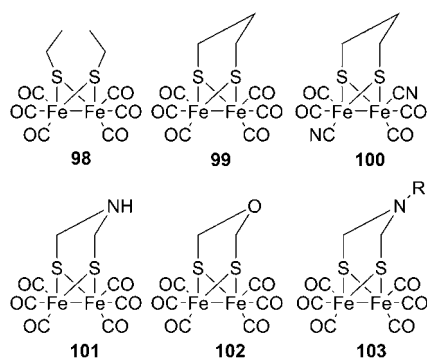
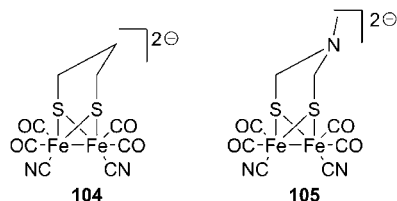


Figure 14.  $\{2\text{Fe}_2\text{S}\}$ -model complexes.



**Figure 15.**  $\{2\text{Fe}2\text{S}(\text{CN})_2\}$ -model complexes.

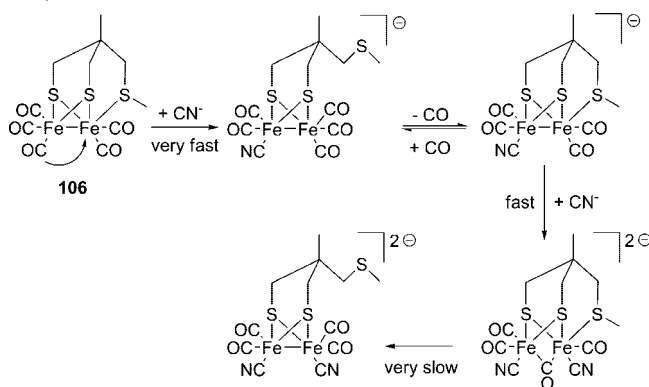
The subsite of the H-cluster can be viewed as a  $\{2\text{Fe}3\text{S}\}$ -assembly rather than a  $\{2\text{Fe}2\text{S}\}$ -unit. There has been considerable work on the synthesis of dithiolate thioether systems which possess the  $\{2\text{Fe}3\text{S}\}$ -arrangement as found in the enzyme.<sup>144,145,299–302</sup> In these systems, the thioether is one of the pendant groups in the tripodal ligand and has allowed a large range of functionality to be introduced at the di-iron core. The thioether ligand is hemilabile and can be reversibly displaced by CO.<sup>299</sup> There is a close correspondence between the energetics of this process and that for inversion at sulfur as observed by NMR.<sup>301</sup> As would be expected, substitution of the thioether with more electron withdrawing R groups displaces the equilibrium toward CO binding.<sup>299</sup> Substitution of the pentacarbonyl dithiolate thioether systems by cyanide has been studied in detail mechanistically and by theoretical methods as described below.<sup>145</sup> Hu et al. have shown that a nonpendant thioether ligand can bind to a simple propanedithiolate di-iron subsite model.<sup>303,304</sup> A dithiolate thioether system with a bridgehead nitrogen unit has been reported.<sup>231</sup> Here it can be mentioned that tripodal dithiolate ligands with appended amine, pyridine, and other groups have been synthesized.<sup>231,299</sup> These molecules have been investigated in the context of both hydride formation and generation of CO binding sites (*vide infra*).

**4.3.2.2. The Enzyme Subsite: Cyanide Ligation.** As discussed above, a major goal of earlier synthetic work was the synthesis of cyanide substituted di-iron units, and  $\{2\text{Fe}2\text{S}\}$ -systems of the type shown in Figure 15 with bridgehead  $\text{CH}_2$  (**104**) and NMe (**105**) were rapidly achieved.<sup>221–223,230</sup> Two studies addressed the mechanism of formation of the dicyanide species **104**,<sup>253,305</sup> and interestingly, Rauchfuss and co-workers showed that substitution of cyanide to give the dicyanide in a single “pot” proceeds faster than addition of cyanide to the monocyanide intermediate.<sup>253</sup> This suggested that the faster second cyanation step might be accounted for by the attack of cyanide on a bridged CO intermediate.<sup>253</sup>

$\{2\text{Fe}3\text{S}\}$ -systems of the type described above also react with cyanide to give dicyanide intermediates. It is been shown unequivocally that a bridging carbonyl dicyanide intermediate is formed which is moderately stable at 0 °C.<sup>144,145</sup> Importantly, it remains the first and only example of subsite structure which possesses both two cyanide ligands and a bridging CO unsupported by phosphine or other abiological ligands. The detailed mechanism of substitution of CO by cyanide in this system has been elucidated, and the overall pathway is shown by Scheme 10.<sup>145</sup>

A DFT study of the reactants, transition states, intermediates, and products of this substitution pathway has been undertaken by Zampella et al.<sup>306</sup> The study showed that the formation of bridging carbonyl transition states is explicitly involved in the intimate mechanism of dicyanation. Importantly, the computed and experimental infrared frequencies of structurally characterized  $\{2\text{Fe}3\text{S}\}$ -species and those of the bridging carbonyl intermediates were found to be in excellent agreement. Subsequently, independent work by

**Scheme 10.** Cyanide Substitution Pathway of the  $\{2\text{Fe}3\text{S}\}$ -Subsite as Deduced from Stopped-Flow FTIR Kinetic Analysis and Labeling Studies (Adapted from Ref 145)



Zilberman et al. provided further theoretical support for the proposed structure of the bridged-CO intermediate.<sup>307</sup>

As discussed above, the resting states of the dicyanide ligated subsite in the enzyme are a mixed-valence  $\text{Fe(I)}-\text{Fe(II)}$  system. Studies of the gas phase and solution phase of oxidation of  $\text{Fe(I)}$  cyanide complexes together with an abiologically substituted subsite will be discussed below.

**4.3.2.3. Bridging CO, Diferrous, and Mixed-Valent Oxidation States: Modeling  $\text{H}_{\text{ox}}$  and  $\text{H}_{\text{ox}}-\text{CO}$  States.** The key features of the resting state structure of  $\text{H}_{\text{ox}}$  and  $\text{H}_{\text{ox}}-\text{CO}$  are a mixed-valent  $\{2\text{Fe}3\text{S}\}$ -system in which a carbon monoxide ligand bridges the two iron atoms which are coordinated by CO and CN (Figure 13). The first experimental evidence that this type of structure could be supported by a  $\text{Fe(I)}-\text{Fe(II)}$  unit was reported by Razavet et al.<sup>302</sup> This work showed that chemical or electrochemical oxidation of a di-iron dicyanide precursor which possesses a pdt ligand produces a transient species in which a CO occupies a bridging position. The FTIR spectra showed bands which were close in wavenumber to those observed in the enzyme system. This lent support to the argument that the subsite in the enzyme was  $\text{Fe(I)}-\text{Fe(II)}$  rather than the  $\text{Fe(III)}-\text{Fe(II)}$  system as discussed in section 4.2.4. DFT calculations related to this species and  $\text{Fe(II)}-\text{Fe(II)}$  analogues have been reported by Zilberman and co-workers, and the authors suggest that higher wavenumber bands in the experimental spectrum could be associated with  $\text{Fe(II)}-\text{Fe(II)}$ .<sup>307</sup>

The mixed-valent bridging carbonyl species is unstable, and much effort has been devoted to the synthesis of stable di-iron units with the bridging CO motif. This was first achieved in diferrous systems.<sup>252,276,277</sup> Enhancement of the electron density at the iron atoms with isocyanide ligands, or a combination of phosphine and cyanide ligands, has allowed the isolation of complexes such as those illustrated in Figure 16. Other diferrous systems in which terminal and bridging CO interchange with terminal and bridging hydride have been uncovered and will be discussed in more detail in the section on hydrides (see section 4.3.3).<sup>262</sup>

The synthesis of mixed-valent  $\text{Fe(I)}-\text{Fe(II)}$  systems has been achieved using more subtle combinations of monophosphine, diphosphine, and carbene units and by the choice of noncoordinating solvents,  $\text{CH}_2\text{Cl}_2$  in oxidation procedures.<sup>248,249,251,283,286,308</sup> Importantly, these mixed-valence species have the “rotated state” in which an iron atom exhibits an essentially square pyramidal coordination with a coordination vacancy as observed in the  $\text{H}_{\text{ox}}$  form of the enzyme. Representative examples are shown in Figure 17.

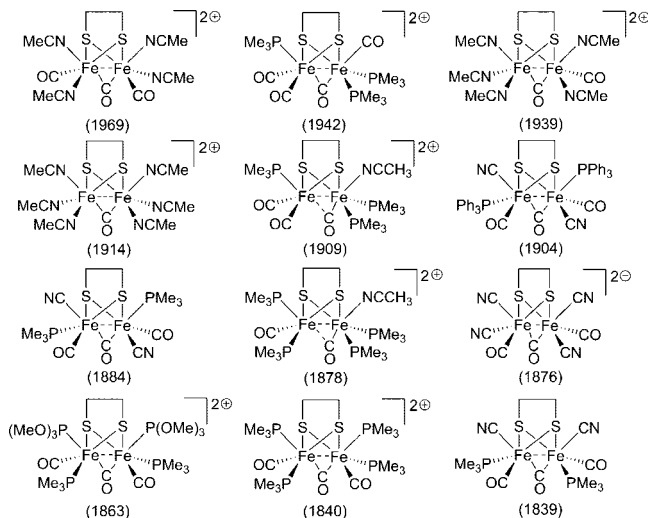


**Figure 16.** Diferrous bridging carbonyl species (bridging  $\nu(\text{CO})$  values are underneath in parentheses,  $\text{cm}^{-1}$ ).

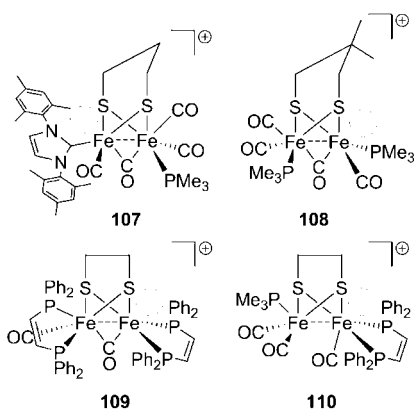
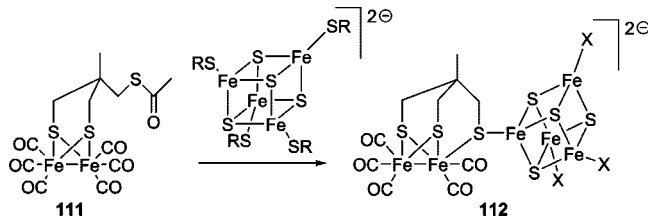


**Figure 17.** Mixed-valent Fe(I)–Fe(II) systems.

**Scheme 11.** Synthesis of  $[\text{Fe}_4\text{S}_4(\text{SR})_x(\text{Fe}_2(\text{CO})_5(\text{CH}_3\text{C}(\text{CH}_2\text{S})_3)_{4-x})]^{2-}$  ( $x = 0, 1, 2$ , and  $3$ ) **112**



It is notable that steric bulk appears to play an important part in the stabilization of these systems, presumably by protecting the five-coordinate site. For example, a sterically crowded carbene ligand has allowed the isolation and crystallographic characterization of the mixed-valent species **107**.<sup>286</sup> Similarly, a bis(diphenylphosphinoethene) ligand has allowed the isolation of a bent semibridging CO complex (**110**).<sup>251</sup> As with the enzyme system, the coordinatively unsaturated species reversibly bind CO<sup>251</sup> and can undergo selective CO-labeling.<sup>287</sup>

**4.3.2.4. H-Cluster Models.** The subsite in the enzyme is linked to a cubane unit by a  $\mu$ -thiolate bridge. Song and co-workers showed that thiophenyl was capable of bridging a subsite structure and the iron atom of a  $\eta^5$ -cyclopentadienyl dicarbonyl iron unit.<sup>227</sup> Beyond a  $\text{Fe}(\mu\text{-SR})\text{Fe}$  linkage, relevance to the H-cluster is somewhat tenuous.

Syntheses of  $\{2\text{Fe}3\text{S}\}$ -cubane cluster assemblies have been achieved via the synthesis of a thioacetyl activated subsite

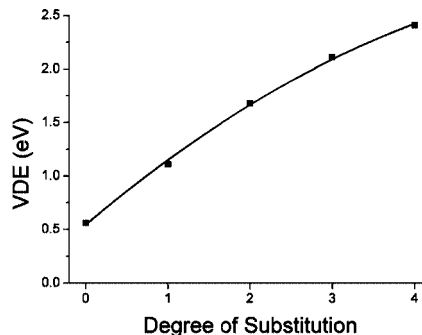


**Figure 18.** Gas-phase photoelectron spectroscopy of isolated  $[\text{Fe}_4\text{S}_4(\text{SEt})_x(\text{Fe}_2(\text{CO})_5(\text{CH}_3\text{C}(\text{CH}_2\text{S})_3)_{4-x})]^{2-}$  (**112**) (unpublished results, Wang L. S., Washington State University, USA).

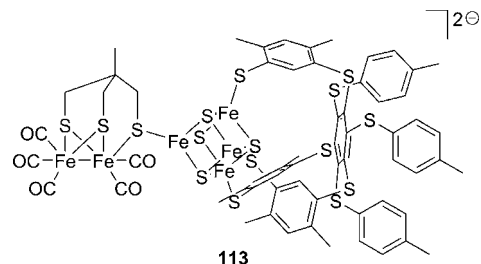


**Figure 19.** H-cluster model **113**.

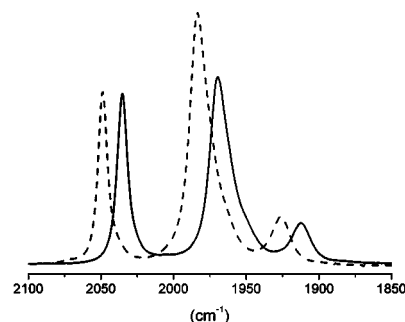


**Figure 20.** IR spectra (acetone nitrile solution) of the  $\{\text{Fe}_6\text{S}_{10}\}$ -core model of the H-cluster **113** (plain) and the simple dithiolate methylthioether complex **106** (dash).

**111.**<sup>300</sup> The complex **111** reacts with phenyl and alkyl thiolate cubanes to give one to four substituted products (Scheme 11).

Of clear significance to the biological system is the interplay between the cubane center and the subsite in the H-cluster and synthetic analogues. “Magnetic bottle” trapping of the mono- to tetrasubstituted anions in a gas phase has allowed measurements of ionization energies and of fragmentation patterns of each of the species.<sup>300</sup> Figure 18 shows the progression of the electron detachment energy as a cubane unit is progressively substituted by the di-iron subsites. This electronic effect is mirrored in the electrochemistry of the subsite substituted clusters, where it is observed that a fully substituted cubane reduces to the trianion at  $-0.59$  V vs SCE whereas the tetraethyl thiolate parent cubane reduces at  $-1.09$  V.<sup>300</sup>

Wrapping up a cubane with a tripodal thiolate ligand<sup>309</sup> has allowed the selective isolation and characterization of a cubane system **113** singly substituted with a di-iron subsite (Figure 19).<sup>300</sup> This has the essential  $\{\text{Fe}_6\text{S}_{10}\}$ -core of the H-cluster. The intrinsic electron withdrawing nature of the pentacarbonyl unit *vis-à-vis* an ethyl thiolate is clearly evident. Figure 20 shows the FTIR of a simple dithiolate methylthioether complex and where the methyl group is

**Table 7. Bridging Hydride Bond Distances (Å) in Crystallographically Characterized Complexes and <sup>1</sup>H NMR  $\mu$ -H Chemical Shifts (ppm)**

compound	$\mu$ -H ( $\delta$ , ppm)	$d_{\text{Fe}(\mu\text{-H})\text{Fe}}$ (Å)	$d_{\text{Fe-Fe}}$ (Å) <sup>a</sup>	ref
[Fe <sub>2</sub> ( $\mu$ -H)( $\mu$ -SMe) <sub>2</sub> (PPhMe <sub>2</sub> ) <sub>2</sub> (CO) <sub>4</sub> ] <sup>+</sup> ( <b>114</b> )	nd	2.595	2.518	189
[Fe <sub>2</sub> ( $\mu$ -H)( $\mu$ -pdt)(PMe <sub>3</sub> ) <sub>2</sub> (CO) <sub>4</sub> ] <sup>+</sup> ( <b>115</b> )	−15.2 <sup>b</sup>	2.578(1)	2.555(2)	255
[Fe <sub>2</sub> ( $\mu$ -H)( $\mu$ -pdt)(PMe <sub>3</sub> ) <sub>2</sub> (CN)(CO) <sub>4</sub> ] <sup>+</sup> ( <b>116</b> )	−17.1 <sup>c</sup>	2.5830(8)	2.5365(11)	256
[Fe <sub>2</sub> ( $\mu$ -H)( $\mu$ -SEt)(PMe <sub>3</sub> ) <sub>2</sub> (CO) <sub>4</sub> ] <sup>+</sup> ( <b>117</b> )	−15.8 <sup>d</sup>	2.5708(4)	2.5097(7)	258
[Fe <sub>2</sub> ( $\mu$ -H)( $\mu$ -edt)(PMe <sub>3</sub> ) <sub>2</sub> (CO) <sub>4</sub> ] <sup>+</sup> ( <b>118</b> )	−17.3 <sup>d</sup>	2.5742(13)	2.5159(6)	258
[Fe <sub>2</sub> ( $\mu$ -H)( $\mu$ -pdt)(PPhMe <sub>2</sub> ) <sub>2</sub> (CO) <sub>4</sub> ] <sup>+</sup> ( <b>119</b> )	−15.0 <sup>d</sup>	2.5859(7)	nd	258
[Fe <sub>2</sub> ( $\mu$ -H)( $\mu$ -SEtPPh <sub>2</sub> ) <sub>2</sub> (CO) <sub>4</sub> ] <sup>+</sup> ( <b>120</b> )	−16.9 <sup>d</sup>	2.580(1)	2.5621(7)	258
[Fe <sub>2</sub> ( $\mu$ -H)( $\mu$ -pdt)(NCMe)(PMe <sub>3</sub> ) <sub>2</sub> (CO) <sub>4</sub> ] <sup>+</sup> ( <b>121</b> )	nd	2.606(2)	nd	311
[Fe <sub>2</sub> ( $\mu$ -H)( $\mu$ -edt)(PMe <sub>3</sub> ) <sub>4</sub> (CO) <sub>2</sub> ] <sup>+</sup> ( <b>122</b> )	−20.6 <sup>c</sup>	2.6102(8)	nd	262
[Fe <sub>2</sub> ( $\mu$ -H)( $\mu$ -adt- <i>p</i> -Ph-NO <sub>2</sub> )(PMe <sub>3</sub> ) <sub>2</sub> (CO) <sub>4</sub> ] <sup>+</sup> ( <b>123</b> )	−15.0 <sup>c</sup>	2.5879(8)	2.5671(10)	237
[Fe <sub>2</sub> ( $\mu$ -H)( $\mu$ -pdt)(Cy <sub>2</sub> PCH <sub>2</sub> PCy <sub>2</sub> )(CO) <sub>4</sub> ] <sup>+</sup> ( <b>124</b> )	−14.5 <sup>d</sup>	2.531(2)	2.5259(10)	312
[Fe <sub>2</sub> ( $\mu$ -H)( $\mu$ -pdt)(dppe)(CO) <sub>4</sub> ] <sup>+</sup> ( <b>125</b> )	−14.1 <sup>c</sup>	2.581(5)	2.547(7)	313
[Fe <sub>2</sub> ( $\mu$ -H)( $\mu$ -pdt)(ImeCH <sub>2</sub> Ime)(CO) <sub>4</sub> ] <sup>+</sup> ( <b>126</b> )	−12.2 <sup>d</sup>	2.6054(6)	2.5774(6)	284
[Fe <sub>2</sub> ( $\mu$ -H)( $\mu$ -pdt-CO <sub>2</sub> Me)(PMe <sub>3</sub> ) <sub>2</sub> (CO) <sub>4</sub> ] <sup>+</sup> ( <b>127</b> )	−15.2 <sup>b</sup>	2.6017(9)	nd	314
[Fe <sub>2</sub> ( $\mu$ -H)( $\mu$ -adt-CH <sub>2</sub> - <i>o</i> -Ph-Br)(PMe <sub>3</sub> ) <sub>2</sub> (CO) <sub>4</sub> ] <sup>+</sup> ( <b>128</b> )	−15.3 <sup>c</sup>	2.5948(8)	2.5870(5)	315

<sup>a</sup> Metal–metal bond distance in the nonprotonated parent compound. <sup>b</sup> In *d*<sub>6</sub>-acetone. <sup>c</sup> In CD<sub>3</sub>CN. <sup>d</sup> In CD<sub>2</sub>Cl<sub>2</sub>. <sup>e</sup> Ime = 1,3-dimethylimidazol-2-ylidene.

formally substituted by a {Fe<sub>4</sub>S<sub>4</sub>}-cubane. Unsurprisingly, the cubane unit is a better donor of charge into the subsite unit than is a methyl group.

X-ray absorption spectroscopic measurements and DFT calculations suggest that the hydrogenase H-cluster model is best described as an electronically inseparable {6Fe}-cluster due to extensive delocalization of frontier molecular orbitals of the iron centers, sulfide, and the noninnocent dithiolate ligands.<sup>310</sup> The difference contour plot between the electron densities of the entire **113** model and the sum of the separate {4Fe}- and {2Fe}-subsites in the {6Fe}-model geometry illustrates the extent of electronic structural changes upon formation of the Fe<sub>p</sub>( $\mu$ -S)(Fe<sub>cubane</sub>) bond. The shape of the most dominant lobes clearly suggests that the delocalization involves the Fe<sub>p</sub> 3d<sub>z<sup>2</sup></sub> orbitals in addition to thiolate C–S  $\sigma$  and CO  $\pi$  orbitals.

#### 4.3.3. Protonation and Hydride Binding at Subsite Molecules

Implicit in the chemistry of [FeFe]-hydrogenase is the formation of hydride intermediates during turnover in either direction, oxidation of H<sub>2</sub>, or proton reduction. The “rotated” square pyramidal site of H<sub>ox</sub> is generally accepted as the site at which a proton or H<sub>2</sub> interacts. However, there are other sites available at which proton or dihydrogen could interact: the metal–metal bond, the apical bridgehead NH, or cyanide ligands. In synthetic complexes, all three of these types of interaction have been recognized, singly or in combination.

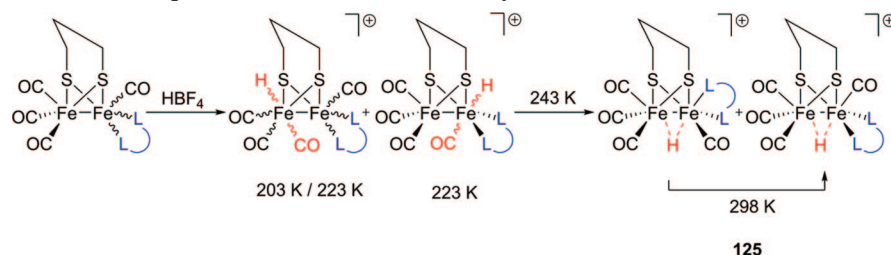
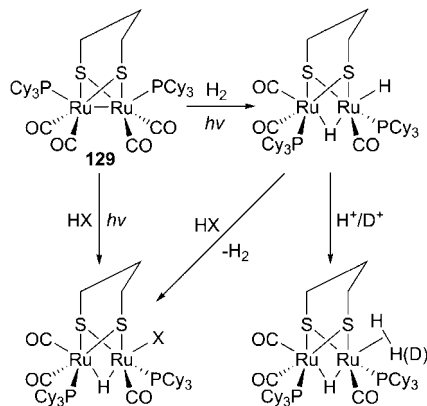
The first hydride complexes of di-iron dithiolate systems (**114**) were discovered in 1976, well before their potential significance in hydrogenase chemistry was recognized.<sup>185</sup> All these systems possessed hydride in a bridging motif.<sup>189,191</sup> Crystallographically characterized bridging hydride species are listed in Table 7. It can be seen from these data that, in the bridging hydrides, the metal–metal bond distance is greater than that in the parent, unprotonated compound. This increase can be relatively large (*ca.* 0.7 Å) (**114**) or rather small (0.07 Å) (**128**).

We will first consider how changes in substitution at a simple pdt-carbonyl core influence the site(s) of protonation and the stability of products. Most protonation studies have been synthetically driven and protonation conditions chosen to effect reaction and allow spectroscopic and or crystallographic characterization; definition of acid strengths in nonaqueous conditions has been largely qualitative. The

parent hexacarbonyl **99** does not protonate measurably with nominally strong acids such as HBF<sub>4</sub> in polar solvents. Formally replacing one CO group by cyanide to give a monoanion substantially increases the electron density and allows protonation, but the preferred site is the cyanide ligand.<sup>254</sup> In contrast, introducing a neutral thioether ligand increases electron density sufficiently for protonation at the metal–metal bond to occur.<sup>299</sup> Substitution of two cyanide ligands gives a highly reactive complex. Protonation is thought to lead to the formation of bridging hydride species to give unstable products which release substoichiometric amounts of H<sub>2</sub>.<sup>254,255</sup> In contrast to the dicyanide, the trimethylphosphine monocyanide species stoichiometrically protonates at the metal–metal bond and at higher acid concentrations also protonates at the cyanide ligand.<sup>254</sup> Work in the 1970s by Poilblanc established that the symmetric di(trimethylphosphine) complex and related systems cleanly protonate at the metal–metal bond to give  $\mu$ -hydride species (**114**).<sup>185,191</sup> The di(trimethylphosphine) species **121** has been recently characterized crystallographically and shown to catalyze H/D exchange from H<sub>2</sub>/D<sub>2</sub> mixtures under photolysis conditions.<sup>311</sup>

An interesting situation arises when bis(diphosphines) are used to generate an asymmetrically substituted complex (**125**). Thus, Schollhammer and co-workers have shown, by NMR studies, that protonation at low-temperature leads to the initial formation of a kinetic product which transforms to the thermodynamically stable  $\mu$ -hydride at higher temperatures (Scheme 12).<sup>313</sup> Later, Rauchfuss and co-workers showed that placing two bis(diphenylphosphinoethene) ligands around the di-iron pdt core also led to the initial formation of a terminal hydride at a rotated bridging carbonyl site which isomerizes very slowly to the more thermodynamically stable  $\mu$ -hydride.<sup>250</sup>

Thus, we can see that the nature of the protonation is substantially controlled by the nature of the substituent on the di-iron dithiolate core. The puzzling feature is perhaps why terminal protonation is kinetically favored. We might expect that the bent metal–metal bond would present little kinetic barrier to direct protonation in any of the complexes, so why is a rearranged bridging carbonyl species preferentially formed? A possible explanation is that there is steric restriction to the approach of an acid to the metal–metal bond provided by the sterically demanding diphosphine ligands. Another explanation may lie with a very fast terminal

**Scheme 12. Protonation at Low-Temperature: Kinetic and Thermodynamic Products****Scheme 13. Ruthenium Analogues of the Di-iron System: Bridging Hydride/Terminal Hydride Product**

CO/bridging CO pre-equilibrium which exposes a square pyramidal site for protonation.

Two systems in which a protonated group and a bridging hydride are present in the same molecule have been recently reported.<sup>316,317</sup> Notably, in the crystal structure of Sun and co-workers, the H...H distance is rather long (nearly 4 Å),<sup>316</sup> and in the related system by Talarmin and co-workers, it is argued that the pendant amino group can function as a proton relay.<sup>317</sup>

Whereas there are numerous bridging hydride species and it is known that some, if not all, of these are capable of participating in electrocatalytic proton reduction (*vide infra*), their relevance to the hydrogenase systems may be tangential. As is clear in the resting state, protonation at the bent Fe–Fe bond is blocked by bridging CO. Indeed, this may be a key role for bridging CO involvement in the catalytic cycle, guiding the protonation to a terminal position.

Terminal hydride systems are rare, but in the past few years, many significant advances have been made. A system described by Rauchfuss and co-workers was based upon ruthenium analogues of the di-iron system in which tricyclohexylphosphine was substituted.<sup>318</sup> Complex **129** can be photolyzed under H<sub>2</sub> to give a bridging hydride/terminal hydride product, the crystal structure of which has been determined.<sup>318</sup> The terminal hydride species reacts with HX to release hydrogen, or if it is protonated with a noncoordinating acid, the formation of a dihydrogen species is observed (Scheme 13). The corresponding chemistry of dicyanide species is limited to the formation of unstable bridging hydride species.

**4.3.4. Electron Transfer and Electrocatalysis**

**4.3.4.1. General Considerations.** Understanding the electron transfer chemistry of synthetic models is fundamental to the design of new systems for electrocatalytic hydrogen production/uptake. Moreover, defining redox states of synthetic systems and how these relate to electrocatalytic

processes contributes toward a better understanding of the biological system. The generation of a mixed-valent Fe(I)–Fe(II) dicyanide species possessing a bridging CO and an {2Fe3S}-core has been discussed in section 4.3.2.3. Electrochemical and chemical generation of stable Fe(I)–Fe(II) mixed-valent species with phosphine coligands has also been discussed above. The following sections largely focus on the reduction chemistry of the di-iron systems, although some discussion of transient oxidation potential is also provided.

The general screening of synthetic systems in terms of their oxidation and their reduction potentials, together with their ability to electrocatalyze proton reduction, has invariably utilized cyclic voltammetry methods. Evans and co-workers have discussed general aspects of catalytic efficiencies in terms of standard potentials for the reduction of substrate acids (HA) and experimental limitations of voltammetric methods when significant uncatalyzed reduction of HA occurs.<sup>319</sup>

Detailed electrochemical studies of the electron transfer chemistry of the model systems are rather few in number, although cursory studies abound. Early studies of the electrochemistry of the di-iron dithiolate and sulfido hexacarbonyl system include that of Darchen and co-workers, who showed that electron transfer catalysis of CO-substitution was possible following reduction<sup>320</sup> and work relating to the chemically reversible interconversion of iron–sulfur clusters and the “butterfly” {Fe<sub>2</sub>(CO)<sub>6</sub>S<sub>2</sub>}-dianions.<sup>321</sup> The first examples of electrocatalytic proton reduction by di-iron dithiolate systems were those reported by Rauchfuss and co-workers in 2001.<sup>254</sup> Subsequently, there have been some 100 papers to date which report such electrocatalysis.

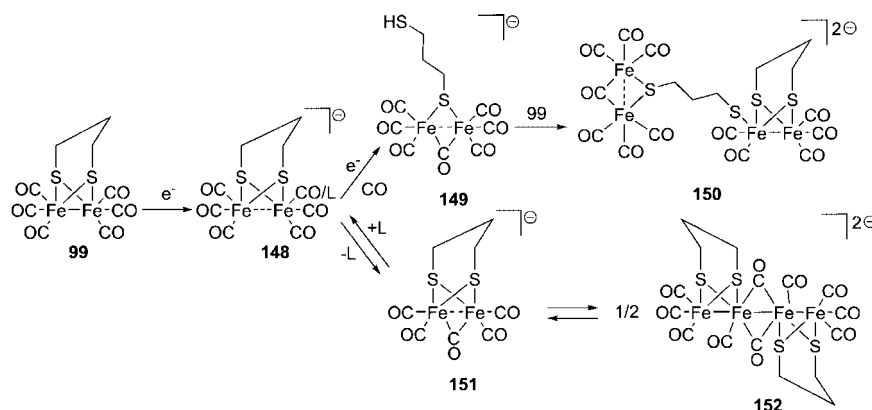
Table 8 summarizes reduction potential data for a range of di-iron subsite units which essentially cover all of the types of structures examined. As expected, replacing the CO on the propane-dithiolate (**99**) or the azadithiolate unit makes the reduction potential of the system more negative (Table 8, entries **8**, **14**, **20–24**). However, increasing the donor ability of the ligands can favor protonation at the metal–metal bond, and this can shift the reduction potentials to more positive values (Table 8, entries **10**, **11**). Similarly, protonation on a coligand, as in the case of the azadithiolate or cyanide, can also lead to easier reduction (Table 8, entries **9**, **11**, **18**, **19**). Where there is further scope for modeling studies is in the possibility of molecular systems designed to enhance sequential proton coupled electron transfer (PCET) or concerted proton–electron transfer (CPET).<sup>324,325</sup>

**4.3.4.2. Electron Transfer and Electrocatalytic Studies of Di-iron Subsite Analogues.** **4.3.4.2.1. Hexacarbonyl Dithiolate Systems.** Several detailed electrochemical studies on dithiolate hexacarbonyl systems have been undertaken. A key question concerning the primary electron transfer chemistry of these systems is whether or not this step is a reversible one-electron or two-electron step. A detailed spectroelectrochemical study of [Fe<sub>2</sub>(CO)<sub>6</sub>(μ-pdt)] (**99**) showed

**Table 8. Primary Redox Potentials of {2Fe2S}-Assemblies**

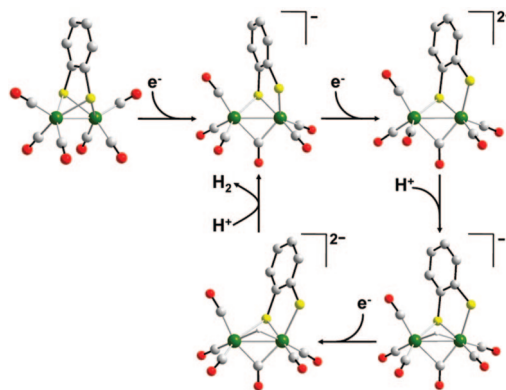
entry	compound	$E_{pc}^a$	ref
1	[Fe <sub>2</sub> (μ-pdt)(CO) <sub>6</sub> ] ( <b>99</b> )	−1.17	320
2	[Fe <sub>2</sub> (μ-adt)(CO) <sub>6</sub> ] ( <b>101</b> )	−1.09	225
3	[Fe <sub>2</sub> (μ-SCH <sub>2</sub> OCH <sub>2</sub> S)(CO) <sub>6</sub> ] ( <b>102</b> )	−1.10	226
4	[Fe <sub>2</sub> (μ-SCH <sub>2</sub> SCH <sub>2</sub> S)(CO) <sub>6</sub> ] ( <b>130</b> )	−1.02	247
5	[Fe <sub>2</sub> (μ-bdt)(CO) <sub>6</sub> ] ( <b>131</b> )	−0.83	263
6	[Fe <sub>2</sub> (μ-SCH <sub>2</sub> (NPh)CH <sub>2</sub> S)(CO) <sub>6</sub> ] ( <b>132</b> )	−1.08	242
7	[Fe <sub>2</sub> (μ-SeCH <sub>2</sub> (NPh)CH <sub>2</sub> Se)(CO) <sub>6</sub> ] ( <b>133</b> )	−1.09	242
8	[Fe <sub>2</sub> (μ-SCH <sub>2</sub> (NBz)CH <sub>2</sub> S)(PMe <sub>3</sub> ) <sub>2</sub> (CO) <sub>4</sub> ] ( <b>134</b> )	−1.69	322
9	[Fe <sub>2</sub> (μ-SCH <sub>2</sub> (NHBz)CH <sub>2</sub> S)(PMe <sub>3</sub> ) <sub>2</sub> (CO) <sub>4</sub> ] <sup>+</sup> ( <b>135</b> )	−1.06	322
10	[Fe <sub>2</sub> (μ-H)(μ-SCH <sub>2</sub> (NBz)CH <sub>2</sub> S)(PMe <sub>3</sub> ) <sub>2</sub> (CO) <sub>4</sub> ] <sup>+</sup> ( <b>136</b> )	−0.61	322
11	[Fe <sub>2</sub> (μ-H)(μ-SCH <sub>2</sub> (NHBz)CH <sub>2</sub> S)(PMe <sub>3</sub> ) <sub>2</sub> (CO) <sub>4</sub> ] <sup>2+</sup> ( <b>137</b> )	−0.51	322
12	[Fe <sub>2</sub> (μ-pdt)(CN)(CO) <sub>5</sub> ] <sup>−</sup> ( <b>138</b> )	−1.35	253
13	[Fe <sub>2</sub> (μ-pdt)(CN) <sub>2</sub> (CO) <sub>4</sub> ] <sup>2−</sup> ( <b>100</b> )	−1.84	253
14	[Fe <sub>2</sub> (CH <sub>3</sub> C(μ-CH <sub>2</sub> S) <sub>2</sub> CH <sub>2</sub> SCH <sub>3</sub> )(CO) <sub>5</sub> ] ( <b>106</b> )	−1.31	301
15	[Fe <sub>2</sub> (CH <sub>3</sub> C(μ-CH <sub>2</sub> S) <sub>2</sub> CH <sub>2</sub> SCH <sub>3</sub> )(CN)(CO) <sub>4</sub> ] <sup>−</sup> ( <b>139</b> )	−1.88	301
16	[Fe <sub>2</sub> (CH <sub>3</sub> C(μ-CH <sub>2</sub> S) <sub>2</sub> CH <sub>2</sub> SCH <sub>3</sub> )(CN) <sub>2</sub> (μ-CO)(CO) <sub>2</sub> ] <sup>2−</sup> ( <b>140</b> )	≤ −2.45	301
17	[Fe <sub>2</sub> (CH <sub>3</sub> C(μ-CH <sub>2</sub> S) <sub>2</sub> CH <sub>2</sub> S{Fe <sub>4</sub> S <sub>4</sub> LS <sub>3</sub> })(CO) <sub>5</sub> ] <sup>b</sup> ( <b>113</b> )	−0.89	300
18	[Fe <sub>2</sub> (μ-H)(μ-pdt)(CN)(PMe <sub>3</sub> )(CO) <sub>4</sub> ] ( <b>141</b> )	−1.14	254
19	[Fe <sub>2</sub> (μ-H)(μ-pdt)(CNH)(PMe <sub>3</sub> )(CO) <sub>4</sub> ] <sup>+</sup> ( <b>142</b> )	−0.99	254
20	[Fe <sub>2</sub> (μ-pdt)(P(OEt) <sub>3</sub> )(CO) <sub>5</sub> ] ( <b>143</b> )	−1.32	261
21	[Fe <sub>2</sub> (μ-pdt)(P(OEt) <sub>3</sub> ) <sub>2</sub> (CO) <sub>4</sub> ] ( <b>144</b> )	−1.68	261
22	[Fe <sub>2</sub> (μ-pdt)(Ime)(CO) <sub>5</sub> ] <sup>c</sup> ( <b>145</b> )	−1.57	280
23	[Fe <sub>2</sub> (μ-pdt)(Ime) <sub>2</sub> (CO) <sub>4</sub> ] <sup>c</sup> ( <b>146</b> )	−1.98	280
24	[Ru <sub>2</sub> (μ-pdt)(CO) <sub>6</sub> ] ( <b>147</b> )	−1.55	323

<sup>a</sup> In CH<sub>3</sub>CN, vs SCE. <sup>b</sup> LS<sub>3</sub> = 1,3,5-tris(4,6-dimethyl-3-mercaptophenylthio)-2,4,6-tris(*p*-tolylthio)benzene. <sup>c</sup> Ime = 1,3-dimethylimidazol-2-ylidene.

**Scheme 14**

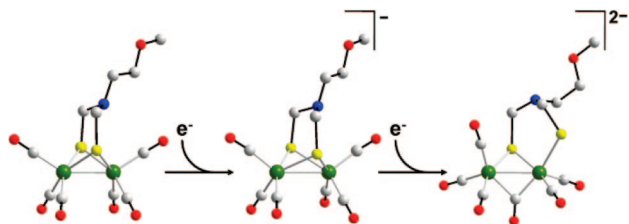
that the primary step involved a reversible single electron transfer to give an unstable 19-electron anion (**148**).<sup>326</sup> Two pathways for the decay of this 19-electron species in the absence of a proton source were identified. One pathway involved further electron transfer and rearrangement to give a bridging carbonyl species from which a thiolate ligand had decoordinated (**149**) (Scheme 14). This species was sufficiently nucleophilic to attack the parent compound to give a tetranuclear product (**150**), which was identified by EXAFS in an electrochemical flow cell experiment. This was independently confirmed by chemical synthesis and X-ray crystal structure analysis by Heinekey and co-workers.<sup>327</sup> The second pathway involves reversible ligand-loss from the 19-electron anion **148** to give the CO-bridge species **151** followed by formation of a symmetrical CO-bridged dimer **152**. Support for this formulation comes from the isolation and characterization of a tetranuclear ethanedithiolate analogue which was synthesized by chemical reduction.<sup>328</sup>

Benzenedithiolate (bdt) systems have been investigated, and it has been suggested that the nature of the bridging dithiolate group can have a significant influence on the primary electron transfer pathway. The reduction of [Fe<sub>2</sub>(CO)<sub>6</sub>(μ-bdt)] (**131**) appears to be chemically reversible, but it actually consists of two overlapping one-electron transfers, with the

**Scheme 15. DFT Calculated Structures and Mechanism of the Catalytic Reduction of Protons to H<sub>2</sub> by [Fe<sub>2</sub>(CO)<sub>6</sub>(μ-bdt)] (**131**) (Adapted from Ref 263)**

second transfer slightly more favorable than the first.<sup>329</sup> This system has been further investigated by Evans and co-workers.<sup>263</sup> They suggest that single electron transfer results in a μ<sub>2</sub> to μ<sub>1</sub> rearrangement of a bridging thiolate (Scheme 15), and this structural rearrangement could explain the slow electron transfer kinetics reported earlier.<sup>329</sup>

**Scheme 16. DFT Calculated Structures and Proposed Reduction Mechanism of  $[\text{Fe}_2(\text{CO})_6(\mu\text{-adt-CH}_2\text{CH}_2\text{OCH}_3)]$  153**



The  $[\text{Fe}_2(\text{CO})_6(\mu\text{-pdt})]$  (**99**) and the  $[\text{Fe}_2(\text{CO})_6(\mu\text{-bdt})]$  (**131**) systems are capable of electrocatalyzing proton reduction. The electrochemistry of the pdt complex has been modeled on the basis of two successive electron/protonation steps, with hydrogen evolution from a dihydride intermediate being rate determining. Evans and co-workers have investigated the electrocatalytic generation of dihydrogen using **131** in the presence of several carboxylic acids and phenols.<sup>263</sup> The catalytic reduction producing dihydrogen using these weak acids occurs at the overpotentials  $-0.4$  to  $-0.7$  V. The mechanism of this process and structures for the intermediates have been discerned by electrochemical and computational analysis. It is argued that the catalyst is the  $\mu_1\mu_2$  dithiolate monoanion, formed by single electron reduction of the starting material, and an ECEC mechanism occurs as shown by Scheme 15. In the bdt case (**131**), rather than decooordination of a  $\mu$ -sulfur ligand as is observed with the pdt system (**99**),  $\mu_2$  to  $\mu_1$  rearrangement of a bridging thiolate is suggested.

The primary electron transfer chemistry of the azapropanedithiolate (adt) **153** system is summarized in Scheme 16.<sup>330</sup> A single reversible electron transfer is followed by a second electron transfer which involves structural rearrangement to give a species in which a  $\mu_2$  to  $\mu_1$  rearrangement of a bridging thiolate has taken place. Catalysis of proton reduction by the adt systems is influenced by protonation at the bridgehead amino group.<sup>331</sup> This raises the reduction potential to a more positive value *vis-à-vis* the pdt analogue **99**, and with weak acids this leads to a catalytically slow hydrogen evolution pathway. With stronger acids, another mechanism is suggested to be operative involving a *third* protonation, and the authors also suggested *two* terminal hydrides which combined to eliminate  $\text{H}_2$ . As far as we can gather, there is no DFT calculation to support these conjectures.

As discussed above, the electron transfer chemistry of the pdt systems can yield a variety of products, specifically, moieties in which the  $\{\text{Fe}_2(\mu\text{-pdt})\}$ -framework has undergone gross structural change, such as decooordination of dithiolate. These species may well engage in hydrogen evolution chemistry, but it has been pointed out that this is of doubtful relevance to the natural system, and mechanistic implication based upon hydrogen evolution from weak acids should be viewed with some caution.<sup>332</sup>

**4.3.4.2.2. Substituted Di-iron Dithiolate Systems.** The most biologically pertinent substitution of the hexacarbonyl systems is replacement of two carbon monoxides by two cyanide ligands. These and related  $\text{Fe(I)}\text{--Fe(I)}$  compounds react with acid to release some dihydrogen, possibly *via* the formation of bridging hydride intermediates.<sup>255</sup> However, no stable products have been isolated.

As discussed in section 4.3.2.1, trimethylphosphine or other phosphine substitutions can enhance the electron

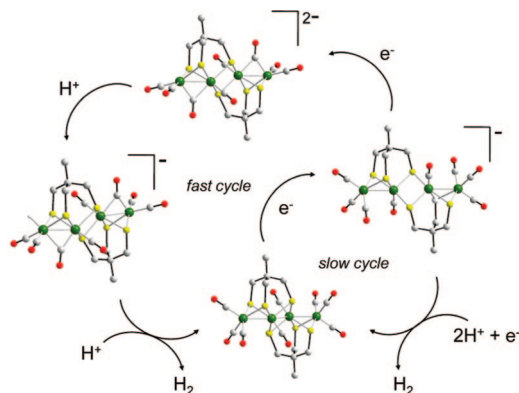
richness of the di-iron center assembly. This inevitably results in the complexes becoming harder to reduce, as is summarized by Table 8 (entries **20**, **21**). However, in acid medium, the complexes can be protonated at the metal–metal bond, and this offers a pathway for reduction at more moderate potentials (Table 8, entries **8–11**). The kinetics of these reductions may, however, be rather sluggish. Substitution of adt complexes offers the possibility of protonation at both the bridgehead dithiolate and the metal–metal bond, making the reduction potential more accessible.

One of the first di-iron dithiolate complexes to be examined for electrocatalysis of hydrogen evolution was a monocyanide monotriphenylphosphine species.<sup>254</sup> In this case, protonation at cyanide was thought to contribute to the lowering of the reduction potential.

The general effect of successive substitution of CO for  $\text{CN}^-$  is that  $E_p^{\text{ox}}$  and  $E_p^{\text{red}}$  are shifted to more negative values, by around 400–500 mV for both  $\{2\text{Fe}2\text{S}\}$ - and  $\{2\text{Fe}3\text{S}\}$ -assemblies (Table 8, entries **1**, **12–16**).<sup>301</sup> This is most likely to be a predominantly electrostatic effect which shifts the HOMO–LUMO redox manifold in tandem, as the negative charge density on the complex is increased. Substitution of CO by  $\text{CN}^-$  at closed shell mononuclear centers usually invokes a shift of around 1 V, as quantified by the ligand parameter  $P_L$ , which is 0.0 and 1.00 V for CO and  $\text{CN}^-$ , respectively.<sup>333,334</sup> This smaller shift in the binuclear systems is consistent with delocalization of charge over the two iron centers, and this is supported by the general shift in all the FTIR terminal carbonyl frequencies to lower values upon substitution of CO by  $\text{CN}^-$ . Formally replacing neutral CO by a neutral pendant thioether ligand leads to a relatively small negative shift in  $E_p^{\text{red}}$  of *ca.* 100 mV (Table 8, entries **1**, **14**) but a considerable negative shift in  $E_p^{\text{ox}}$  of nearly 500 mV.<sup>301</sup> Thus, the LUMO, which is almost certainly an Fe–Fe antibonding ( $\sigma^*$ ) orbital, can have little CO or thioether ligand character. In contrast, replacing the strong  $\pi$ -acid CO by the thioether ligand significantly perturbs the HOMO, which is evidently very sensitive to the Fe atom environment.

In two particularly significant recent papers, Rauchfuss and co-workers have provided insight into the comparative chemistry of terminal and bridging hydride species.<sup>250,335</sup> First, they have shown that a dithiolate bridgehead O or NH can significantly influence the kinetics of formation/deprotonation of a terminal hydride and have argued that in the natural system either type of function could act as a proton relay kinetically favoring terminal hydride versus bridging hydride formation.<sup>335</sup> Second, they have shown that a terminal hydride species at a “symmetrical” electron-rich tetraphosphine substituted system reduces at a potential some 200 mV positive of its companion bridging hydride isomer.<sup>250</sup> The terminal hydride species is stable below  $-20$  °C; the bridging hydride species is the thermodynamically species stable at room temperature.

**4.3.4.2.3. How Relevant Is the Electrochemistry of the Di-iron Systems and Their Derivatives to Biological and the Design of Competent Synthetic Electrocatalysis?** The *raison d'être* for synthesis of the di-iron subsite and H-cluster model systems is, of course, to provide an opportunity to study their electron-transfer chemistry and catalytic performance, both to inform an understanding of the natural system and to pathfind new hydrogen evolution/uptake catalysts which might provide alternatives to platinum. Virtually every di-iron system synthesized since 1999 has been studied by electrochemical methods. Most often this has involved

**Scheme 17. DFT Calculated Structures and Mechanism of Proton Reduction by **154****<sup>334</sup>

cursory examination by cyclic voltammetry and often claims with respect to redox states and intermediates which at best might be described as speculative. There are however an increasing series of more definitive studies detailing fundamental mechanisms.

However, if one was to summarize the intrinsic limitation of all studies which purport to model the electron-transfer chemistry of the natural system, it is that they are virtually all operating at the wrong oxidation states. The natural system performs catalysis of proton reduction at the Fe(I)–Fe(II)/Fe(I)–Fe(I) level with limited exceptions; all the model systems operate at best at the Fe(I)–Fe(I)/Fe(I)–Fe(0) level.

If we stand back and look at the natural system and compare it with the various studies of the di-iron system at the Fe(I)–Fe(I) level, it can be argued that electron-transfer to a hexacarbonyl or phosphine derivative enhances the electron density on the molecule, favoring protonation in the same way that the cyanide ligands enhance the electron density in the natural system. Thus, cyanide allows both protonation at higher oxidation levels and turnover at higher oxidation states. It is in this area, most likely enhanced with development in supramolecular and/or matrix chemistry, that we should expect to see advances. A clear failure of the synthetic di-iron systems is their inability to oxidize dihydrogen to protons, and this is of course related to their operation at potentials substantially removed from thermodynamic reversibility.

**4.3.4.2.4. Electrocatalysis by Higher Oxidation State Iron Assemblies.** A mixed-valence {Fe(I)–Fe(II)–Fe(II)–Fe(I)}-hexathiolate carbonyl assembly **154**, in which two dithiolate tetracarbonyl di-iron centers with a “butterfly” configuration of the {2Fe3S}-cores are fused by two bridging thiolates which form a central planar {2Fe2S}-unit, has been synthesized.<sup>336</sup> This molecule was found to be kinetically extremely efficient in electrocatalysis of hydrogen evolution. The mechanistic basis of this efficiency has been ascribed to rearrangement following two electron transfer, which leads to a terminal CO/bridging CO rearrangement which allows the exposure of a square pyramidal site at which the proton can rapidly bind, the so-called “rotated-state”.<sup>337</sup> Detailed spectroelectrochemical and DFT calculations have indicated a mechanistic pathway as outlined in Scheme 17.<sup>338</sup> Whereas the reversible protonation of the second metal site is possible but will be a mechanistically redundant reaction, the large driving force for H<sub>2</sub> evolution with rearrangement to the thermodynamically stable parent molecule most likely accounts for the fast kinetics. The rate constant for the formation of dihydrogen, the rate limiting step, is estimated

to be >2000 s<sup>−1</sup>, which compares with *ca.* 6000 s<sup>−1</sup> for the enzyme system.<sup>131</sup> Notably, catalysis by the Fe(I)–Fe(I) core of [Fe<sub>2</sub>(CO)<sub>6</sub>(μ-pdt)] (**99**) is merely 5 s<sup>−1</sup>.<sup>326</sup>

Notably, this is the first synthetic system in which electrocatalysis takes place at redox levels [Fe(I)–Fe(II)/Fe(I)–Fe(I)] and net charge levels [1<sup>−</sup>/2<sup>−</sup>] pertinent to the enzyme, and which, moreover, also involves switching between terminal and bridging CO states during turnover. This system, however, operates at a potential removed from the thermodynamic equilibrium of the H<sup>+</sup>/H<sub>2</sub> couple.

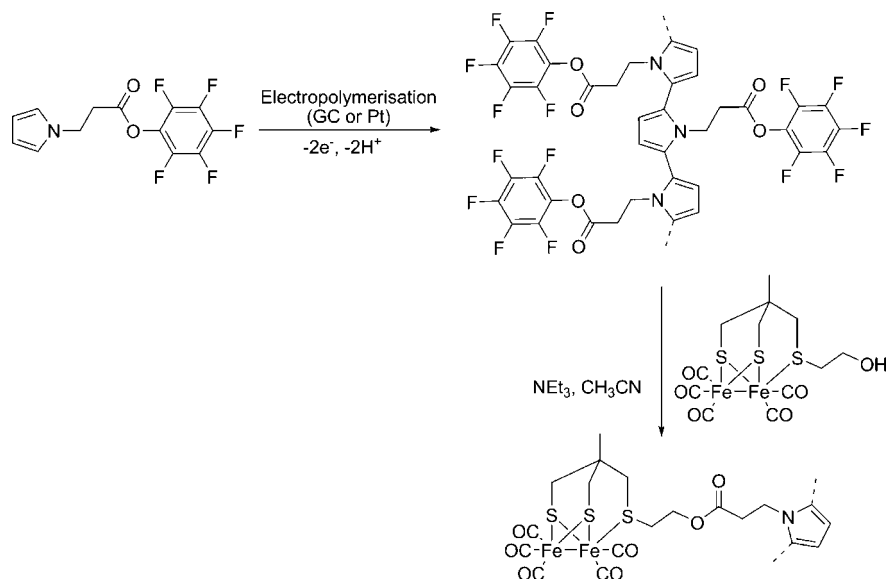
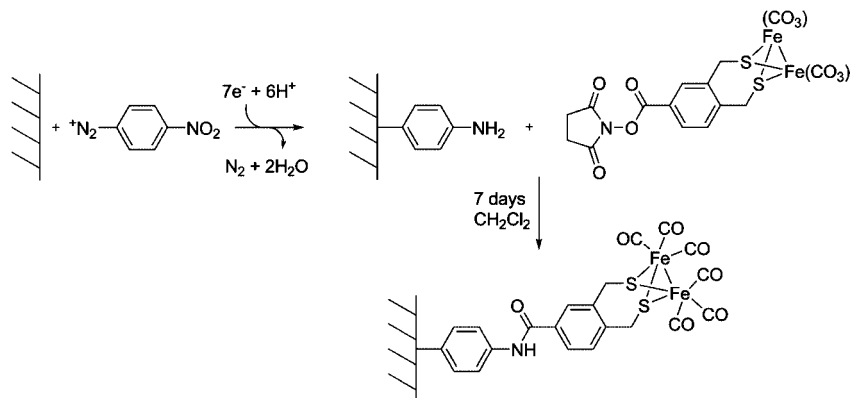
**4.3.4.2.5. Functionalized Electrodes, Solid State Materials, and Confinement in Peptides.** Anchoring organic and organometallic systems to electrodes goes back a long way.<sup>339</sup> Indeed, the first example of covalent binding of a redox active system to an electrode was reported some 30 years ago, whereby silanization of an antimony–tin-oxide surface allowed ligation of iron–sulfur cluster moieties.<sup>340</sup> Later it was shown that iron–sulfur cluster analogues of the electron-transfer centers in the {Fe<sub>4</sub>S<sub>4</sub>}-ferredoxin redox proteins can be built into poly(pyrroles) and that such arrays sustain fast charge propagation through an electrode-bound polymer film.<sup>341</sup>

Incorporating synthetic analogues of the catalytic machinery of iron-only hydrogenase within an electropolymer presents a greater challenge, but one which might afford new electrode materials for electrocatalysis of dihydrogen uptake/evolution. This is particularly attractive if catalysis can be matched to the conducting regime of the supporting polymer or if fast electron-transfer relays are coinorporated. Some first steps in this direction have been reported with the assembly of solid-state materials with structures related to the subsite of iron-only hydrogenase confined within a poly(pyrrole) framework (Scheme 18). In this system, which does not possess an intrinsic electron transfer relay, proton reduction was reported to be sluggish. Functionalization of carbon surfaces using the diazo methodology of Savéant<sup>342</sup> has also been reported (Scheme 19).<sup>343</sup> This system is however unstable under acidic turnover conditions, probably because of hydrolysis of the amide bonds.

A very wide range of -NH<sub>2</sub>, -OH, pyridinium, iodo, and aromatic functionalities have been introduced onto {2Fe2S}- and {2Fe3S}-cores with demonstrable and potential utility for surface and polymer modification.<sup>299,314</sup>

### 4.3.5. Photocatalysis of Hydrogen Evolution Using Sacrificial Electron-Donors

The solar generation of dihydrogen by water splitting utilizing inexpensive catalysts is a grand challenge.<sup>11,344–346</sup> Various studies in which a photosensitizer present in solution or linked to a subsite moiety have been undertaken with the aim of producing molecular hydrogen photochemically. Sun, Song, and their respective co-workers have prepared several assemblies where the {Fe<sub>2</sub>S<sub>2</sub>}-core is covalently linked to a ruthenium tris-bipyridine (**155**, **156**, and **157**),<sup>232,234,347,348</sup> a rhenium bipyridine complex (**158**),<sup>349</sup> or a metal-free porphyrin photosensitizer (**159**)<sup>350</sup> (Figure 21). Some noncovalently bounded zinc porphyrins have also been synthesized with an azadithiolate ligand bridging the hexacarbonyl di-iron center (**160** and **161**).<sup>241,351</sup> Of these photosystems, the first to demonstrably produce dihydrogen did not employ the linking of the photosensitizer to the di-iron unit.<sup>352</sup> The system employed [Ru(bpy)<sub>3</sub>]<sup>2+</sup> as a photosensitizer, which was reductively quenched by a thiocarbamate, to generate the highly reducing ruthenium monocation. This species in

**Scheme 18. Active Ester Functionalized Poly(pyrroles) for Covalent Binding of {2Fe3S}-Assemblies into Electropolymeric Materials on Glassy Carbon (GC) or Platinum****Scheme 19. Two-Step Procedure for Monolayer Grafting a Di-iron Complex on a Glassy Carbon Surface**

turn reduced a synthetic di-iron subsite, leading to the electrocatalytic evolution of hydrogen.

Subsequently, a supramolecular system (**161**) has been reported for visible light-driven hydrogen generation.<sup>241</sup> In this system it has been argued that the unproductive charge recombination common to the covalently linked supramolecular systems is circumvented by detachment of the pyridine linker ligand from the Zn chromophore following excitation and electron transfer. Nevertheless, a low turnover number is observed in a 2 h photolysis (0.16 based on the di-iron complex and 16 based on the photosensitizer). Another system prepared by the same group showed that a three-component catalyst composed of a bridging azadithiolate di-iron complex, a ruthenium tris-bipyridine photosensitizer, and a sacrificial electron donor (ascorbic acid) (Scheme 20) can produce molecular hydrogen with higher turnover numbers in a 3 h photolysis (4.3 based on the di-iron complex and 86 based on the photosensitizer).<sup>353</sup> These three systems have some promise and provide a basic strategy for further improvement.

## 5. Concluding Remarks

Over the last five or so years, there has been very substantial progress in chemical modeling of the [FeFe]-hydrogenase system, most notably in the area of structural analogues, mixed valence states, and the elucidation of

hydride chemistry, where the works of Darensbourg, Rauchfuss, Schollhammer, Pickett, and their colleagues have made decisive impacts.<sup>251,300,308,313</sup> We are still missing a complete picture of both structure and how the [FeFe]-hydrogenases work: in particular, is there a bridging NH dithiolate? If so, does it have a role in heterogeneous formation or splitting of  $H_2$ ? Is molecular hydrogen ligated to Fe at any stage during turnover? Do bridging hydride intermediates have a role? Here we might expect further chemical studies of model systems in combination with advanced spectroscopic studies on the natural system, such as those coming out of the Mulheim Max Planck Institut, to provide clarity on structure/function.<sup>346</sup>

Where we need to be somewhat circumspect with respect to achievements in the chemistry of the [FeFe]-hydrogenase area is the absence of functional models which can drive  $H_2/2H^+ + 2e^-$  interconversion reversibly at low overpotentials, noting indeed the absence of any model [FeFe]-system which electrocatalyses the oxidation of  $H_2$ . This is an area critical to designing systems of potential technological relevance for replacing platinum in fuel/producer cells and where we might hope greater advances to be made in the not too distant future.

[NiFe]-hydrogenase chemistry has received rather less research effort. On the structural side, advances in assembling a primary sulfur coordination environment of Ni linking by

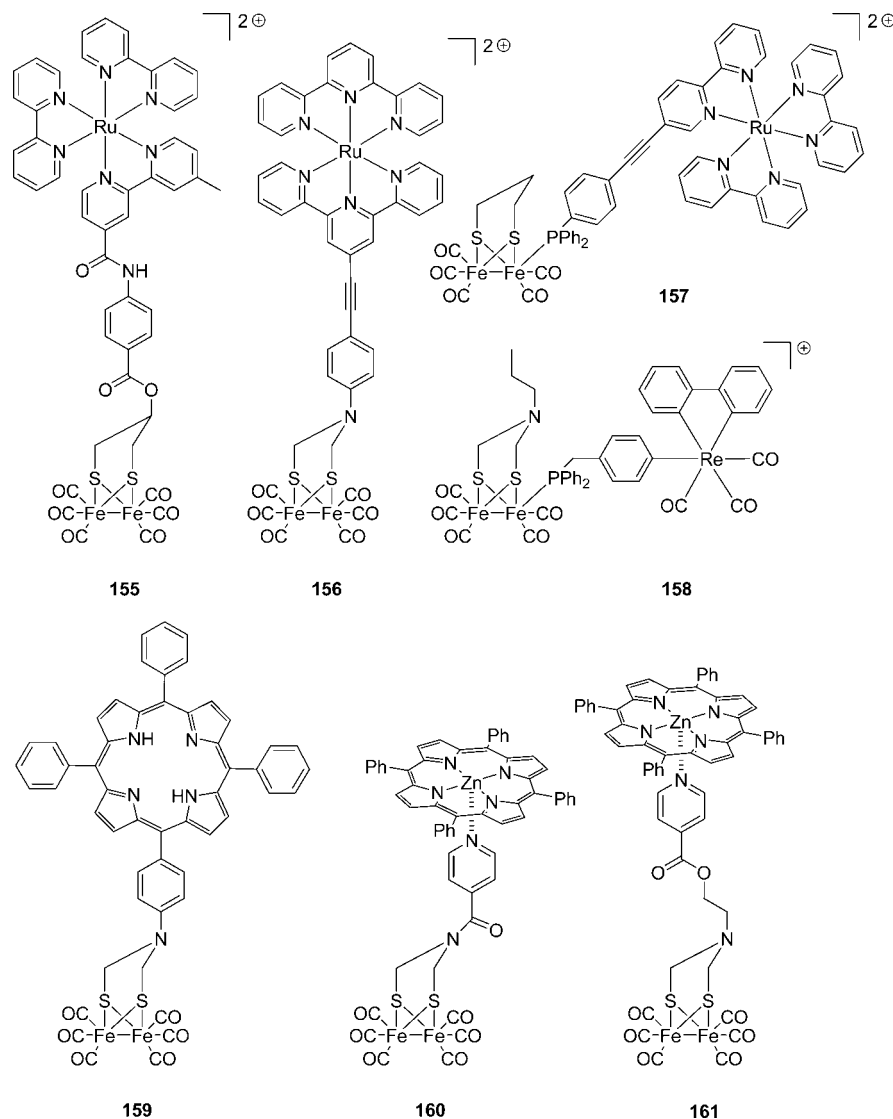
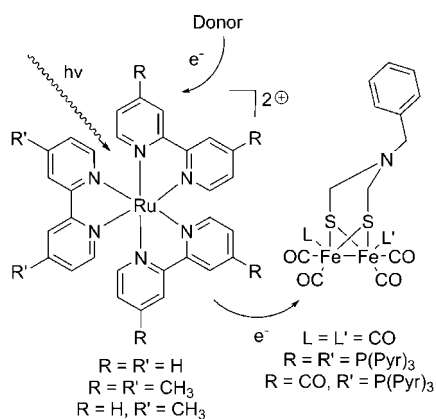


**Figure 21.** Di-iron centers coupled with photosensitizers.

**Scheme 20**



thiolate bridges to the Fe have been made, notably by Tatsumi and co-workers:<sup>101</sup> the challenge remains to incorporate the  $\{Fe(CN)_2(CO)\}$ -motif. On the functional side, some of the most interesting chemistry has come from somewhat abiological systems, most notably the [NiRu]-systems of Ogo,<sup>129</sup> the intriguing [GeRu]-system of Tatsumi<sup>130</sup> and the delightful Ni-diphosphine hydride chemistry of the DuBois.<sup>117,119,122</sup>

Chemistry related to the [Fe]-hydrogenase system is still in its infancy, but model chemistry is beginning to contribute some clarity with respect to oxidation state.<sup>33</sup> Again, we can expect more spectroscopic and X-ray crystallographic structural data on the enzyme system which will hopefully unshroud the coordination geometry of the active site. Undoubtedly, there will be major advances in the structural and functional analogue chemistry of this fascinating “cluster-free” hydrogenase over the next two or three years.

Solar generation of dihydrogen from water remains a world class problem; thus, the anchoring of electrocatalysts based on di-iron subsites to photosensitizers is receiving some attention.<sup>241,353</sup> Arguably, this is the less challenging half-reaction of water splitting, since efficient water oxidation to dioxygen *via* molecular catalysts rather than Pt is nontrivial. Nevertheless, there is the prospect of major advances in efficiency of electrocatalysts for reduction as analogue (and not so analogue) hydrogenase chemistry advances which should impute into the design of tandem water splitting solar devices.

## 6. Abbreviations

bme-daco  
bmes

bis(mercaptoethyl)-1,5-diazacyclooctane  
bis(mercaptoethylene)sulfide

bmps	bis(mercaptophenyl)sulfide
DFT	density functional theory
dppe	1,2-bis(diphenylphosphino)ethane
dppp	1,3-bis(diphenylphosphino)propane
ENDOR	electron nuclear double resonance
EPR	electron paramagnetic resonance
EXAFS	extended X-ray absorption fine structure
FTIR	Fourier-transform infrared
Hmd	H <sub>2</sub> -forming methylenetetrahydromethanopterin
IMe	1,3-dimethylimidazol-2-ylidene
HYSCORE	hyperfine sublevel correlation spectroscopy
nd	not determined
NHE	normal hydrogen electrode
NRVS	nuclear resonance vibrational spectroscopy
pd	1,3-propanedithiolate
SCE	saturated calomel electrode
tmtu	tetramethylthiourea
tptp	tris(3-phenyl-2-thiophenyl)phosphine
tsalen	N,N'-ethylenebis(thiosalicylideneiminatio)

## 7. References

- Darensbourg, M. Y.; Lyon, E. J.; Smece, J. J. *Coord. Chem. Rev.* **2000**, *206*, 533.
- King, R. B.; Bitterwolf, T. E. *Coord. Chem. Rev.* **2000**, *206*, 563.
- Marr, A. C.; Spencer, D. J. E.; Schroder, M. *Coord. Chem. Rev.* **2001**, *219*, 1055.
- Darensbourg, M. Y.; Lyon, E. J.; Zhao, X.; Georgakaki, I. P. *Proc. Natl. Acad. Sci. U. S. A.* **2003**, *100*, 3683.
- Evans, D. J.; Pickett, C. J. *Chem. Soc. Rev.* **2003**, *32*, 268.
- Best, S. P. *Coord. Chem. Rev.* **2005**, *249*, 1536.
- Bouwman, E.; Reedijk, J. *Coord. Chem. Rev.* **2005**, *249*, 1555.
- Capon, J. F.; Gloaguen, F.; Schollhammer, P.; Talarmin, J. *Coord. Chem. Rev.* **2005**, *249*, 1664.
- Liu, X. M.; Ibrahim, S. K.; Tard, C.; Pickett, C. J. *Coord. Chem. Rev.* **2005**, *249*, 1641.
- Song, L. C. *Acc. Chem. Res.* **2005**, *38*, 21.
- Sun, L. C.; Akermarck, B.; Ott, S. *Coord. Chem. Rev.* **2005**, *249*, 1653.
- Canaguier, S.; Artero, V.; Fontecave, M. *Dalton Trans.* **2008**, 315.
- Capon, J. F.; Gloaguen, F.; Pétilion, F.; Schollhammer, P.; Talarmin, J. C. R. *Chimie* **2008**, *11*, 842.
- Chiou, T. W.; Liaw, W. F. C. R. *Chimie* **2008**, *11*, 818.
- Capon, J. F.; Gloaguen, F.; Petillon, F. Y.; Schollhammer, P.; Talarmin, J. *Eur. J. Inorg. Chem.* **2008**, 4671.
- Gloaguen, F.; Rauchfuss, T. B. *Chem. Soc. Rev.* **2009**, *38*, 100.
- Winter, M.; Brodd, R. J. *Chem. Rev.* **2004**, *104*, 4245.
- Borup, R.; Meyers, J.; Pivovar, B.; Kim, Y. S.; Mukundan, R.; Garland, N.; Myers, D.; Wilson, M.; Garzon, F.; Wood, D.; Zelenay, P.; More, K.; Stroh, K.; Zawodzinski, T.; Boncella, J.; McGrath, J. E.; Inaba, M.; Miyatake, K.; Hori, M.; Ota, K.; Ogumi, Z.; Miyata, S.; Nishikata, A.; Siroama, Z.; Uchimoto, Y.; Yasuda, K.; Kimijima, K. I.; Iwashita, N. *Chem. Rev.* **2007**, *107*, 3904.
- Shima, S.; Thauer, R. K. *Chem. Rec.* **2007**, *7*, 37.
- Zirngibl, C.; Dongen, W.; Schworer, B.; Bunau, R.; Richter, M.; Klein, A.; Thauer, R. K. *Eur. J. Biochem.* **1992**, *208*, 511.
- Zirngibl, C.; Hedderich, R.; Thauer, R. K. *FEBS Lett.* **1990**, *261*, 112.
- Shima, S.; Pilak, O.; Vogt, S.; Schick, M.; Stagni, M. S.; Meyer-Klaucke, W.; Warkentin, E.; Thauer, R. K.; Ermler, U. *Science* **2008**, *321*, 572.
- Shima, S.; Lyon, E. J.; Thauer, R. K.; Mienert, B.; Bill, E. *J. Am. Chem. Soc.* **2005**, *127*, 10430.
- Rawson, J. M.; Winpenny, R. E. P. *Coord. Chem. Rev.* **1995**, *139*, 313.
- Lyon, E. J.; Shima, S.; Boecher, R.; Thauer, R. K.; Grevels, F. W.; Bill, E.; Roseboom, W.; Albracht, S. P. J. *J. Am. Chem. Soc.* **2004**, *126*, 14239.
- Korbas, M.; Vogt, S.; Meyer-Klaucke, W.; Bill, E.; Lyon, E. J.; Thauer, R. K.; Shima, S. *J. Biol. Chem.* **2006**, *281*, 30804.
- Kubas, G. J. *Chem. Rev.* **2007**, *107*, 4152.
- Fairhurst, S. A.; Henderson, R. A.; Hughes, D. L.; Ibrahim, S. K.; Pickett, C. J. *J. Chem. Soc., Chem. Commun.* **1995**, 1569.
- Vogt, S.; Lyon, E. J.; Shima, S.; Thauer, R. K. *J. Biol. Inorg. Chem.* **2008**, *13*, 97.
- Kure, B.; Matsumoto, T.; Ichikawa, K.; Fukuzumi, S.; Higuchi, Y.; Yagi, T.; Ogo, S. *Dalton Trans.* **2008**, 4747.
- Yang, X. Z.; Hall, M. B. *J. Am. Chem. Soc.* **2008**, *130*, 14036.
- Hiromoto, T.; Ataka, K.; Pilak, O.; Vogt, S.; Stagni, M. S.; Meyer-Klaucke, W.; Warkentin, E.; Thauer, R. K.; Shima, S.; Ermler, U. *FEBS Lett.* **2009**, *583*, 585.
- Wang, X. F.; Li, Z. M.; Zeng, X. R.; Luo, Q. Y.; Evans, D. J.; Pickett, C. J.; Liu, X. M. *Chem. Commun.* **2008**, 3555.
- Lyon, E. J.; Shima, S.; Buurman, G.; Chowdhuri, S.; Batschauer, A.; Steinbach, K.; Thauer, R. K. *Eur. J. Biochem.* **2004**, *271*, 195.
- Sadique, A. R.; Brennessel, W. W.; Holland, P. L. *Inorg. Chem.* **2008**, *47*, 784.
- Guo, Y. S.; Wang, H. X.; Xiao, Y. M.; Vogt, S.; Thauer, R. K.; Shima, S.; Volkers, P. I.; Rauchfuss, T. B.; Pelmenchikov, V.; Case, D. A.; Alp, E. E.; Sturhahn, W.; Yoda, Y.; Cramer, S. P. *Inorg. Chem.* **2008**, *47*, 3969.
- Takacs, J.; Soos, E.; Nagy-Magos, Z.; Marko, L.; Gervasio, G.; Hoffmann, T. *Inorg. Chim. Acta* **1989**, *166*, 39.
- Liaw, W. F.; Chen, C. H.; Lee, G. H.; Peng, S. M. *Organometallics* **1998**, *17*, 2370.
- Mauro, A. E.; Casagrande, O. L.; Nogueira, V. M.; Santos, R. H. A.; Gambardella, M. T. P.; Lechat, J. R.; Filho, M. F. J. *Polyhedron* **1993**, *12*, 297.
- Royer, A. M.; Rauchfuss, T. B.; Wilson, S. R. *Inorg. Chem.* **2008**, *47*, 395.
- Lubitz, W.; Reijerse, E.; van Gestel, M. *Chem. Rev.* **2007**, *107*, 4331.
- De Lacey, A. L.; Fernandez, V. M.; Rousset, M.; Cammack, R. *Chem. Rev.* **2007**, *107*, 4304.
- Siegbahn, P. E. M.; Tye, J. W.; Hall, M. B. *Chem. Rev.* **2007**, *107*, 4414.
- Vignais, P. M.; Billoud, B. *Chem. Rev.* **2007**, *107*, 4206.
- Bagley, K. A.; Duin, E. C.; Roseboom, W.; Albracht, S. P. J.; Woodruff, W. H. *Biochemistry* **1995**, *34*, 5527.
- Volbeda, A.; Charon, M. H.; Piras, C.; Hatchikian, E. C.; Frey, M.; Fontecillacamps, J. C. *Nature (London)* **1995**, *373*, 580.
- Volbeda, A.; Martin, L.; Cavazza, C.; Matho, M.; Faber, B. W.; Roseboom, W.; Albracht, S. P. J.; Garcin, E.; Rousset, M.; Fontecilla-Camps, J. C. *J. Biol. Inorg. Chem.* **2005**, *10*, 239.
- Garcin, E.; Vernede, X.; Hatchikian, E. C.; Volbeda, A.; Frey, M.; Fontecilla-Camps, J. C. *Structure* **1999**, *7*, 557.
- Volbeda, A.; Garcin, E.; Piras, C.; deLacey, A. L.; Fernandez, V. M.; Hatchikian, E. C.; Frey, M.; FontecillaCamps, J. C. *J. Am. Chem. Soc.* **1996**, *118*, 12989.
- Ogata, H.; Hirota, S.; Nakahara, A.; Komori, H.; Shibata, N.; Kato, T.; Kano, K.; Higuchi, Y. *Structure* **2005**, *13*, 1635.
- Ogata, H.; Mizoguchi, Y.; Mizuno, N.; Miki, K.; Adachi, S.; Yasuoka, N.; Yagi, T.; Yamauchi, O.; Hirota, S.; Higuchi, Y. *J. Am. Chem. Soc.* **2002**, *124*, 11628.
- Higuchi, Y.; Ogata, H.; Miki, K.; Yasuoka, N.; Yagi, T. *Structure* **1999**, *7*, 549.
- Leroux, F.; Dementin, S.; Burlatt, B.; Cournac, L.; Volbeda, A.; Champ, S.; Martin, L.; Guigliarelli, B.; Bertrand, P.; Fontecilla-Camps, J.; Rousset, M.; Leger, C. *Proc. Natl. Acad. Sci. U. S. A.* **2008**, *105*, 11188.
- Pardo, A.; De Lacey, A. L.; Fernandez, V. M.; Fan, H. J.; Fan, Y.; Hall, M. B. *J. Biol. Inorg. Chem.* **2006**, *11*, 286.
- Bruschi, M.; Zampella, G.; Fantucci, P.; De Gioia, L. *Coord. Chem. Rev.* **2005**, *249*, 1620.
- Foerster, S.; van Gestel, M.; Brecht, M.; Lubitz, W. *J. Biol. Inorg. Chem.* **2005**, *10*, 51.
- Brecht, M.; van Gestel, M.; Buhrke, T.; Friedrich, B.; Lubitz, W. *J. Am. Chem. Soc.* **2003**, *125*, 13075.
- De Lacey, A. L.; Hatchikian, E. C.; Volbeda, A.; Frey, M.; FontecillaCamps, J. C.; Fernandez, V. M. *J. Am. Chem. Soc.* **1997**, *119*, 7181.
- DeLacey, A. L.; Stadler, C.; Fernandez, V. N.; Hatchikian, E. C.; Fan, H. J.; Li, S. H.; Hall, M. B. *J. Biol. Inorg. Chem.* **2002**, *7*, 318.
- Bleijlevens, B.; van Broekhuizen, F. A.; De Lacey, A. L.; Roseboom, W.; Fernandez, V. M.; Albracht, S. P. J. *J. Biol. Inorg. Chem.* **2004**, *9*, 743.
- Fichtner, C.; Laurich, C.; Bothe, E.; Lubitz, W. *Biochemistry* **2006**, *45*, 9706.
- Hatchikian, C. E.; Traore, A. S.; Fernandez, V. M.; Cammack, R. *Eur. J. Biochem.* **1990**, *187*, 635.
- Romao, C. V.; Pereira, I. A. C.; Xavier, A. V.; LeGall, J.; Teixeira, M. *Biochem. Biophys. Res. Commun.* **1997**, *240*, 75.
- Schroder, O.; Bleijlevens, B.; de Jongh, T. E.; Chen, Z. J.; Li, T. S.; Fischer, J.; Forster, J.; Friedrich, C. G.; Bagley, K. A.; Albracht, S. P. J.; Lubitz, W. *J. Biol. Inorg. Chem.* **2007**, *12*, 212.
- Yamamura, T.; Miyamae, H.; Katayama, Y.; Sasaki, Y. *Chem. Lett.* **1985**, *14*, 269.
- Yamamura, T. *Chem. Lett.* **1986**, *15*, 801.
- Snyder, B. S.; Rao, C. P.; Holm, R. H. *Aust. J. Chem.* **1986**, *39*, 963.
- Rosenfield, S. G.; Armstrong, W. H.; Mascharak, P. K. *Inorg. Chem.* **1986**, *25*, 3014.

- (69) Nicholson, J. R.; Christou, G.; Huffman, J. C.; Folting, K. *Polyhedron* **1987**, *6*, 863.
- (70) Yamamura, T.; Kurihara, H.; Nakamura, N.; Kuroda, R.; Asakura, K. *Chem. Lett.* **1990**, *19*, 101.
- (71) Yamamura, T.; Arai, H.; Kurihara, H.; Kuroda, R. *Chem. Lett.* **1990**, *19*, 1975.
- (72) Sellmann, D.; Funfgelder, S.; Pohlmann, G.; Knoch, F.; Moll, M. *Inorg. Chem.* **1990**, *29*, 4772.
- (73) Fox, S.; Wang, Y.; Silver, A.; Millar, M. *J. Am. Chem. Soc.* **1990**, *112*, 3218.
- (74) Halcrow, M. A.; Christou, G. *Chem. Rev.* **1994**, *94*, 2421.
- (75) Jiang, J. F.; Acunzo, A.; Koch, S. A. *J. Am. Chem. Soc.* **2001**, *123*, 12109.
- (76) Jiang, J. F.; Koch, S. A. *Inorg. Chem.* **2002**, *41*, 158.
- (77) Jiang, J. F.; Koch, S. A. *Angew. Chem., Int. Ed.* **2001**, *40*, 2629.
- (78) Chen, C. H.; Chang, Y. S.; Yang, C. Y.; Chen, T. N.; Lee, C. M.; Liaw, W. F. *Dalton Trans.* **2004**, 137.
- (79) Liaw, W. F.; Lee, J. H.; Gau, H. B.; Chen, C. H.; Jung, S. J.; Hung, C. H.; Chen, W. Y.; Hu, C. H.; Lee, G. H. *J. Am. Chem. Soc.* **2002**, *124*, 1680.
- (80) Lai, C. H.; Lee, W. Z.; Miller, M. L.; Reibenspies, J. H.; Darensbourg, D. J.; Darensbourg, M. Y. *J. Am. Chem. Soc.* **1998**, *120*, 10103.
- (81) Darensbourg, D. J.; Reibenspies, J. H.; Lai, C. H.; Lee, W. Z.; Darensbourg, M. Y. *J. Am. Chem. Soc.* **1997**, *119*, 7903.
- (82) Sellmann, D.; Geipel, F.; Heinemann, F. W. *Chem.—Eur. J.* **2002**, *8*, 958.
- (83) Rauchfuss, T. B.; Contakes, S. M.; Hsu, S. C. N.; Reynolds, M. A.; Wilson, S. R. *J. Am. Chem. Soc.* **2001**, *123*, 6933.
- (84) Liaw, W. F.; Lee, N. H.; Chen, C. H.; Lee, C. M.; Lee, G. H.; Peng, S. M. *J. Am. Chem. Soc.* **2000**, *122*, 488.
- (85) Hsu, H. F.; Koch, S. A.; Popescu, C. V.; Munck, E. *J. Am. Chem. Soc.* **1997**, *119*, 8371.
- (86) Lai, C. H.; Reibenspies, J. H.; Darensbourg, M. Y. *Angew. Chem., Int. Ed.* **1996**, *35*, 2390.
- (87) Osterloh, F.; Saak, W.; Haase, D.; Pohl, S. *Chem. Commun.* **1997**, 979.
- (88) Zhu, W. F.; Marr, A. C.; Wang, Q.; Neese, F.; Spencer, D. J. E.; Blake, A. J.; Cooke, P. A.; Wilson, C.; Schroder, M. *Proc. Natl. Acad. Sci. U. S. A.* **2005**, *102*, 18280.
- (89) Stenson, P. A.; Marin-Becerra, A.; Wilson, C.; Blake, A. J.; McMaster, J.; Schroder, M. *Chem. Commun.* **2006**, 317.
- (90) Steinfeld, G.; Kersting, B. *Chem. Commun.* **2000**, 205.
- (91) Davies, S. C.; Evans, D. J.; Hughes, D. L.; Longhurst, S.; Sanders, J. R. *Chem. Commun.* **1999**, 1935.
- (92) Smith, M. C.; Barclay, J. E.; Cramer, S. P.; Davies, S. C.; Gu, W. W.; Hughes, D. L.; Longhurst, S.; Evans, D. J. *J. Chem. Soc., Dalton Trans.* **2002**, 2641.
- (93) Smith, M. C.; Barclay, J. E.; Davies, S. C.; Hughes, D. L.; Evans, D. J. *Dalton Trans.* **2003**, 4147.
- (94) Duff, S. E.; Hitchcock, P. B.; Davies, S. C.; Barclay, J. E.; Evans, D. J. *Acta Crystallogr., Sect. E: Struct. Rep. Online* **2005**, *61*, M1316.
- (95) Duff, S. E.; Hitchcock, P. B.; Davies, S. C.; Barclay, J. E.; Evans, D. J. *Acta Crystallogr., Sect. E: Struct. Rep. Online* **2005**, *61*, M1313.
- (96) Lindahl, P. A. *J. Biol. Inorg. Chem.* **2004**, *9*, 516.
- (97) Liaw, W. F.; Chiang, C. Y.; Lee, G. H.; Peng, S. M.; Lai, C. H.; Darensbourg, M. Y. *Inorg. Chem.* **2000**, *39*, 480.
- (98) Verhagen, J. A. W.; Lutz, M.; Spek, A. L.; Bouwman, E. *Eur. J. Inorg. Chem.* **2003**, 3968.
- (99) Sellmann, D.; Geipel, F.; Lauderbach, F.; Heinemann, F. W. *Angew. Chem., Int. Ed.* **2002**, *41*, 632.
- (100) Li, Z. L.; Ohki, Y.; Tatsumi, K. *J. Am. Chem. Soc.* **2005**, *127*, 8950.
- (101) Ohki, Y.; Yasumura, K.; Kuge, K.; Tanino, S.; Ando, M.; Li, Z.; Tatsumi, K. *Proc. Natl. Acad. Sci. U. S. A.* **2008**, *105*, 7652.
- (102) Ohki, Y.; Sakamoto, M.; Tatsumi, K. *J. Am. Chem. Soc.* **2008**, *130*, 11610.
- (103) Cowie, M.; DeKock, R. L.; Wagenmaker, T. R.; Seyferth, D.; Henderson, R. A.; Gallagher, M. K. *Organometallics* **1989**, *8*, 119.
- (104) Lozano, A. A.; Santana, M. D.; Garcia, G.; Barclay, J. E.; Davies, S. C.; Evans, D. J. *Z. Anorg. Allg. Chem.* **2005**, *631*, 2062.
- (105) Liaw, W. F.; Lee, J. H.; Gau, H. B.; Chen, C. H.; Lee, G. H. *Inorg. Chim. Acta* **2001**, *322*, 99.
- (106) Chalbot, M. U.; Mills, A. M.; Spek, A. L.; Long, G. J.; Bouwman, E. *Eur. J. Inorg. Chem.* **2003**, 453.
- (107) Sellmann, D.; Lauderbach, F.; Heinemann, F. W. *Eur. J. Inorg. Chem.* **2005**, 371.
- (108) Wang, Q.; Barclay, J. E.; Blake, A. J.; Davies, E. S.; Evans, D. J.; Marr, A. C.; McInnes, E. J. L.; McMaster, J.; Wilson, C.; Schroder, M. *Chem.—Eur. J.* **2004**, *10*, 3384.
- (109) Watson, W. H.; Nagl, A.; Don, M. J.; Richmond, M. G. *J. Chem. Crystallogr.* **1999**, *29*, 871.
- (110) Holliday, R. L.; Roof, L. C.; Hargus, B.; Smith, D. M.; Wood, P. T.; Pennington, W. T.; Kolis, J. W. *Inorg. Chem.* **1995**, *34*, 4392.
- (111) Bouwman, E.; Henderson, R. K.; Spek, A. L.; Reedijk, J. *Eur. J. Inorg. Chem.* **1999**, 217.
- (112) Colpas, G. J.; Day, R. O.; Maroney, M. J. *Inorg. Chem.* **1992**, *31*, 5053.
- (113) Mills, D. K.; Hsiao, Y. M.; Farmer, P. J.; Atnip, E. V.; Reibenspies, J. H.; Darensbourg, M. Y. *J. Am. Chem. Soc.* **1991**, *113*, 1421.
- (114) Glaser, T.; Kesting, F.; Beissel, T.; Bill, E.; Weyhermüller, T.; Meyer-Klaucke, W.; Wieghardt, K. *Inorg. Chem.* **1999**, *38*, 722.
- (115) Smith, M. C.; Longhurst, S.; Barclay, J. E.; Cramer, S. P.; Davies, S. C.; Hughes, D. L.; Gu, W. W.; Evans, D. J. *J. Chem. Soc., Dalton Trans.* **2001**, 1387.
- (116) Sellmann, D.; Lauderbach, F.; Geipel, F.; Heinemann, F. W.; Moll, M. *Angew. Chem., Int. Ed.* **2004**, *43*, 3141.
- (117) Wilson, A. D.; Frazee, K.; Twamle, B.; Miller, S. M.; DuBois, D. L.; DuBois, M. R. *J. Am. Chem. Soc.* **2008**, *130*, 1061.
- (118) DuBois, M. R.; DuBois, D. L. *C. R. Chimie* **2008**, *11*, 805.
- (119) Wilson, A. D.; Shoemaker, R. K.; Miedaner, A.; Muckerman, J. T.; DuBois, D. L.; DuBois, M. R. *Proc. Natl. Acad. Sci. U. S. A.* **2007**, *104*, 6951.
- (120) Redin, K.; Wilson, A. D.; Newell, R.; DuBois, M. R.; DuBois, D. L. *Inorg. Chem.* **2007**, *46*, 1268.
- (121) Frazee, K.; Wilson, A. D.; Appel, A. M.; DuBois, M. R.; DuBois, D. L. *Organometallics* **2007**, *26*, 3918.
- (122) Wilson, A. D.; Newell, R. H.; McNevin, M. J.; Muckerman, J. T.; DuBois, M. R.; DuBois, D. L. *J. Am. Chem. Soc.* **2006**, *128*, 358.
- (123) Henry, R. M.; Shoemaker, R. K.; DuBois, D. L.; DuBois, M. R. *J. Am. Chem. Soc.* **2006**, *128*, 3002.
- (124) Henry, R. M.; Shoemaker, R. K.; Newell, R. H.; Jacobsen, G. M.; DuBois, D. L.; DuBois, M. R. *Organometallics* **2005**, *24*, 2481.
- (125) Curtis, C. J.; Miedaner, A.; Ciancanelli, R.; Ellis, W. W.; Noll, B. C.; DuBois, M. R.; DuBois, D. L. *Inorg. Chem.* **2003**, *42*, 216.
- (126) DuBois, M. R.; DuBois, D. L. *Chem. Soc. Rev.* **2009**, *38*, 62.
- (127) Oudart, Y.; Artero, V.; Pecaut, J.; Lebrun, C.; Fontecave, M. *Eur. J. Inorg. Chem.* **2007**, 2613.
- (128) Oudart, Y.; Artero, V.; Pecaut, J.; Fontecave, M. *Inorg. Chem.* **2006**, *45*, 4334.
- (129) Ogo, S.; Kabe, R.; Uehara, K.; Kure, B.; Nishimura, T.; Menon, S. C.; Harada, R.; Fukuzumi, S.; Higuchi, Y.; Ohhara, T.; Tamada, T.; Kuroki, R. *Science* **2007**, *316*, 585.
- (130) Matsumoto, T.; Nakaya, Y.; Itakura, N.; Tatsumi, K. *J. Am. Chem. Soc.* **2008**, *130*, 2458.
- (131) Adams, M. W. W. *Biochim. Biophys. Acta* **1990**, *1020*, 115.
- (132) Vignais, P. M.; Billoud, B.; Meyer, J. *FEMS Microbiol. Rev.* **2001**, *25*, 455.
- (133) Nicolet, Y.; Lemon, B. J.; Fontecilla-Camps, J. C.; Peters, J. W. *Trends Biochem. Sci.* **2000**, *25*, 138.
- (134) Peters, J. W.; Lanzilotta, W. N.; Lemon, B. J.; Seefeldt, L. C. *Science* **1998**, *282*, 1853.
- (135) Nicolet, Y.; Piras, C.; Legrand, P.; Hatchikian, C. E.; Fontecilla-Camps, J. C. *Structure* **1999**, *7*, 13.
- (136) Lemon, B. J.; Peters, J. W. *Biochemistry* **1999**, *38*, 12969.
- (137) Pandey, A. S.; Harris, T. V.; Giles, L. J.; Peters, J. W.; Szilagyi, R. K. *J. Am. Chem. Soc.* **2008**, *130*, 4533.
- (138) Spek, M. T.; Arends, A. F.; Happe, R. P.; Yun, S. Y.; Bagley, K. A.; Stufkens, D. J.; Hagen, W. R.; Albracht, S. P. J. *Eur. J. Biochem.* **1996**, *237*, 629.
- (139) Pierik, A. J.; Hulstein, M.; Hagen, W. R.; Albracht, S. P. J. *Eur. J. Biochem.* **1998**, *258*, 572.
- (140) De Lacey, A. L.; Stadler, C.; Cavazza, C.; Hatchikian, E. C.; Fernandez, V. M. *J. Am. Chem. Soc.* **2000**, *122*, 11232.
- (141) Lemon, B. J.; Peters, J. W. *J. Am. Chem. Soc.* **2000**, *122*, 3793.
- (142) Nicolet, Y.; de Lacey, A. L.; Vernede, X.; Fernandez, V. M.; Hatchikian, E. C.; Fontecilla-Camps, J. C. *J. Am. Chem. Soc.* **2001**, *123*, 1596.
- (143) Popescu, C. V.; Munck, E. *J. Am. Chem. Soc.* **1999**, *121*, 7877.
- (144) Razavet, M.; Borg, S. J.; George, S. J.; Best, S. P.; Fairhurst, S. A.; Pickett, C. J. *Chem. Commun.* **2002**, 700.
- (145) George, S. J.; Cui, Z.; Razavet, M.; Pickett, C. J. *Chem.—Eur. J.* **2002**, *8*, 4037.
- (146) Fiedler, A. T.; Brunold, T. C. *Inorg. Chem.* **2005**, *44*, 9322.
- (147) Bruschi, M.; Greco, C.; Fantucci, P.; De Gioia, L. *Inorg. Chem.* **2008**, *47*, 6056.
- (148) Silakov, A.; Reijerse, E. J.; Albracht, S. P. J.; Hatchikian, E. C.; Lubitz, W. *J. Am. Chem. Soc.* **2007**, *129*, 11447.
- (149) Roseboom, W.; De Lacey, A. L.; Fernandez, V. M.; Hatchikian, E. C.; Albracht, S. P. J. *J. Biol. Inorg. Chem.* **2006**, *11*, 102.
- (150) Chen, Z. J.; Lemon, B. J.; Huang, S.; Swartz, D. J.; Peters, J. W.; Bagley, K. A. *Biochemistry* **2002**, *41*, 2036.
- (151) Albracht, S. P. J.; Roseboom, W.; Hatchikian, E. C. *J. Biol. Inorg. Chem.* **2006**, *11*, 88.
- (152) Bennett, B.; Lemon, B. J.; Peters, J. W. *Biochemistry* **2000**, *39*, 7455.
- (153) Cao, Z. X.; Hall, M. B. *J. Am. Chem. Soc.* **2001**, *123*, 3734.

- (154) Reihlen, H.; Gruhl, A.; von Hessling, G. *Liebigs Ann. Chem.* **1929**, 472, 268.
- (155) Dahl, L. F.; Wei, C. H. *Inorg. Chem.* **1963**, 2, 328.
- (156) Hieber, W.; Spacu, P. Z. *Anorg. Allg. Chem.* **1937**, 233, 353.
- (157) Hieber, W.; Scharfenberg, C. *Ber. Dtsch. Chem. Ges.* **1940**, 73, 1012.
- (158) Hieber, W.; Gruber, J. Z. *Anorg. Allg. Chem.* **1958**, 296, 91.
- (159) Hieber, W.; Beck, W. Z. *Anorg. Allg. Chem.* **1960**, 305, 265.
- (160) Seyferth, D.; Henderson, R. S. *J. Am. Chem. Soc.* **1979**, 101, 508.
- (161) Seyferth, D.; Henderson, R. S.; Gallagher, M. K. *J. Organomet. Chem.* **1980**, 193, C75.
- (162) Seyferth, D.; Song, L. C.; Henderson, R. S. *J. Am. Chem. Soc.* **1981**, 103, 5103.
- (163) Chieh, C.; Seyferth, D.; Song, L. C. *Organometallics* **1982**, 1, 473.
- (164) Seyferth, D.; Henderson, R. S.; Song, L. C. *Organometallics* **1982**, 1, 125.
- (165) Mak, T. C. W.; Book, L.; Chieh, C.; Gallagher, M. K.; Song, L. C.; Seyferth, D. *Inorg. Chim. Acta* **1983**, 73, 159.
- (166) Seyferth, D.; Womack, G. B.; Song, L. C.; Cowie, M.; Hames, B. W. *Organometallics* **1983**, 2, 928.
- (167) Seyferth, D.; Womack, G. B.; Cowie, M.; Hames, B. W. *Organometallics* **1984**, 3, 1891.
- (168) Seyferth, D.; Henderson, R. S.; Song, L. C.; Womack, G. B. *J. Organomet. Chem.* **1985**, 292, 9.
- (169) Seyferth, D.; Kiwan, A. M. *J. Organomet. Chem.* **1985**, 286, 219.
- (170) Seyferth, D.; Kiwan, A. M.; Sinn, E. *J. Organomet. Chem.* **1985**, 281, 111.
- (171) Seyferth, D.; Womack, G. B.; Dewan, J. C. *Organometallics* **1985**, 4, 398.
- (172) Seyferth, D.; Archer, C. M. *Organometallics* **1986**, 5, 2572.
- (173) Seyferth, D.; Womack, G. B.; Henderson, R. S.; Cowie, M.; Hames, B. W. *Organometallics* **1986**, 5, 1568.
- (174) Hoke, J. B.; Dewan, J. C.; Seyferth, D. *Organometallics* **1987**, 6, 1816.
- (175) Seyferth, D.; Hoke, J. B.; Dewan, J. C. *Organometallics* **1987**, 6, 895.
- (176) Seyferth, D.; Womack, G. B.; Gallagher, M. K.; Cowie, M.; Hames, B. W.; Fackler, J. P.; Mazany, A. M. *Organometallics* **1987**, 6, 283.
- (177) Seyferth, D.; Hoke, J. B.; Rheingold, A. L.; Cowie, M.; Hunter, A. D. *Organometallics* **1988**, 7, 2163.
- (178) Seyferth, D.; Womack, G. B.; Archer, C. M.; Dewan, J. C. *Organometallics* **1989**, 8, 430.
- (179) Seyferth, D.; Womack, G. B.; Archer, C. M.; Fackler, J. P.; Marler, D. O. *Organometallics* **1989**, 8, 443.
- (180) Seyferth, D.; Archer, C. M.; Ruschke, D. P.; Cowie, M.; Hilts, R. W. *Organometallics* **1991**, 10, 3363.
- (181) Seyferth, D.; Anderson, L. L.; Villafane, F.; Cowie, M.; Hilts, R. W. *Organometallics* **1992**, 11, 3262.
- (182) Seyferth, D.; Anderson, L. L.; Davis, W. M. *J. Organomet. Chem.* **1993**, 459, 271.
- (183) Seyferth, D.; Hoke, J. B.; Dewan, J. C.; Hofmann, P.; Schnellbach, M. *Organometallics* **1994**, 13, 3452.
- (184) Seyferth, D.; Ruschke, D. P.; Davis, W. M. *Organometallics* **1994**, 13, 4695.
- (185) Fauvel, K.; Mathieu, R.; Poilblanc, R. *Inorg. Chem.* **1976**, 15, 976.
- (186) Arabi, M. S.; Mathieu, R.; Poilblanc, R. *Inorg. Chim. Acta* **1977**, 23, L17.
- (187) Leborgne, G.; Grandjean, D.; Mathieu, R.; Poilblanc, R. *J. Organomet. Chem.* **1977**, 131, 429.
- (188) Mathieu, R.; Poilblanc, R. *J. Organomet. Chem.* **1977**, 142, 351.
- (189) Savariault, J. M.; Bonnet, J. J.; Mathieu, R.; Galy, J. C. R. *Acad. Sci., Ser. C* **1977**, 284, 663.
- (190) Poilblanc, R. *New J. Chem.* **1978**, 2, 145.
- (191) Arabi, M. S.; Mathieu, R.; Poilblanc, R. *J. Organomet. Chem.* **1979**, 177, 199.
- (192) Bonnet, J. J.; Mathieu, R.; Poilblanc, R.; Ibers, J. A. *J. Am. Chem. Soc.* **1979**, 101, 7487.
- (193) Mathieu, R.; Poilblanc, R.; Lemoine, P.; Gross, M. *J. Organomet. Chem.* **1979**, 165, 243.
- (194) Shaver, A.; Fitzpatrick, P. J.; Steliou, K.; Butler, I. S. *J. Organomet. Chem.* **1979**, 172, C59.
- (195) Shaver, A.; Fitzpatrick, P. J.; Steliou, K.; Butler, I. S. *J. Am. Chem. Soc.* **1979**, 101, 1313.
- (196) Bonnet, J. J.; Mathieu, R.; Ibers, J. A. *Inorg. Chem.* **1980**, 19, 2448.
- (197) Leborgne, G.; Mathieu, R. *J. Organomet. Chem.* **1981**, 208, 201.
- (198) Patin, H.; Mignani, G.; Benoit, A.; Lemarouille, J. Y.; Grandjean, D. *Inorg. Chem.* **1981**, 20, 4351.
- (199) Broadhurst, P. V.; Johnson, B. F. G.; Lewis, J.; Raithby, P. R. *J. Chem. Soc., Chem. Commun.* **1982**, 140.
- (200) Dettlaf, G.; Hubener, P.; Klimes, J.; Weiss, E. *J. Organomet. Chem.* **1982**, 229, 63.
- (201) Chernyshev, E. A.; Kuzmin, O. V.; Lebedev, A. V.; Gusev, A. I.; Los, M. G.; Alekseev, N. V.; Nametkin, N. S.; Tyurin, V. D.; Krapivin, A. M.; Kubasova, N. A.; Zaikin, V. G. *J. Organomet. Chem.* **1983**, 252, 143.
- (202) Nametkin, N. S.; Kolobkov, B. I.; Tyurin, V. D.; Muratov, A. N.; Nekhaev, A. I.; Mavlonov, M.; Sideridu, A. Y.; Aleksandrov, G. G.; Lebedev, A. V.; Tashev, M. T.; Dustov, H. B. *J. Organomet. Chem.* **1984**, 276, 393.
- (203) Nekhaev, A. I.; Alekseeva, S. D.; Nametkin, N. S.; Tyurin, V. D.; Kolobkov, B. I.; Aleksandrov, G. G.; Parpiev, N. A.; Tashev, M. T.; Dustov, H. B. *J. Organomet. Chem.* **1985**, 297, C33.
- (204) Adams, R. D.; Babin, J. E. *Inorg. Chem.* **1986**, 25, 3418.
- (205) Gaete, W.; Ros, J.; Yanez, R.; Solans, X.; Fontaltaba, M. *J. Organomet. Chem.* **1986**, 316, 169.
- (206) Gaete, W.; Ros, J.; Yanez, R.; Solans, X.; Miravittles, C.; Aguilo, M. *Inorg. Chim. Acta* **1986**, 119, 55.
- (207) Lotz, S.; Vanrooyen, P. H.; Vandyk, M. M. *Organometallics* **1987**, 6, 499.
- (208) Messelhauser, J.; Gutensohn, K. U.; Lorenz, I. P.; Hiller, W. *J. Organomet. Chem.* **1987**, 321, 377.
- (209) Wu, X. T.; Bose, K. S.; Sinn, E.; Averill, B. A. *Organometallics* **1989**, 8, 251.
- (210) Dillen, J. L. M.; Vandyk, M. M.; Lotz, S. *J. Chem. Soc., Dalton Trans.* **1989**, 2199.
- (211) Banister, A. J.; Gorrell, I. B.; Clegg, W.; Jorgensen, K. A. *J. Chem. Soc., Dalton Trans.* **1989**, 2229.
- (212) Choi, N.; Kabe, Y.; Ando, W. *Organometallics* **1992**, 11, 1506.
- (213) Delgado, E.; Hernandez, E.; Rossell, O.; Seco, M.; Puebla, E. G.; Ruiz, C. *J. Organomet. Chem.* **1993**, 455–177.
- (214) Westmeyer, M. D.; Rauchfuss, T. B.; Verma, A. K. *Inorg. Chem.* **1996**, 35, 7140.
- (215) Cherng, J. J.; Tsai, Y. C.; Ueng, C. H.; Lee, G. H.; Peng, S. M.; Shieh, M. *Organometallics* **1998**, 17, 255.
- (216) Alvarez-Toledano, C.; Enriquez, J.; Toscano, R. A.; Martinez-Garcia, M.; Cortes-Cortes, E.; Osornio, Y. M.; Garcia-Mellado, O.; Gutierrez-Perez, R. *J. Organomet. Chem.* **1999**, 577, 38.
- (217) Delgado, E.; Hernandez, E.; Mansilla, N.; Zamora, F.; Martinez-Cruz, L. A. *Inorg. Chim. Acta* **1999**, 284, 14.
- (218) Imhof, W. *Organometallics* **1999**, 18, 4845.
- (219) Wang, Z. X.; Jia, C. S.; Zhou, Z. Y.; Zhou, X. G. *J. Organomet. Chem.* **1999**, 580, 201.
- (220) Hourihane, R.; Gray, G.; Spalding, T.; Deeney, T. *J. Organomet. Chem.* **2000**, 595, 191.
- (221) Le Cloirec, A.; Best, S. P.; Borg, S.; Davies, S. C.; Evans, D. J.; Hughes, D. L.; Pickett, C. J. *Chem. Commun.* **1999**, 2285.
- (222) Lyon, E. J.; Georgakaki, I. P.; Reibenspies, J. H.; Darensbourg, M. Y. *Angew. Chem., Int. Ed.* **1999**, 38, 3178.
- (223) Schmidt, M.; Contakes, S. M.; Rauchfuss, T. B. *J. Am. Chem. Soc.* **1999**, 121, 9736.
- (224) Li, H. X.; Rauchfuss, T. B. *J. Am. Chem. Soc.* **2002**, 124, 726.
- (225) Wang, Z.; Liu, J. H.; He, C. J.; Jiang, S.; Akermark, B.; Sun, L. C. *J. Organomet. Chem.* **2007**, 692, 5501.
- (226) Song, L. C.; Yang, Z. Y.; Bian, H. Z.; Liu, Y.; Wang, H. T.; Liu, X. F.; Hu, Q. M. *Organometallics* **2005**, 24, 6126.
- (227) Song, L. C.; Yang, Z. Y.; Bian, H. Z.; Hu, Q. M. *Organometallics* **2004**, 23, 3082.
- (228) Song, L. C.; Wang, L. X.; Yin, B. S.; Li, Y. L.; Zhang, X. G.; Zhang, Y. W.; Luo, X.; Hu, Q. M. *Eur. J. Inorg. Chem.* **2008**, 291.
- (229) Song, L. C.; Wang, H. T.; Ge, J. H.; Mei, S. Z.; Gao, J.; Wang, L. X.; Gai, B.; Zhao, L. Q.; Yan, J.; Wang, Y. Z. *Organometallics* **2008**, 27, 1409.
- (230) Lawrence, J. D.; Li, H. X.; Rauchfuss, T. B.; Benard, M.; Rohmer, M. M. *Angew. Chem., Int. Ed.* **2001**, 40, 1768.
- (231) Lawrence, J. D.; Li, H. X.; Rauchfuss, T. B. *Chem. Commun.* **2001**, 1482.
- (232) Ott, S.; Kritikos, M.; Akermark, B.; Sun, L. C. *Angew. Chem., Int. Ed.* **2003**, 42, 3285.
- (233) Liu, T. B.; Wang, M.; Shi, Z.; Cui, H. G.; Dong, W. B.; Chen, J. S.; Akermark, B.; Sun, L. C. *Chem.—Eur. J.* **2004**, 10, 4474.
- (234) Ott, S.; Borgstrom, M.; Kritikos, M.; Lomoth, R.; Bergquist, J.; Akermark, B.; Hammarstrom, L.; Sun, L. C. *Inorg. Chem.* **2004**, 43, 4683.
- (235) Ott, S.; Kritikos, M.; Akermark, B.; Sun, L. C.; Lomoth, R. *Angew. Chem., Int. Ed.* **2004**, 43, 1006.
- (236) Wang, F. J.; Wang, M.; Liu, X. Y.; Jin, K.; Dong, W. B.; Li, G. H.; Akermark, B.; Sun, L. C. *Chem. Commun.* **2005**, 3221.
- (237) Dong, W. B.; Wang, M.; Liu, X. Y.; Jin, K.; Li, G. H.; Wang, F. J.; Sun, L. C. *Chem. Commun.* **2006**, 305.
- (238) Gao, W. M.; Liu, J. H.; Ma, C. B.; Weng, L. H.; Jin, K.; Chen, C. N.; Akermark, B.; Sun, L. C. *Inorg. Chim. Acta* **2006**, 359, 1071.
- (239) Jiang, S.; Liu, J. H.; Sun, L. C. *Inorg. Chem. Commun.* **2006**, 9, 290.
- (240) Schwartz, L.; Eilers, G.; Eriksson, L.; Gogoll, A.; Lomoth, R.; Ott, S. *Chem. Commun.* **2006**, 520.

- (241) Li, X. Q.; Wang, M.; Zhang, S.; Pan, J. X.; Na, Y.; Liu, J. H.; Akermark, B.; Sun, L. C. *J. Phys. Chem. B* **2008**, *112*, 8198.
- (242) Gao, S.; Fan, J. L.; Sun, S.; Peng, X. J.; Zhao, X.; Hou, J. *Dalton Trans.* **2008**, 2128.
- (243) Si, G.; Wang, W. G.; Wang, H. Y.; Tung, C. H.; Wu, L. Z. *Inorg. Chem.* **2008**, *47*, 8101.
- (244) Stanley, J. L.; Heiden, Z. M.; Rauchfuss, T. B.; Wilson, S. R. *Organometallics* **2008**, *27*, 119.
- (245) Windhager, J.; Seidel, R. A.; Apfel, U. P.; Görls, H.; Linti, G.; Weigand, W. *Chem. Biodiversity* **2008**, *5*, 2023.
- (246) Windhager, J.; Rudolph, M.; Brautigam, S.; Görls, H.; Weigand, W. *Eur. J. Inorg. Chem.* **2007**, 2748.
- (247) Song, L. C.; Yang, Z. Y.; Hua, Y. J.; Wang, H. T.; Liu, Y.; Hu, Q. M. *Organometallics* **2007**, *26*, 2106.
- (248) Justice, A. K.; Nilges, M. J.; Rauchfuss, T. B.; Wilson, S. R.; De Gioia, L.; Zampella, G. *J. Am. Chem. Soc.* **2008**, *130*, 5293.
- (249) Justice, A. K.; De Gioia, L.; Nilges, M. J.; Rauchfuss, T. B.; Wilson, S. R.; Zampella, G. *Inorg. Chem.* **2008**, *47*, 7405.
- (250) Barton, B. E.; Rauchfuss, T. B. *Inorg. Chem.* **2008**, *47*, 2261.
- (251) Justice, A. K.; Rauchfuss, T. B.; Wilson, S. R. *Angew. Chem., Int. Ed.* **2007**, *46*, 6152.
- (252) van der Vlugt, J. I.; Rauchfuss, T. B.; Wilson, S. R. *Chem.—Eur. J.* **2006**, *12*, 90.
- (253) Gloaguen, F.; Lawrence, J. D.; Schmidt, M.; Wilson, S. R.; Rauchfuss, T. B. *J. Am. Chem. Soc.* **2001**, *123*, 12518.
- (254) Gloaguen, F.; Lawrence, J. D.; Rauchfuss, T. B. *J. Am. Chem. Soc.* **2001**, *123*, 9476.
- (255) Zhao, X.; Georgakaki, I. P.; Miller, M. L.; Yarbrough, J. C.; Darensbourg, M. Y. *J. Am. Chem. Soc.* **2001**, *123*, 9710.
- (256) Gloaguen, F.; Lawrence, J. D.; Rauchfuss, T. B.; Benard, M.; Rohmer, M. M. *Inorg. Chem.* **2002**, *41*, 6573.
- (257) Zhao, X.; Hsiao, Y. M.; Lai, C. H.; Reibenspies, J. H.; Darensbourg, M. Y. *Inorg. Chem.* **2002**, *41*, 699.
- (258) Zhao, X.; Georgakaki, I. P.; Miller, M. L.; Mejia-Rodriguez, R.; Chiang, C. Y.; Darensbourg, M. Y. *Inorg. Chem.* **2002**, *41*, 3917.
- (259) Chong, D. S.; Georgakaki, I. P.; Mejia-Rodriguez, R.; Samabria-Chinchilla, J.; Soriaga, M. P.; Darensbourg, M. Y. *Dalton Trans.* **2003**, 4158.
- (260) Mejia-Rodriguez, R.; Chong, D. S.; Reibenspies, J. H.; Soriaga, M. P.; Darensbourg, M. Y. *J. Am. Chem. Soc.* **2004**, *126*, 12004.
- (261) Li, P.; Wang, M.; He, C. J.; Li, G. H.; Liu, X. Y.; Chen, C. N.; Akermark, B.; Sun, L. C. *Eur. J. Inorg. Chem.* **2005**, 2506.
- (262) van der Vlugt, J. I.; Rauchfuss, T. B.; Whaley, C. M.; Wilson, S. R. *J. Am. Chem. Soc.* **2005**, *127*, 16012.
- (263) Felton, G. A. N.; Vannucci, A. K.; Chen, J. Z.; Lockett, L. T.; Okumura, N.; Petro, B. J.; Zakai, U. I.; Evans, D. H.; Glass, R. S.; Lichtenberger, D. L. *J. Am. Chem. Soc.* **2007**, *129*, 12521.
- (264) Loscher, S.; Schwartz, L.; Stein, M.; Ott, S.; Haumann, M. *Inorg. Chem.* **2007**, *46*, 11094.
- (265) Adam, F. I.; Hogarth, G.; Kabir, S. E.; Richards, I. C. R. *Chimie* **2008**, *11*, 890.
- (266) Hogarth, G.; Richards, I.; Subasi, E. *Transition Met. Chem.* **2008**, *33*, 729.
- (267) Olsen, M. T.; Bruschi, M.; De Gioia, L.; Rauchfuss, T. B.; Wilson, S. R. *J. Am. Chem. Soc.* **2008**, *130*, 12021.
- (268) Schwartz, L.; Singh, P. S.; Eriksson, L.; Lomoth, R.; Ott, S. C. R. *Chimie* **2008**, *11*, 875.
- (269) Si, Y. T.; Hu, M. Q.; Chen, C. N. C. R. *Chimie* **2008**, *11*, 932.
- (270) Song, L. C.; Li, C. G.; Gao, J.; Yin, B. S.; Luo, X.; Zhang, X. G.; Bao, H. L.; Hu, Q. M. *Inorg. Chem.* **2008**, *47*, 4545.
- (271) Wang, Z.; Jiang, W. F.; Liu, J. H.; Jiang, W.; Wang, Y.; Akermark, B.; Sun, L. C. *J. Organomet. Chem.* **2008**, *693*, 2828.
- (272) Wang, N.; Wang, M.; Liu, T. B.; Li, P.; Zhang, T. T.; Darensbourg, M. Y.; Sun, L. C. *Inorg. Chem.* **2008**, *47*, 6948.
- (273) Song, L. C.; Li, C. G.; Ge, J. H.; Yang, Z. Y.; Wang, H. T.; Zhang, J.; Hu, Q. M. *J. Inorg. Biochem.* **2008**, *102*, 1973.
- (274) Lawrence, J. D.; Rauchfuss, T. B.; Wilson, S. R. *Inorg. Chem.* **2002**, *41*, 6193.
- (275) Nehring, J. L.; Heinekey, D. M. *Inorg. Chem.* **2003**, *42*, 4288.
- (276) Boyke, C. A.; Rauchfuss, T. B.; Wilson, S. R.; Rohmer, M. M.; Benard, M. *J. Am. Chem. Soc.* **2004**, *126*, 15151.
- (277) Boyke, C. A.; van der Vlugt, J. I.; Rauchfuss, T. B.; Wilson, S. R.; Zampella, G.; De Gioia, L. *J. Am. Chem. Soc.* **2005**, *127*, 11010.
- (278) Hou, J.; Peng, X. J.; Liu, J. F.; Gao, Y. L.; Zhao, X.; Gao, S.; Han, K. L. *Eur. J. Inorg. Chem.* **2006**, 4679.
- (279) Tye, J. W.; Lee, J.; Wang, H. W.; Mejia-Rodriguez, R.; Reibenspies, J. H.; Hall, M. B.; Darensbourg, M. Y. *Inorg. Chem.* **2005**, *44*, 5550.
- (280) Capon, J. F.; El Hassnaoui, S.; Gloaguen, F.; Schollhammer, P.; Talarmin, J. *Organometallics* **2005**, *24*, 2020.
- (281) Duan, L. L.; Wang, M.; Li, P.; Na, Y.; Wang, N.; Sun, L. C. *Dalton Trans.* **2007**, 1277.
- (282) Jiang, S.; Liu, J. H.; Shi, Y.; Wang, Z.; Akermark, B.; Sun, L. H. *Polyhedron* **2007**, *26*, 1499.
- (283) Liu, T. B.; Darensbourg, M. Y. *J. Am. Chem. Soc.* **2007**, *129*, 7008.
- (284) Morvan, D.; Capon, J. F.; Gloaguen, F.; Le Goff, A.; Marchivie, M.; Michaud, F.; Schollhammer, P.; Talarmin, J.; Yaouanc, J. J.; Pichon, R.; Kervarec, N. *Organometallics* **2007**, *26*, 2042.
- (285) Thomas, C. M.; Darensbourg, M. Y.; Hall, M. B. *J. Inorg. Biochem.* **2007**, *101*, 1752.
- (286) Thomas, C. M.; Liu, T. B.; Hall, M. B.; Darensbourg, M. Y. *Inorg. Chem.* **2008**, *47*, 7009.
- (287) Thomas, C. M.; Liu, T. B.; Hall, M. B.; Darensbourg, M. Y. *Chem. Commun.* **2008**, 1563.
- (288) Singleton, M. L.; Jenkins, R. M.; Klemashevich, C. L.; Darensbourg, M. Y. C. R. *Chimie* **2008**, *11*, 861.
- (289) Song, L. C.; Yan, C. G.; Hu, Q. M.; Huang, X. Y. *J. Organomet. Chem.* **1995**, *505*, 119.
- (290) Song, L. C.; Yan, C. G.; Hu, Q. M.; Wang, R. J.; Mak, T. C. W.; Huang, X. Y. *Organometallics* **1996**, *15*, 1535.
- (291) Song, L. C.; Zeng, G. H.; Mei, S. Z.; Lou, S. X.; Hu, Q. M. *Organometallics* **2006**, *25*, 3468.
- (292) Apfel, U. P.; Halpin, Y.; Gottschaldt, M.; Görls, H.; Vos, J. G.; Weigand, W. *Eur. J. Inorg. Chem.* **2008**, 5112.
- (293) Cheah, M. H.; Borg, S. J.; Bondin, M. I.; Best, S. P. *Inorg. Chem.* **2004**, *43*, 5635.
- (294) Das, P.; Capon, J. F.; Gloaguen, F.; Petillon, F. Y.; Schollhammer, P.; Talarmin, J.; Muir, K. W. *Inorg. Chem.* **2004**, *43*, 8203.
- (295) Song, L. C.; Zeng, G. H.; Lou, S. X.; Zan, H. N.; Ming, J. B.; Hu, Q. M. *Organometallics* **2008**, *27*, 3714.
- (296) Volkens, P.; Rauchfuss, T. B. *J. Inorg. Biochem.* **2007**, *101*, 1748.
- (297) de Hatten, X.; Bothe, E.; Merz, K.; Huc, I.; Metzler-Nolte, N. *Eur. J. Inorg. Chem.* **2008**, 4530.
- (298) Jones, A. K.; Lichtenstein, B. R.; Dutta, A.; Gordon, G.; Dutton, P. L. *J. Am. Chem. Soc.* **2007**, *129*, 14844.
- (299) Xu, F. F.; Tard, C.; Wang, X. F.; Ibrahim, S. K.; Hughes, D. L.; Zhong, W.; Zeng, X. R.; Luo, Q. Y.; Liu, X. M.; Pickett, C. J. *Chem. Commun.* **2008**, 606.
- (300) Tard, C.; Liu, X. M.; Ibrahim, S. K.; Bruschi, M.; De Gioia, L.; Davies, S. C.; Yang, X.; Wang, L. S.; Sowers, G.; Pickett, C. J. *Nature (London)* **2005**, *433*, 610.
- (301) Razavet, M.; Davies, S. C.; Hughes, D. L.; Barclay, J. E.; Evans, D. J.; Fairhurst, S. A.; Liu, X. M.; Pickett, C. J. *Dalton Trans.* **2003**, 586.
- (302) Razavet, M.; Davies, S. C.; Hughes, D. L.; Pickett, C. J. *Chem. Commun.* **2001**, 847.
- (303) Hu, M. Q.; Ma, C. B.; Zhang, X. F.; Chen, F.; Chen, C. N.; Liu, Q. T. *Chem. Lett.* **2006**, *35*, 840.
- (304) Hu, M. Q.; Ma, C. B.; Si, Y. T.; Chen, C. N.; Liu, Q. T. *J. Inorg. Biochem.* **2007**, *101*, 1370.
- (305) Lyon, E. J.; Georgakaki, I. P.; Reibenspies, J. H.; Darensbourg, M. Y. *J. Am. Chem. Soc.* **2001**, *123*, 3268.
- (306) Zampella, G.; Bruschi, M.; Fantucci, P.; De Gioia, L. *J. Am. Chem. Soc.* **2005**, *127*, 13180.
- (307) Zilberman, S.; Stiefel, E. I.; Cohen, M. H.; Car, R. *J. Phys. Chem. B* **2006**, *110*, 7049.
- (308) Singleton, M. L.; Bhuvanesh, N.; Reibenspies, J. H.; Darensbourg, M. Y. *Angew. Chem., Int. Ed.* **2008**, *47*, 9492.
- (309) Stack, T. D. P.; Holm, R. H. *J. Am. Chem. Soc.* **1987**, *109*, 2546.
- (310) Schwab, D. E.; Tard, C.; Brecht, E.; Peters, J. W.; Pickett, C. J.; Szilagyi, R. K. *Chem. Commun.* **2006**, 3696.
- (311) Zhao, X.; Chiang, C. Y.; Miller, M. L.; Rampersad, M. V.; Darensbourg, M. Y. *J. Am. Chem. Soc.* **2003**, *125*, 518.
- (312) Adam, F. I.; Hogarth, G.; Richards, I. *J. Organomet. Chem.* **2007**, *692*, 3957.
- (313) Ezzaher, S.; Capon, J. F.; Gloaguen, F.; Petillon, F. Y.; Schollhammer, P.; Talarmin, J. *Inorg. Chem.* **2007**, *46*, 3426.
- (314) Thomas, C. M.; Rudiger, O.; Liu, T.; Carson, C. E.; Hall, M. B.; Darensbourg, M. Y. *Organometallics* **2007**, *26*, 3976.
- (315) Wang, F. J.; Wang, M.; Liu, X. Y.; Jin, K.; Donga, W. B.; Sun, L. C. *Dalton Trans.* **2007**, 3812.
- (316) Wang, N.; Wang, M.; Zhang, T. T.; Li, P.; Liu, J. H.; Sun, L. C. *Chem. Commun.* **2008**, 5800.
- (317) Ezzaher, S.; Capon, J. F.; Gloaguen, F.; Petillon, F.; Schollhammer, P.; Talarmin, J.; Kervarec, N. *Inorg. Chem.* **2009**, *48*, 2.
- (318) Justice, A. K.; Linck, R. C.; Rauchfuss, T. B.; Wilson, S. R. *J. Am. Chem. Soc.* **2004**, *126*, 13214.
- (319) Felton, G. A. N.; Glass, R. S.; Lichtenberger, D. L.; Evans, D. H. *Inorg. Chem.* **2006**, *45*, 9181.
- (320) Darchen, A.; Mousser, H.; Patin, H. *J. Chem. Soc., Chem. Commun.* **1988**, 968.
- (321) Alani, F. T.; Pickett, C. J. *J. Chem. Soc., Dalton Trans.* **1988**, 2329.
- (322) Eilers, G.; Schwartz, L.; Stein, M.; Zampella, G.; de Gioia, L.; Ott, S.; Lomoth, R. *Chem.—Eur. J.* **2007**, *13*, 7075.
- (323) Justice, A. K.; Linck, R. C.; Rauchfuss, T. B. *Inorg. Chem.* **2006**, *45*, 2406.
- (324) Costentin, C. *Chem. Rev.* **2008**, *108*, 2145.

- (325) Huynh, M. H. V.; Meyer, T. J. *Chem. Rev.* **2007**, *107*, 5004.
- (326) Borg, S. J.; Behrsing, T.; Best, S. P.; Razavet, M.; Liu, X. M.; Pickett, C. J. *J. Am. Chem. Soc.* **2004**, *126*, 16988.
- (327) de Carcer, I. A.; DiPasquale, A.; Rheingold, A. L.; Heinekey, D. M. *Inorg. Chem.* **2006**, *45*, 8000.
- (328) Best, S. P.; Borg, S. J.; White, J. M.; Razavet, M.; Pickett, C. J. *Chem. Commun.* **2007**, 4348.
- (329) Capon, J. F.; Gloaguen, F.; Schollhammer, P.; Talarmin, J. J. *Electroanal. Chem.* **2004**, *566*, 241.
- (330) Capon, J. F.; Ezzaher, S.; Gloaguen, F.; Petillon, F. Y.; Schollhammer, P.; Talarmin, J.; Davin, T. J.; McGrady, J. E.; Muir, K. W. *New J. Chem.* **2007**, *31*, 2052.
- (331) Capon, J. F.; Ezzaher, S.; Gloaguen, F.; Petillon, F. Y.; Schollhammer, P.; Talarmin, J. *Chem.—Eur. J.* **2008**, *14*, 1954.
- (332) Borg, S. J.; Ibrahim, S. K.; Pickett, C. J.; Best, S. P. C. R. *Chimie* **2008**, *11*, 852.
- (333) Chatt, J.; Kan, C. T.; Leigh, G. J.; Pickett, C. J.; Stanley, D. R. *J. Chem. Soc., Dalton Trans.* **1980**, 2032.
- (334) Pombeiro, A. J. L. *Eur. J. Inorg. Chem.* **2007**, 1473.
- (335) Barton, B. E.; Olsen, M. T.; Rauchfuss, T. B. *J. Am. Chem. Soc.* **2008**, *130*, 16834.
- (336) Tard, C.; Liu, X. M.; Hughes, D. L.; Pickett, C. J. *Chem. Commun.* **2005**, 133.
- (337) Georgakaki, I. P.; Thomson, L. M.; Lyon, E. J.; Hall, M. B.; Darensbourg, M. Y. *Coord. Chem. Rev.* **2003**, *238*, 255.
- (338) Cheah, M. H.; Tard, C.; Borg, S. J.; Liu, X. M.; Ibrahim, S. K.; Pickett, C. J.; Best, S. P. *J. Am. Chem. Soc.* **2007**, *129*, 11085.
- (339) Snell, K. D.; Keenan, A. G. *Chem. Soc. Rev.* **1979**, *8*, 259.
- (340) Burt, R. J.; Leigh, G. J.; Pickett, C. J. *J. Chem. Soc., Chem. Commun.* **1976**, 940.
- (341) Moutet, J. C.; Pickett, C. J. *J. Chem. Soc., Chem. Commun.* **1989**, 188.
- (342) Allongue, P.; Delamar, M.; Desbat, B.; Fagebaume, O.; Hitmi, R.; Pinson, J.; Saveant, J. M. *J. Am. Chem. Soc.* **1997**, *119*, 201.
- (343) Vijaikanth, V.; Capon, J. F.; Gloaguen, F.; Schollhammer, P.; Talarmin, J. *Electrochem. Commun.* **2005**, *7*, 427.
- (344) Amouyal, E. *Sol. Energy Mater. Sol. Cells* **1995**, *38*, 249.
- (345) Esswein, M. J.; Nocera, D. G. *Chem. Rev.* **2007**, *107*, 4022.
- (346) Lubitz, W.; Reijerse, E. J.; Messinger, J. *Energy Environ. Sci.* **2008**, *1*, 15.
- (347) Wolpher, H.; Borgstrom, M.; Hammarstrom, L.; Bergquist, J.; Sundstrom, V.; Stenbjorn, S.; Sun, L. C.; Akermark, B. *Inorg. Chem. Commun.* **2003**, *6*, 989.
- (348) Ekstrom, J.; Abrahamsson, M.; Olson, C.; Bergquist, J.; Kaynak, F. B.; Eriksson, L.; Licheng, S. C.; Becker, H. C.; Akermark, B.; Hammarstrom, L.; Ott, S. *Dalton Trans.* **2006**, 4599.
- (349) Gao, W. M.; Liu, J. H.; Jiang, W.; Wang, M.; Weng, L. H.; Åkermark, B.; Sun, L. C. C. R. *Chimie* **2008**, *11*, 915.
- (350) Song, L. C.; Tang, M. Y.; Su, F. H.; Hu, Q. M. *Angew. Chem., Int. Ed.* **2006**, *45*, 1130.
- (351) Song, L. C.; Tang, M. Y.; Mei, S. Z.; Huang, J. H.; Hu, Q. M. *Organometallics* **2007**, *26*, 1575.
- (352) Na, Y.; Pan, J. X.; Wang, M.; Sun, L. C. *Inorg. Chem.* **2007**, *46*, 3813.
- (353) Na, Y.; Wang, M.; Pan, J. X.; Zhang, P.; Akermark, B.; Sun, L. C. *Inorg. Chem.* **2008**, *47*, 2805.

CR800542Q